

Acyclic CB[n]-Type Molecular Containers: Effect of Solubilizing Group on their Function as Solubilizing Excipients

Supporting Information

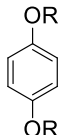
by Ben Zhang, Peter Y. Zavalij, and Lyle Isaacs*

Department of Chemistry and Biochemistry, University of Maryland, College Park, MD
20742

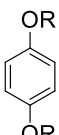
Table of Contents	Pages
General experimental details	S2
Synthetic procedures and characterization data	S2 – S23
Procedure to measure the solubility of drugs with Host 2a , 2f and 2h	S24 – S28
Binding Models (1:1 and Competition) implemented in Scientist™	S29 – S31
Determination of binding constants	S32 – S55
Binding Models (pK _a shift) implemented in Scientist™	S56
Determination of pK _a shift of dye 7	S57 – S60
Details of the X-ray crystallographic structure of 2h and 2f	S61 – S66

General Experimental. Starting materials were purchased from commercial suppliers and were used without further purification or were prepared by literature procedures. Compound **1b**, **1e**, and **2b** were prepared according to literature procedures.^{1,2} Melting points were measured on a Meltemp apparatus in open capillary tubes and are uncorrected. IR spectra were measured on a JASCO FT/IR 4100 spectrometer and are reported in cm^{-1} . NMR spectra were measured on Bruker DRX-400 instrument operating at 400 MHz for ^1H and 125 MHz for ^{13}C . Mass spectrometry was performed using a JEOL AccuTOF electrospray instrument (ESI). UV-Vis absorbance was measured on Varian Cary 100UV spectrophotometer.

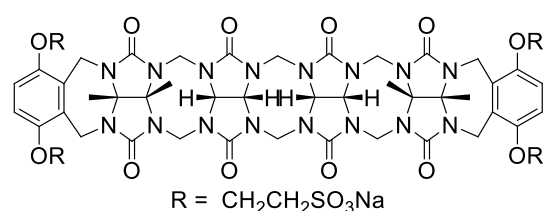
Synthetic Procedures and Characterization. The synthesis of **1e** and **2b** have been reported previously in literature.^{1,2}


R = $\text{CH}_2\text{CH}_2\text{SO}_3\text{Na}$

Compound 1a. Compound **1e** (2.000 g, 6.13 mmol) and Na_2SO_3 (3.100 g, 24.5 mmol) was mixed and dissolved in H_2O (20 mL). The mixture was stirred at 100°C under N_2 for 12 h. The mixture was allowed to cool to RT and then acetone (40 mL) was added. The product precipitated as white crystals. The solid was collected by filtration and then purified by recrystallization from water. Drying under high vacuum gave **1a** as a white solid (2.012 g, 88%). M.p. $> 270^\circ\text{C}$. IR (ATR, cm^{-1}): 3053w, 2994w, 2972w, 2882w, 1618w, 1512s, 1478m, 1265m, 1169s, 1038s, 817w, 747m, 597m, 477m. ^1H NMR (400 MHz, D_2O): 6.98 (s, 4H), 4.35 (t, $J = 6.2$, 4H), 3.32 (t, $J = 6.2$, 4H). ^{13}C NMR (125 MHz, D_2O , 1,4-dioxane as internal reference): δ 151.5, 115.5, 63.3, 49.3, (4 out of 4 resonances were observed). High-Res MS (ESI): m/z 162.0120 ($[\text{M} - 2\text{Na}]^{2-}$), calculated for $\text{C}_{10}\text{H}_{12}\text{O}_8\text{S}_2^{2-}$ 161.9987.


R = $\text{CH}_2\text{CH}_2\text{CH}_2\text{CH}_2\text{SO}_3\text{Na}$

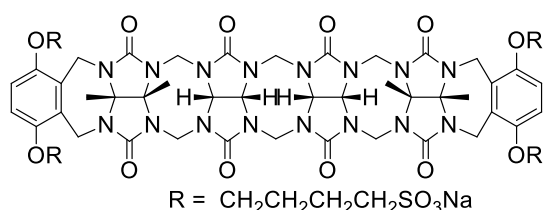
Compound 1c. A solution of butanesultone (24.500 g, 200 mmol) in 1,4-dioxane (160 mL) was added into a solution of hydroquinone (8.800 g, 80.0 mmol) in aqueous NaOH solution (10 wt%, 120 mL). The mixture was stirred at RT. for 12 h then filtered to collect the crude solid. The solid was stirred with acetone (200 mL) then dried under high vacuum to yield **1c** as a white solid (25.112 g, 80%). M.p. $> 270^\circ\text{C}$. IR (ATR, cm^{-1}): 2961w, 2857w, 1622w, 1510s, 1475w, 1237s, 1184s, 1049s, 822m, 604m, 534m, 479w. ^1H NMR (400 MHz, D_2O): 6.98 (s, 4H), 4.05 (t, $J = 5.7$, 4H), 2.95 (t, $J = 7.0$, 4H), 1.80 - 2.00 (m, 8H). ^{13}C NMR (125 MHz, D_2O , 1, 4-dioxane as internal reference): δ 152.1, 115.8, 68.3, 50.1, 26.8, 20.3 (6 out of 6 resonances were observed). High-Res MS (ESI): m/z 381.0677 ($[\text{M} - 2\text{Na} + \text{H}]$), calculated for $\text{C}_{14}\text{H}_{20}\text{O}_8\text{S}_2\text{H}$ 381.0678.



Compound 2a. Compound **1a** (0.285 g, 0.77 mmol) was added into a solution of **3** (0.181 g, 0.23 mmol) in TFA (2 mL). The mixture was stirred and heated at 70°C for 4 h. The solvent was removed with under reduced pressure and the solid was further dried under high vacuum.

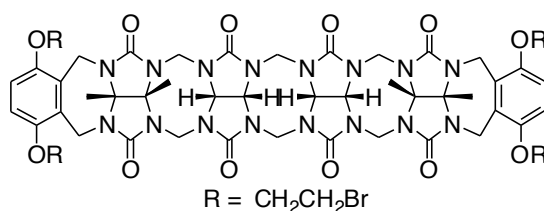
The solid was washed with the mixture of water and acetone (1:2, v/v, 30 mL) twice and then

dissolved in water and adjusted to pH = 7 by adding 1 M aqueous NaOH. The solvent was removed under reduced pressure and then the solid was further dried under high vacuum to yield **2a** as a white solid (0.208 g, 61%). M.p. > 300 °C. IR (ATR, cm⁻¹): 2990w, 1726s, 1480s, 1381m, 1318m, 1182, 1087s, 968m, 938m, 822m, 799s, 759m, 526m. ¹H NMR (400 MHz, D₂O): 6.93 (s, 4H), 5.67 (d, *J* = 15.5, 2H), 5.56 (d, *J* = 16.0, 4H), 5.44 (d, *J* = 7.6, 2H), 5.38 (d, *J* = 7.6, 2H), 5.35 (d, *J* = 16.3, 4H) 4.45 - 4.25 (m, 8H), 4.24 (d, *J* = 16.0, 4H), 4.21 (d, *J* = 16.3, 4H) 4.10 (d, *J* = 15.5, 2H), 3.55 - 3.40 (m, 4H), 3.35 - 3.20 (m, 4H), 1.79 (s, 6H), 1.75 (s, 6H). ¹³C NMR (125 MHz, D₂O, 1,4-dioxane as internal reference): δ 168.3, 167.8, 161.5, 139.5, 126.3, 90.3, 89.0, 82.8, 82.7, 77.4, 64.2, 62.0, 59.9, 46.7, 27.5, 26.5 (16 out of 16 resonances were observed). High-Res MS (ESI): *m/z* 708.1271 ([*M* - 3Na + H]²⁻), calculated for C₅₀H₅₇N₁₆O₂₄S₄Na²⁻ 708.1256.



Compound 2c. Compound **1c** (6.500 g, 15.4 mmol) was added into a solution of **3** (3.000 g, 3.84 mmol) in TFA (30 mL). The mixture was stirred and heated at 70 °C for 4 h. The solvent was removed with under reduced pressure and the solid was further dried under high vacuum.

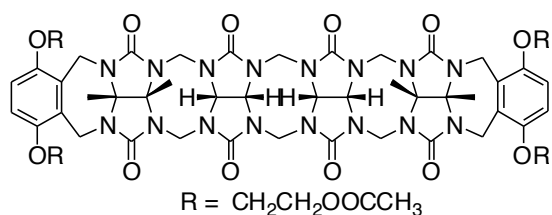
The solid was washed twice with the mixture of water and acetone (1:2, v/v, 300 mL) twice and then dissolved in water and adjusted to pH = 7 by adding 1 M aqueous NaOH. The solvent was removed under reduced pressure and then the solid was further dried under high vacuum to yield **2c** as a white solid (2.331 g, 40%). M.p. > 300 °C. IR (ATR, cm⁻¹): 3936w, 1729s, 1474s, 1380m, 1185s, 1088s, 1043s, 963m, 974m, 823m, 799s, 760m, 603m. ¹H NMR (400 MHz, D₂O): 7.00 (s, 4H), 5.62 (d, *J* = 15.2, 2H), 5.51 (d, *J* = 16.0, 4H), 5.45 (d, *J* = 8.9, 2H), 5.35 (d, *J* = 8.9, 2H), 5.24 (d, *J* = 16.0, 4H), 4.30 (d, *J* = 16.0, 4H), 4.25 (d, *J* = 16.0, 4H), 4.04 (d, *J* = 15.2, 2H), 3.90 - 3.75 (m, 8H), 2.90 - 2.75 (m, 4H), 2.70 - 2.55 (m, 4H), 1.72 (s, 12H), 1.80 - 1.40 (m, 16H). ¹³C NMR (125 MHz, D₂O, 1,4-dioxane as internal reference): δ 162.5, 162.3, 156.8, 134.1, 122.4, 85.2, 83.8, 77.5, 76.8, 57.1, 54.6, 41.3, 34.2, 27.4, 22.1, 21.4 (16 out of 18 resonances were observed). High-Res MS (ESI): *m/z* 753.1977 ([*M* - 4Na + 2H]²⁺), calculated for C₅₈H₇₄N₁₆O₂₄S₄²⁺ 753.1972.



Compound 2d. Compound **1e** (1.700 g, 5.21 mmol) and compound **3** (1.200 g, 1.53 mmol) were mixed in a round bottom flask. TFA (12 mL) was added, and the mixture was stirred at 70 °C for 3 h. The reaction mixture was poured into MeOH (100 mL), and the solid was collected

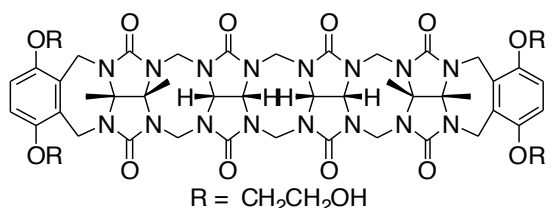
with filtration. The crude product was stirred with water (150 mL) and then acetone (150 mL) at RT and the solid was isolated by filtration. Drying at high vacuum gave the product **2d** as a white powder (1.714 g, 79 %). M.p. 283 - 285 °C. IR (ATR, cm⁻¹): 3000br, 1704m, 1456m, 1311m, 1225s, 1177s, 1080s, 966m, 922m, 818m, 794s, 754m, 666m. ¹H NMR (400 MHz, DMSO): 6.91 (s, 4H), 5.59 (d, *J* = 14.4, 2H), 5.51 (d, *J* = 15.2, 4H), 5.38 (d, *J* = 9.0, 2H), 5.30 - 5.25 (m, 6H), 4.50 - 4.40 (m, 4H), 4.25 - 4.20 (m, 10H), 4.06 (d, *J* = 15.2, 4H), 3.90 - 3.80 (m, 8H), 1.69 (s, 6H), 1.66 (s, 6H). ¹³C NMR (125 MHz, DMSO): δ 155.3, 154.0 150.3,

128.8, 116.0, 77.3, 76.2, 70.1, 70.8, 70.7, 70.3, 52.9, 48.2, 34.5, 32.8, 16.6, 15.6, (16 out of 16 resonances were observed). MS (ESI): m/z 765 ($[M + p\text{-xylenediamine} + 2H]^{2+}$)



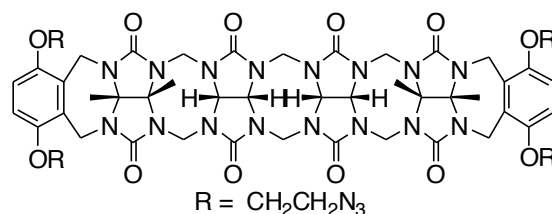
Compound 2g. Compound **1d** (1.021 g, 5.12 mmol) and **3** (1.000 g, 1.28 mmol) was mixed as solid and then dissolved in a mixture of TFA and Ac_2O (1:1, 10 mL). The mixture was stirred at 70 °C for 3.5 h and then was poured into MeOH (150 mL). The solid was collected by filtration

and was washed with acetone (100 mL) and water (100 mL). After drying under high vacuum, compound **2g** was obtained as a white powder (1.512 g, 90 %). M.p. > 300 °C. IR (ATR, cm^{-1}): 2925w, 1732s, 1464s, 1377m, 1314m, 1228s, 1184s, 1083m, 974m, 822m, 797m. ^1H NMR (400 MHz, DMSO): 6.84 (s, 4H), 5.58 (d, $J = 16.3$, 2H), 5.48 (d, $J = 15.6$, 4H), 5.37 (d, $J = 9.0$, 2H), 5.27 (d, $J = 9.0$, 2H), 5.23 (d, $J = 16.0$, 4H), 4.45-4.30 (m, 4H), 4.30-4.05 (m, 16H), 3.50-3.45 (m, 4H), 2.06 (s, 12H), 1.67 (s, 6H), 1.63 (s, 6H). ^{13}C NMR (125 MHz, DMSO): δ 170.4, 155.3, 153.9, 150.3, 128.4, 115.0, 77.3, 76.2, 71.8, 70.4, 68.6, 63.1, 53.1, 48.3, 34.4, 20.7, 16.6, 15.6 (18 out of 18 resonances were observed). MS (ESI): m/z 745 ($[M + p\text{-xylenediamine} + 2H]^{2+}$).



Compound 2h. Compound **2g** (0.400 g, 0.305 mmol) was added into an aqueous solution of LiOH (2.5 M, 7.5 mL). The mixture was stirred at 50 °C for 0.5 h and then the solid was collected by filtration. The solid was wash with 0.1 M HCl to nertral and then stirred with EtOH (30 mL),

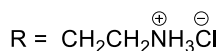
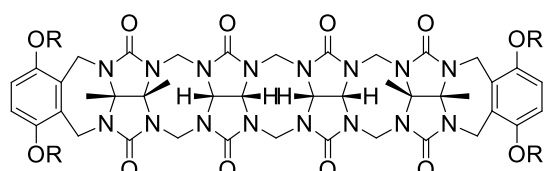
and water (30 mL). After drying under high vacuum, a white solid was obtained (0.234 g, 67%). M.p. > 300 °C. IR (ATR, cm^{-1}): 3428br, 2932w, 1728s, 1476s, 1379s, 1256s, 1184m, 1085m, 967m, 798m. ^1H NMR (400 MHz, D_2O): 6.95 (s, 4H), 5.62 (d, $J = 15.3$, 2H), 5.52 (d, $J = 15.7$, 4H), 5.43 (d, $J = 8.0$, 2H), 5.20 (d, $J = 8.0$, 2H), 4.72 (d, $J = 16.2$, 4H), 4.28 (d, $J = 15.7$, 4H), 4.23 (d, $J = 16.2$, 4H), 4.19 (d, $J = 15.3$, 2H), 3.85-3.50 (m, 8H), 3.45-2.85 (m, 8H), 1.76 (s, 12H). ^{13}C NMR (125 MHz, D_2O , 1,4-dioxane as internal reference): δ 155.8, 149.8, 127.2, 114.7, 78.8, 77.4, 71.0, 70.2, 60.0, 52.0, 47.8, 34.6, 15.7, 14.8 (16 out of 18 resonances were observed). High-Res MS (ESI): m/z 639.2886 ($[M + p\text{-xylenediamine} + 2H]^{2+}$), calculated for $\text{C}_{58}\text{H}_{74}\text{N}_{18}\text{O}_{16}^{2+}$ 639.2765.



Compound 2e. Compound **2d** (0.500 g, 0.359 mmol) and NaN_3 (0.281 g, 4.32 mmol) were mixed together and was then dissolved in DMSO (5.0 mL). The mixed was stirred at 80 °C for 12 h and was then poured into H_2O (50 mL). The solid was collected by filtration and was

then washed with MeOH (50 mL). After drying under vacuum, a white solid was obtained (0.423 g, 95%). M.p. > 300 °C. IR (ATR, cm^{-1}): 2932w, 2106m, 1730s, 1466s, 1378m, 1314m, 1230m, 1086m, 973w, 798m, ^1H NMR (400 MHz, DMSO): 6.88 (s, 4H), 5.57 (d,

$J = 14.6$, 2H), 5.47 (d, $J = 15.1$, 4H), 5.37 (d, $J = 8.7$, 2H), 5.25 (d, $J = 8.7$, 2H), 5.24 (d, $J = 16.1$, 4H), 4.25 – 4.20 (m, 4H), 4.14 (d, $J = 16.1$, 4H), 4.15 – 4.05 (m, 4H), 4.05 (d, $J = 14.6$, 4H), 4.03 (d, $J = 15.1$, 2H), 3.85-3.75 (m, 4H), 3.55-3.45 (m, 4H), 1.69 (s, 6H), 1.66 (s, 6H). ^{13}C NMR (125 MHz, DMSO): δ 155.1, 153.8, 150.2, 128.3, 115.0, 77.1, 76.0, 70.6, 70.2, 69.6, 52.8, 50.4, 34.2, 16.5, 15.4 (16 out of 16 resonances were observed). High-Res MS (ESI): m/z 689.3025 ($[\text{M} + p - \text{xylenediamine} + 2\text{H}]^{2+}$), calculated for $\text{C}_{58}\text{H}_{70}\text{N}_{30}\text{O}_{12}^{2+}$ 689.2894.



Compound 2f. Compound **2e** (0.031 g, 0.0242 mmol) was mixed with triphenylphosphine (0.051 g, 0.193 mmol) and was then dissolved in the mixed solvent of DMSO (4 mL) and H_2O (1 mL). The mixture was stirred at 80 °C for 6 h and pH was adjusted to 1 with 6M HCl. The

resulting solution was poured into acetone (80 mL) and the solid was collected by filtration. The crude product was then crystallized with a mix solvent of H_2O (0.5 mL) and acetone (1.5 mL). The solid was then collected by centrifuge and after drying under vacuum, a white solid was obtained (0.012 g, 39%). M.p. > 300 °C. IR (ATR, cm^{-1}): 3435br, 3045m, 1726s, 1479s, 1379w, 1318s, 1257s, 1231s, 1180s, 1093s. ^1H NMR (400 MHz, D_2O): 6.44 (s, 4H), 5.58 (d, $J = 15.3$, 2H), 5.52 (d, $J = 15.8$, 4H), 5.46 (d, $J = 9.2$, 2H), 5.28 (d, $J = 9.2$, 2H), 5.27 (d, $J = 16.5$, 4H), 4.31 (d, $J = 15.8$, 4H), 4.29 (d, $J = 16.5$, 4H), 4.13 (d, $J = 15.3$, 2H), 3.85 - 3.75 (m, 4H), 3.65-3.55 (m, 4H), 3.350-3.10 (m, 8H), 1.78 (s, 6H), 1.77 (s, 6H). ^{13}C NMR (125 MHz, D_2O , 1,4-dioxane as internal reference): δ 155.9, 155.7, 148.2, 126.8, 112.1, 78.6, 77.5, 70.1, 70.0, 64.0, 51.5, 47.8, 38.4, 34.5, 17.0, 15.5, (16 out of 16 resonances were observed). High-Res MS (ESI): m/z 1137.5092 ($[\text{M} - 4\text{HCl} + \text{H}]^+$), calculated for $\text{C}_{50}\text{H}_{65}\text{N}_{20}\text{O}_{12}^+$ 1137.5091.

References

- 1) Ma, D.; Hettiarachchi, G.; Nguyen, D.; Zhang, B.; Wittenberg, J. B.; Zavalij, P. Y.; Briken, V.; Isaacs, L., *Nat. Chem.* **2012**, *4*, 503-510.
- 2) George, W. N.; Giles, M.; McCulloch, I.; De Mello, J. C.; Steinke, J. H. G., *Soft Matter.*, **2007**, *3*, 1381-1387.

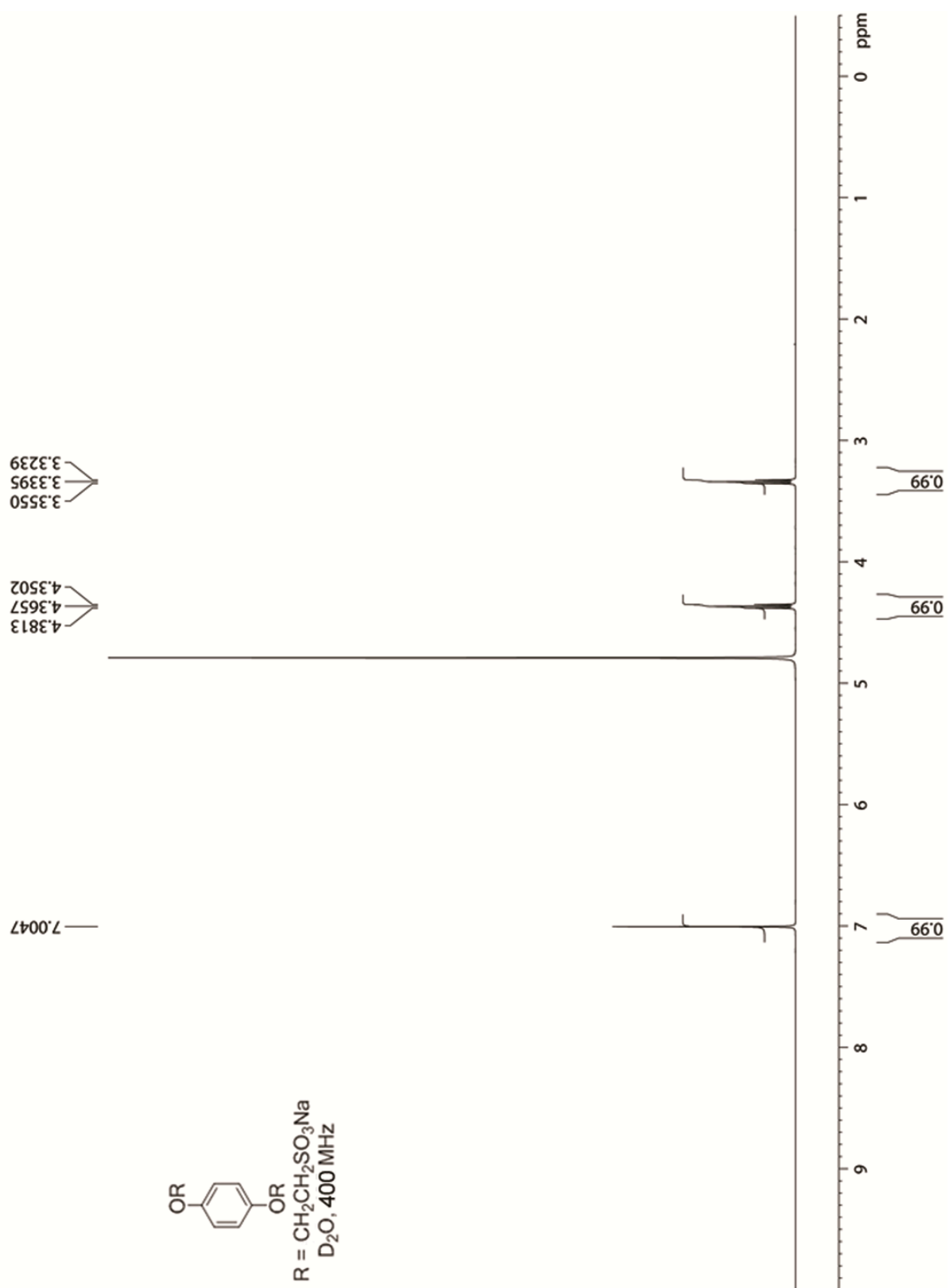


Figure S1. ¹H NMR spectra (400 MHz, D₂O, RT) recorded for **1a**.

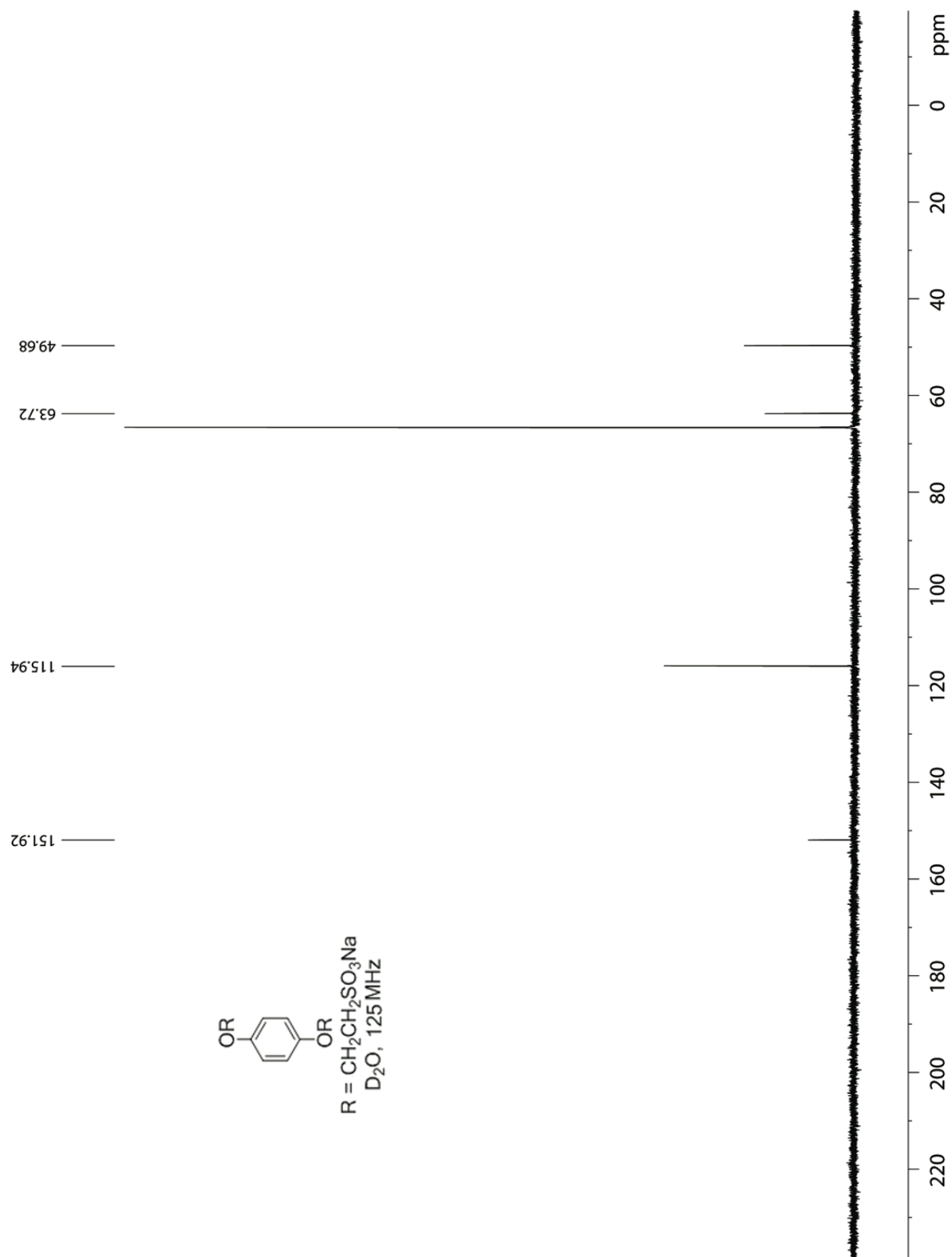


Figure S2. ¹³C NMR spectra (125 MHz, D₂O, RT, 1,4-dioxane as internal reference) recorded for **1a**.

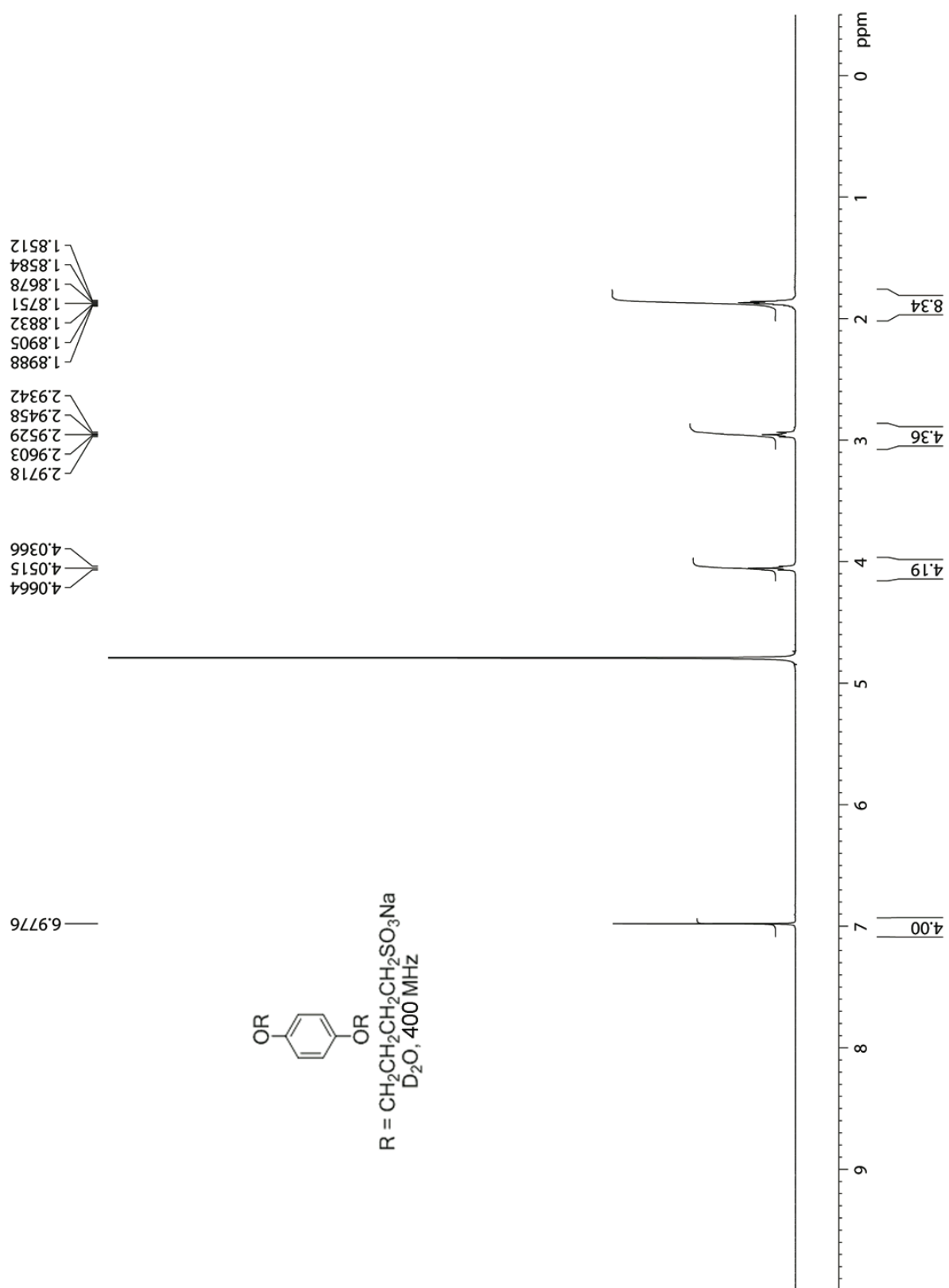


Figure S3. ^1H NMR spectra (400 MHz, D_2O , RT) recorded for **1c**.

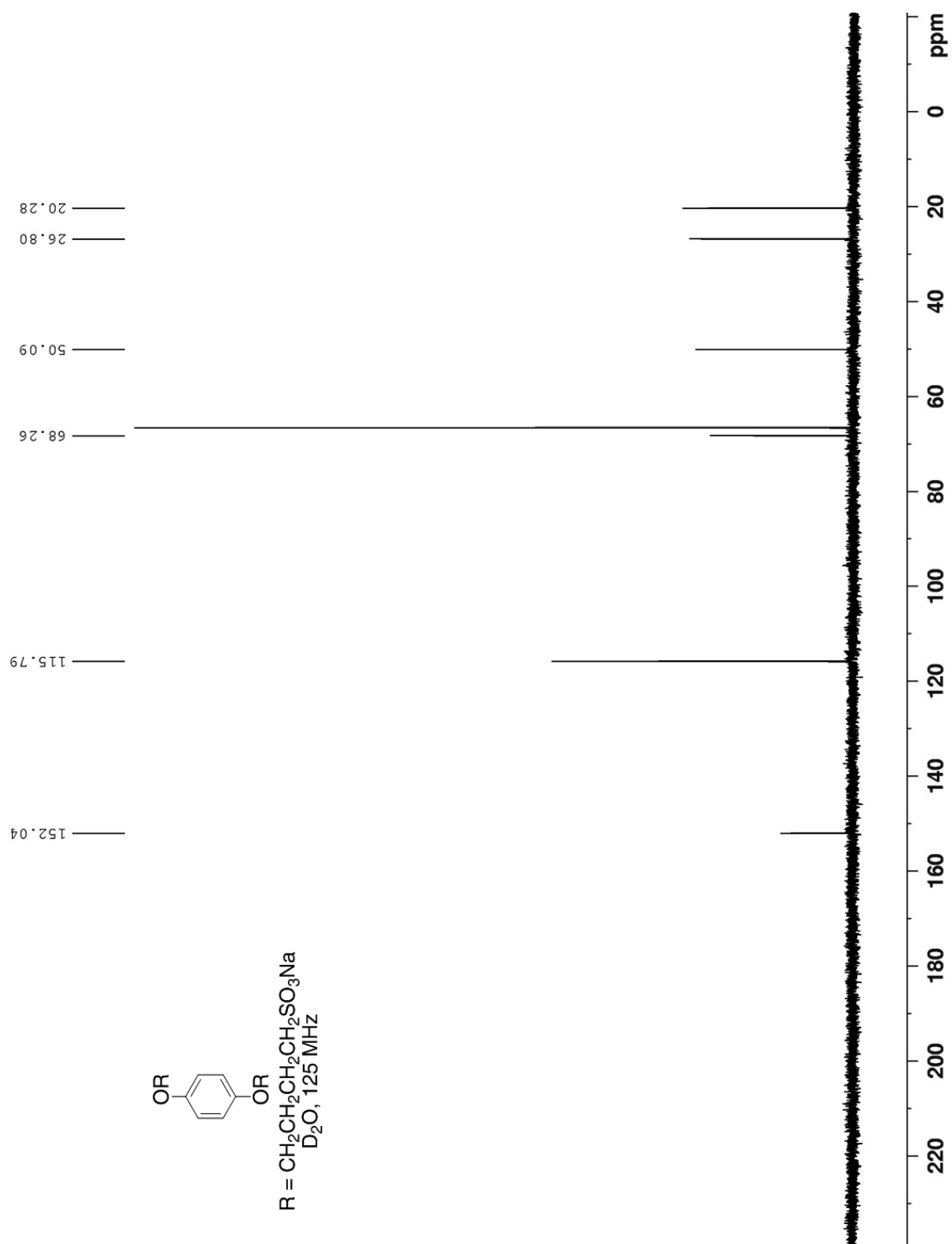


Figure S4. ^{13}C NMR spectra (125 MHz, D_2O , RT, 1,4-dioxane as internal reference) recorded for **1c**.

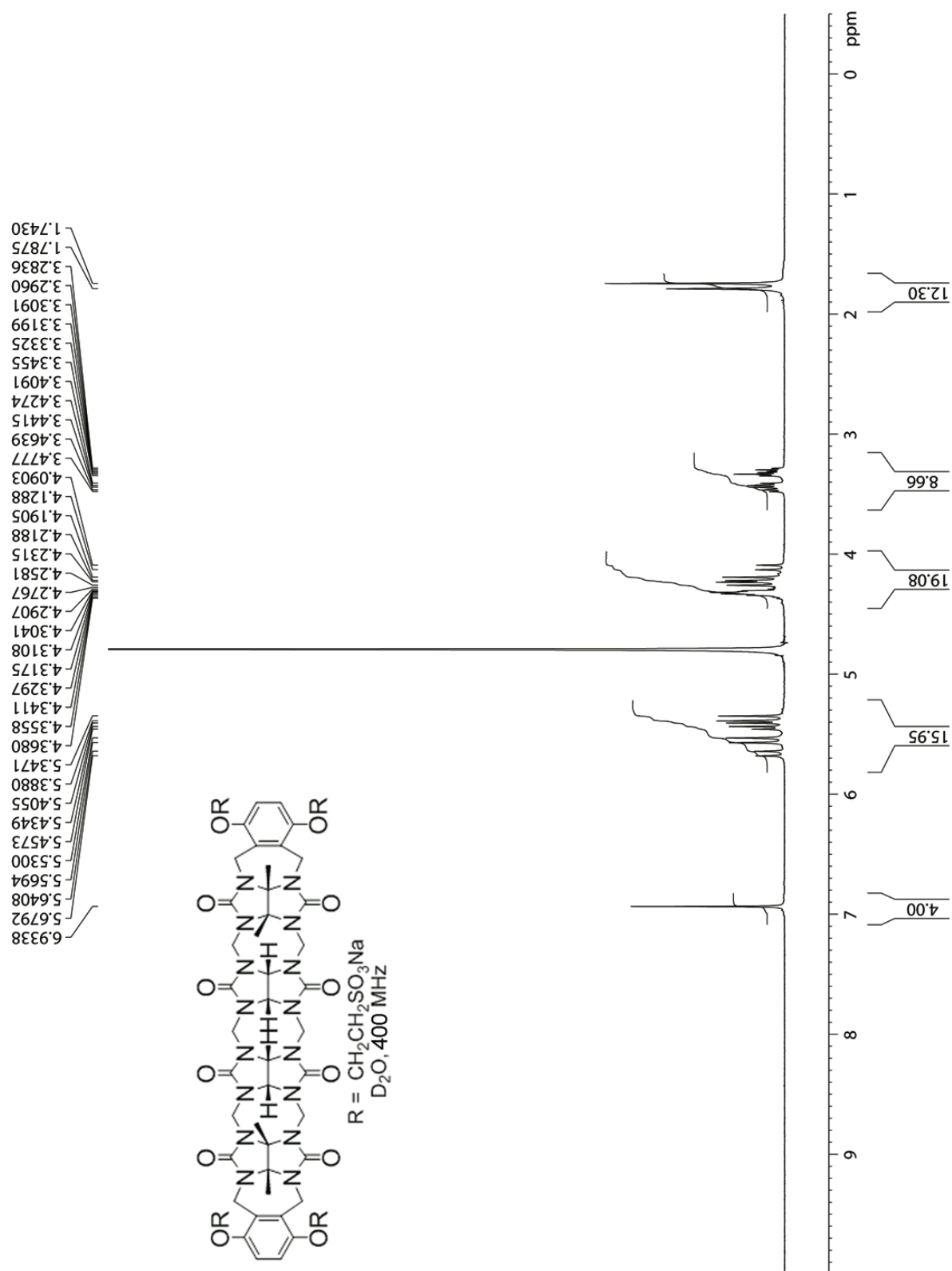


Figure S5. ^1H NMR spectra (400 MHz, D_2O , RT) recorded for **2a**.

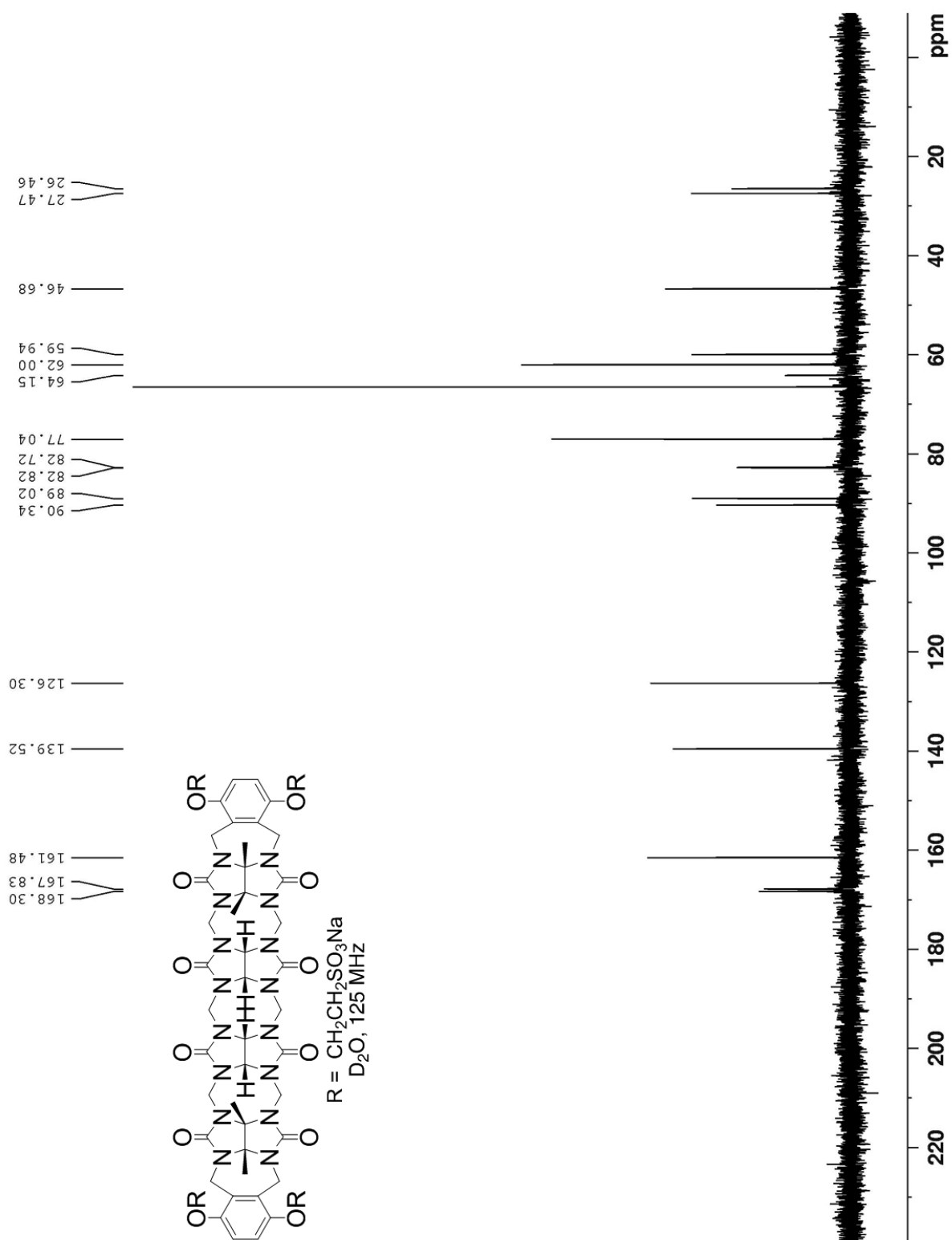


Figure S6. ^{13}C NMR spectra (125 MHz, D_2O , RT, 1,4-dioxane as internal reference) recorded for **2a**.

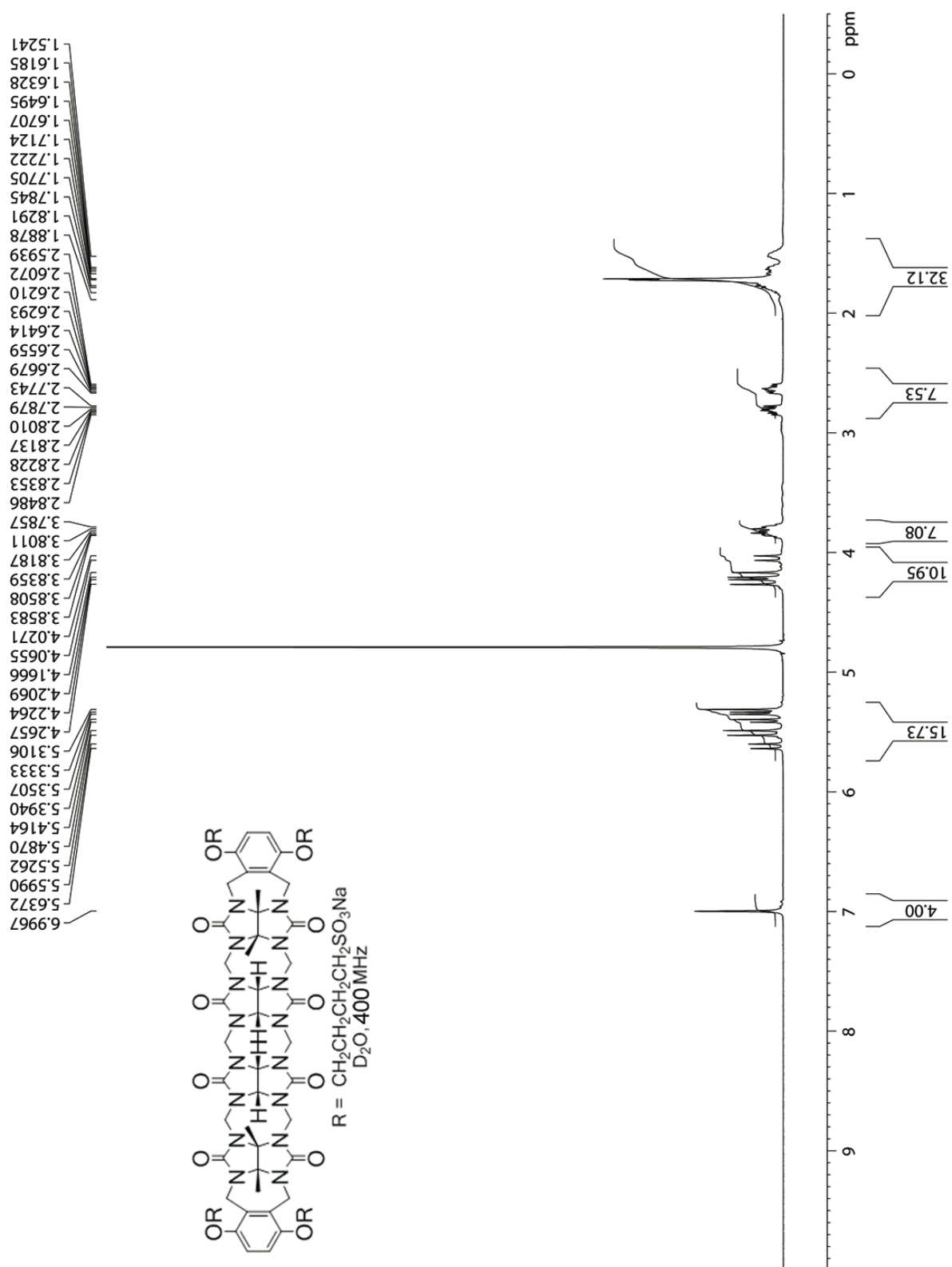


Figure S7. ^1H NMR spectra (400 MHz, D_2O , RT) recorded for **2c**.

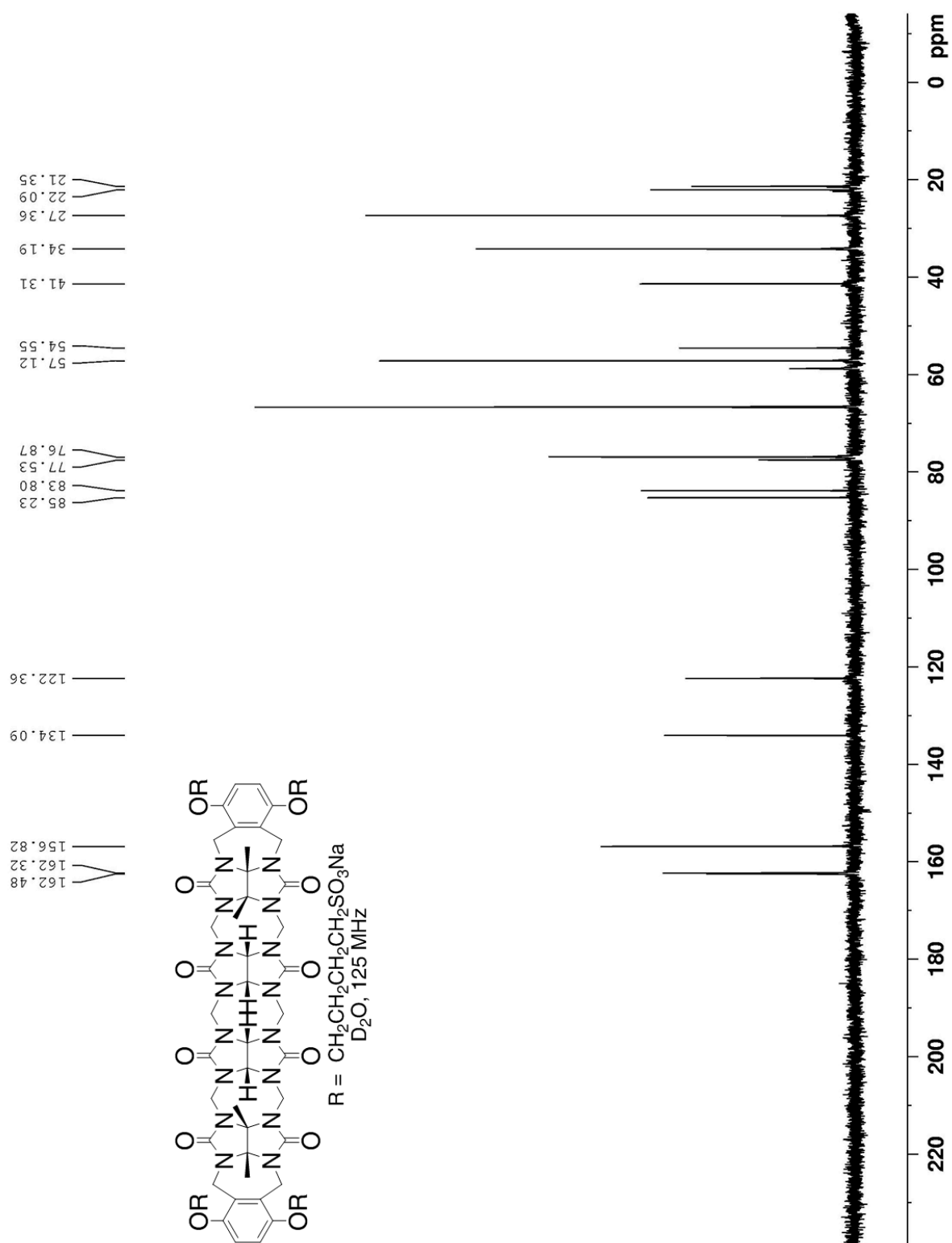


Figure S8. ^{13}C NMR spectra (125 MHz, D_2O , RT, 1,4-dioxane as internal reference) recorded for **2c**.

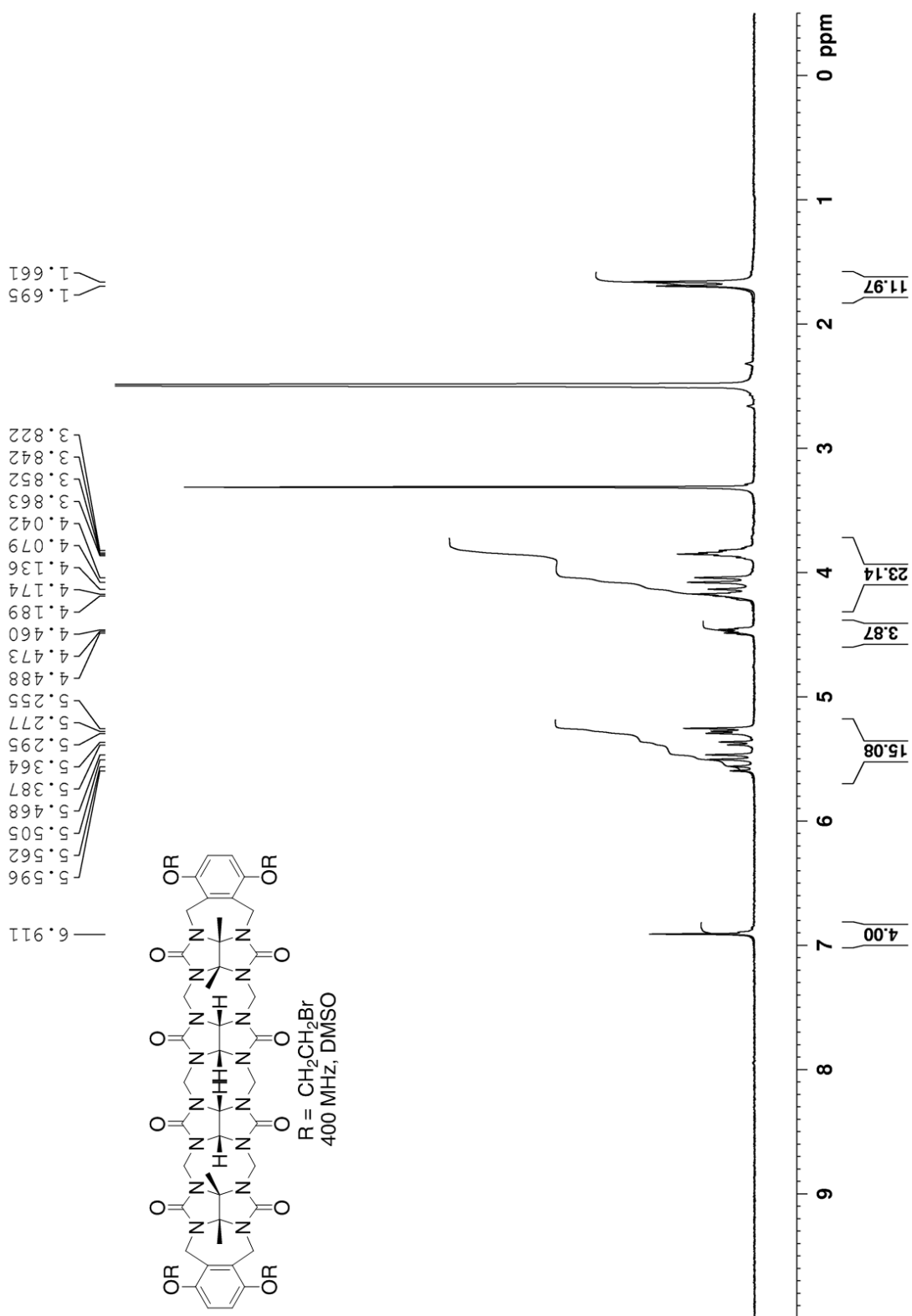


Figure S9. ¹H NMR spectra (400 MHz, DMSO, RT) recorded for **2d**.

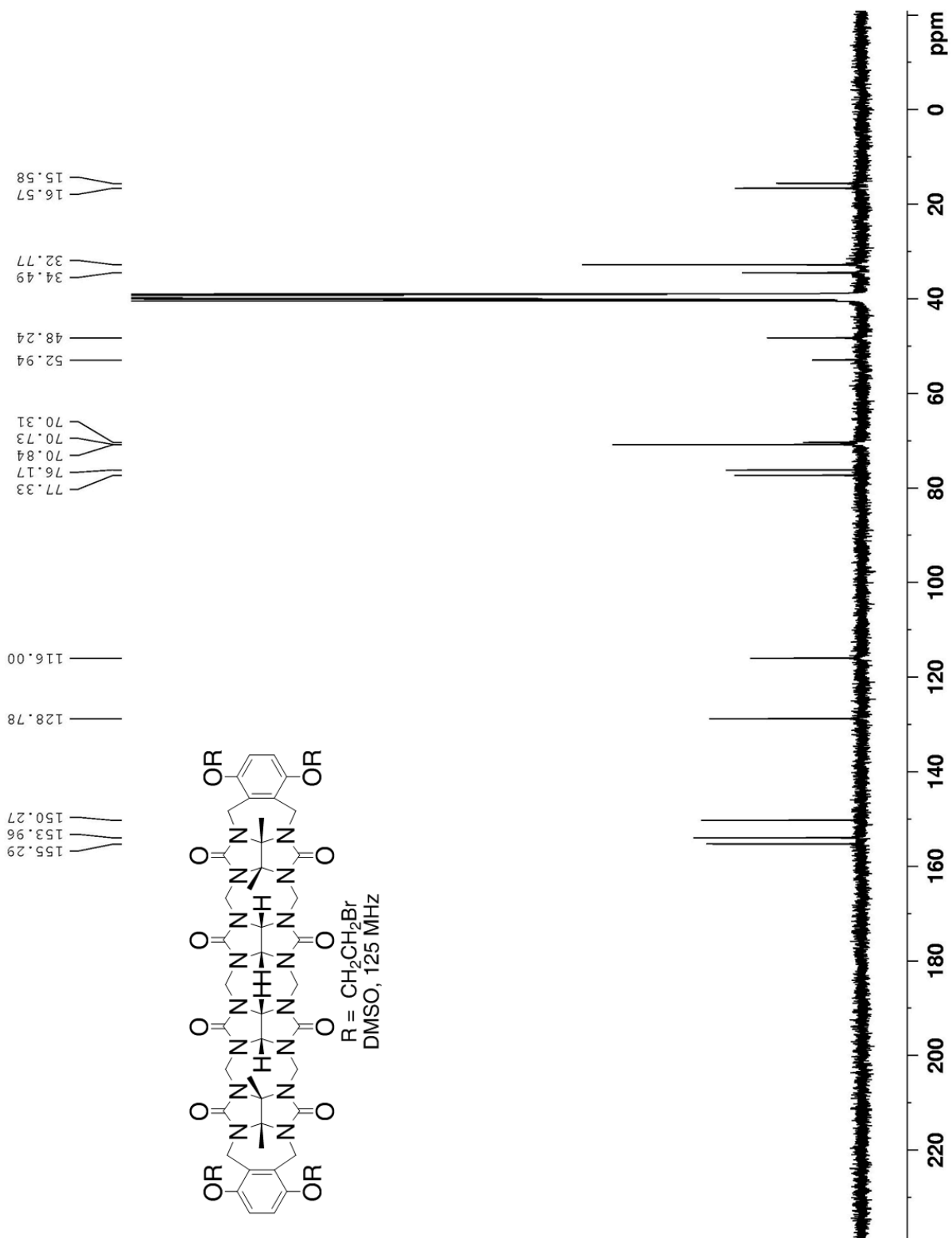


Figure S10. ^{13}C NMR spectra (125 MHz, DMSO, RT) recorded for **2d**.

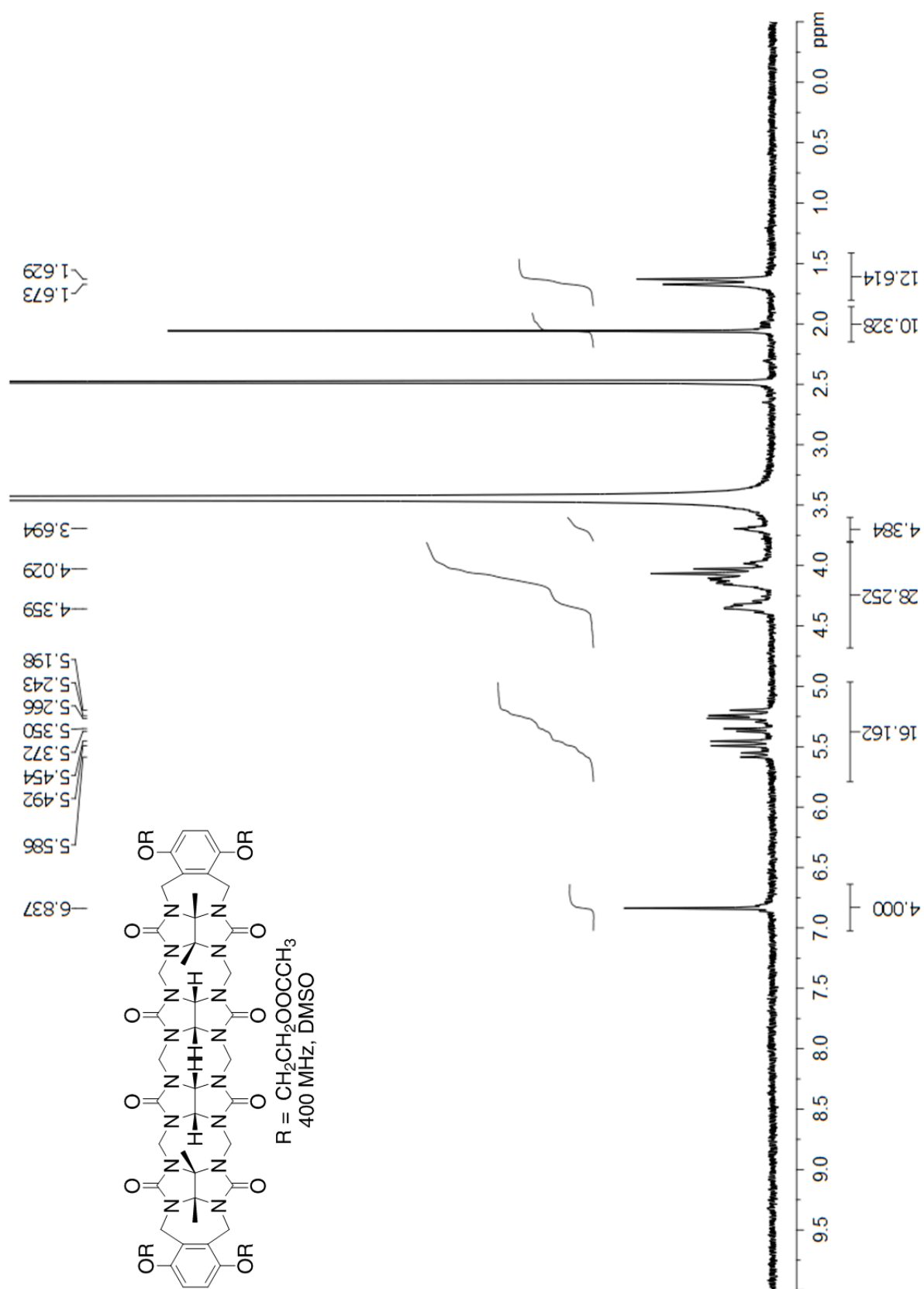


Figure S11. ^1H NMR spectra (400 MHz, DMSO, RT) recorded for **2g**.

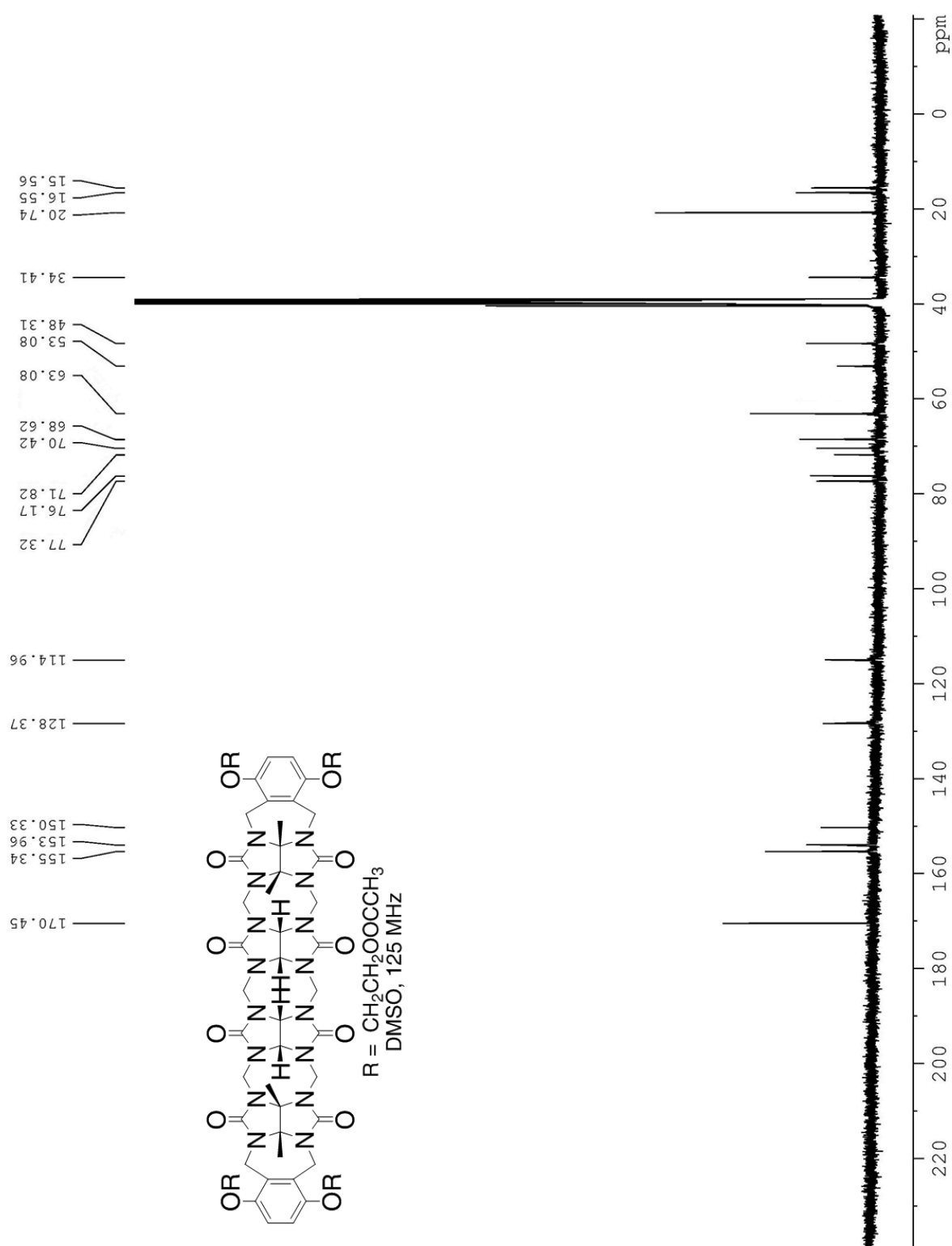


Figure S12. ¹³C NMR spectra (125 MHz, DMSO, RT) recorded for **2g**.

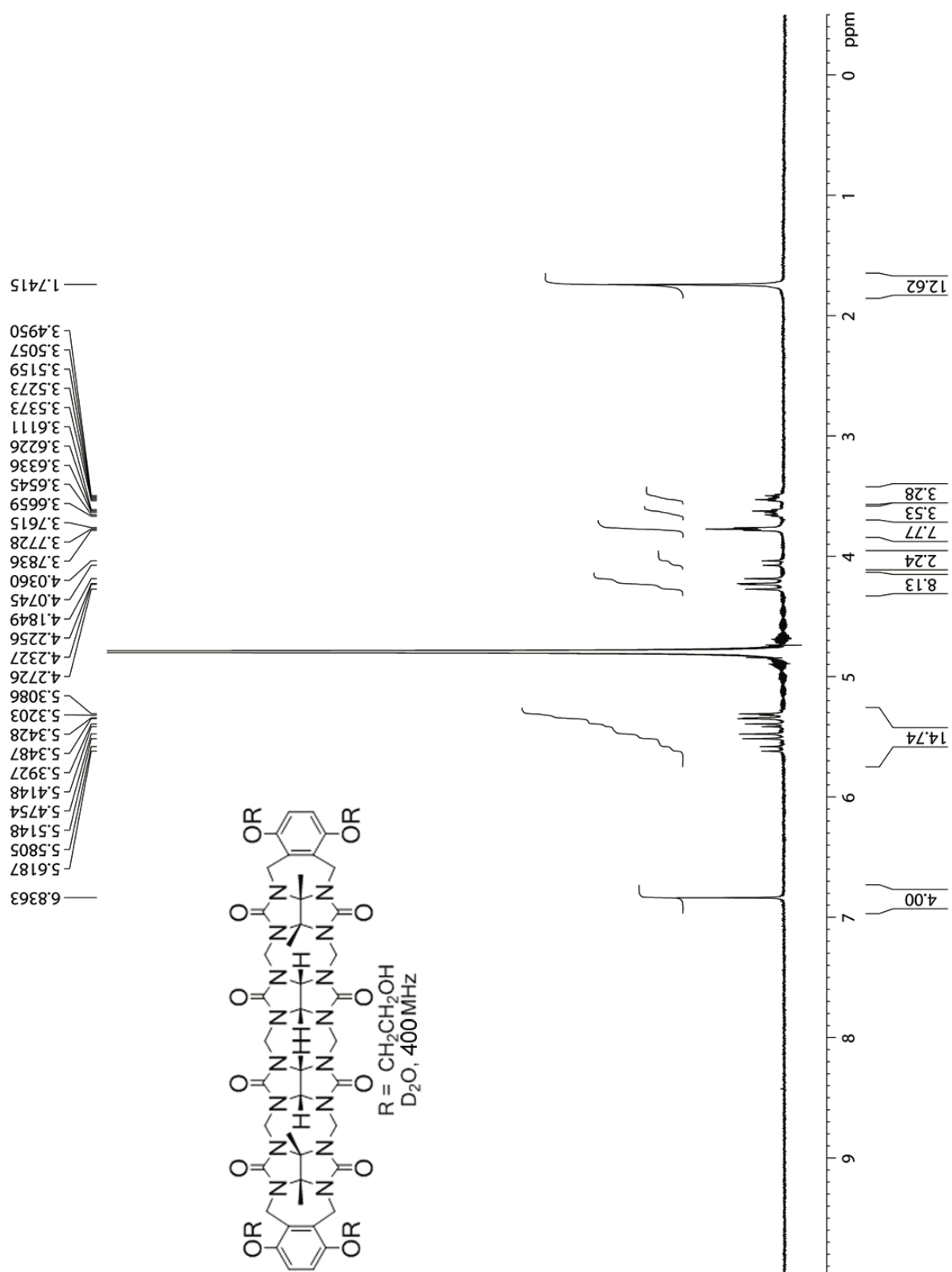


Figure S13. ^1H NMR spectra (400 MHz, D_2O , RT) recorded for **2h**.

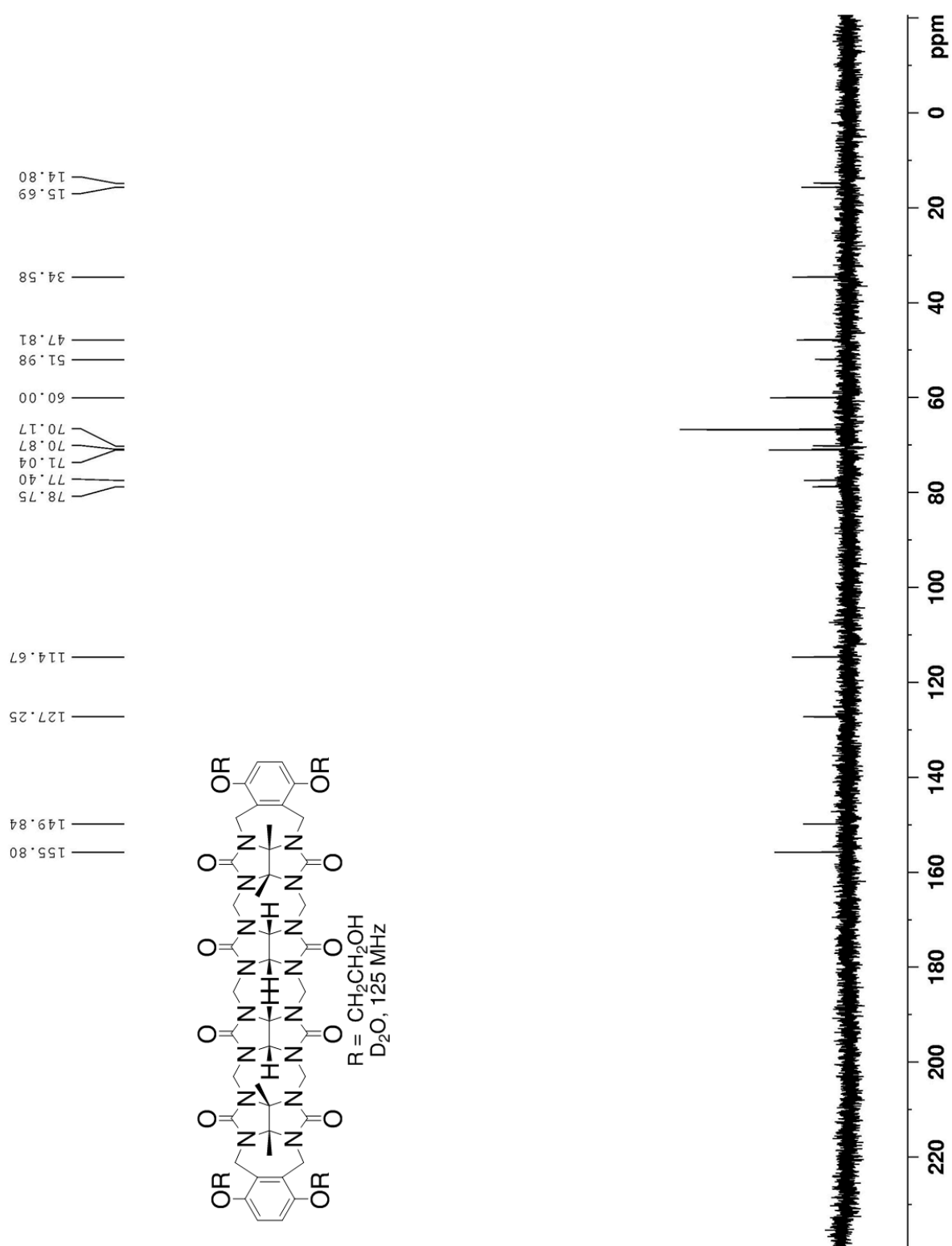


Figure S13. ^{13}C NMR spectra (125 MHz, D_2O , RT, 1,4-dioxane as internal reference) recorded for **2h**.

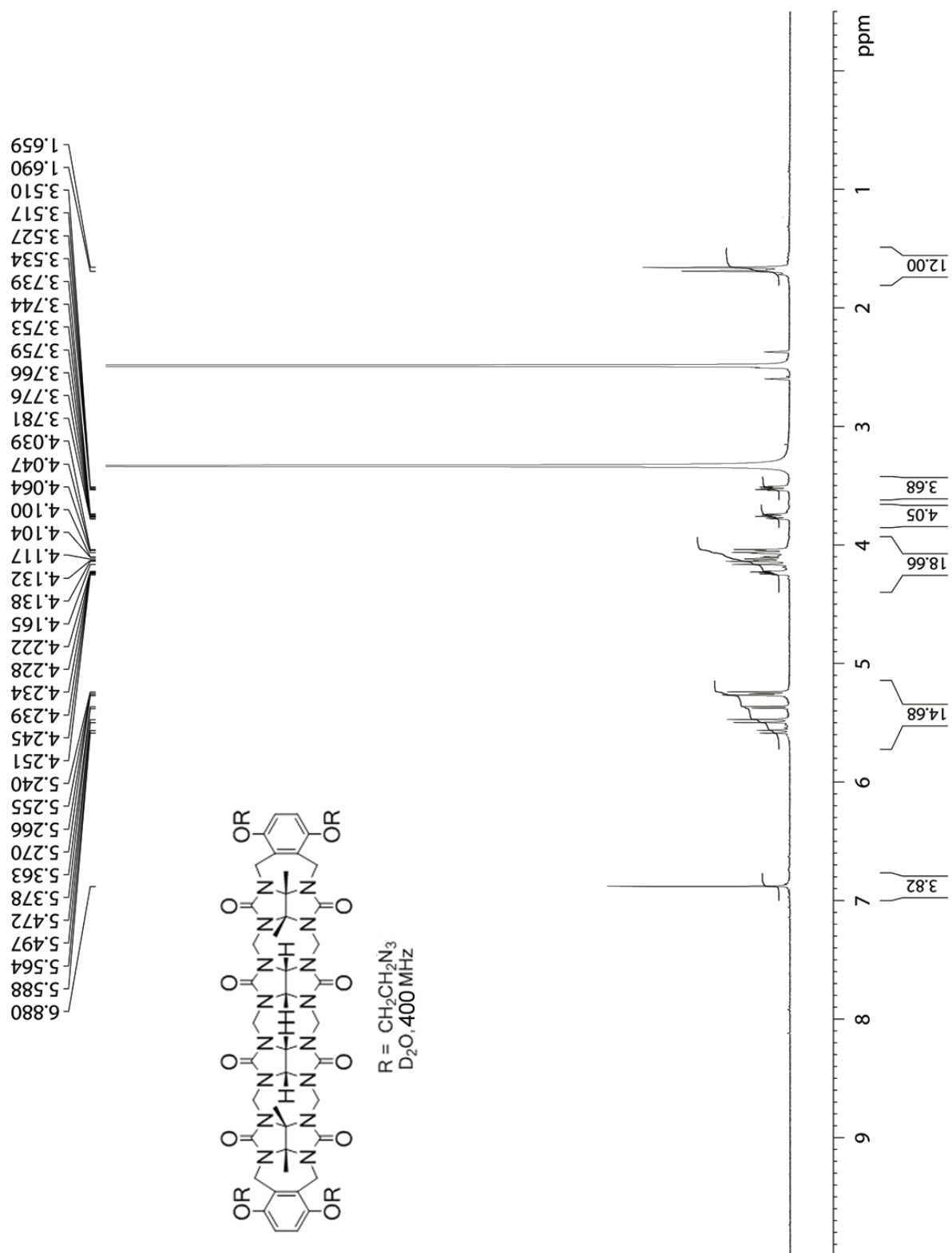


Figure S14. ^1H NMR spectra (400 MHz, DMSO, RT) recorded for **2e**.

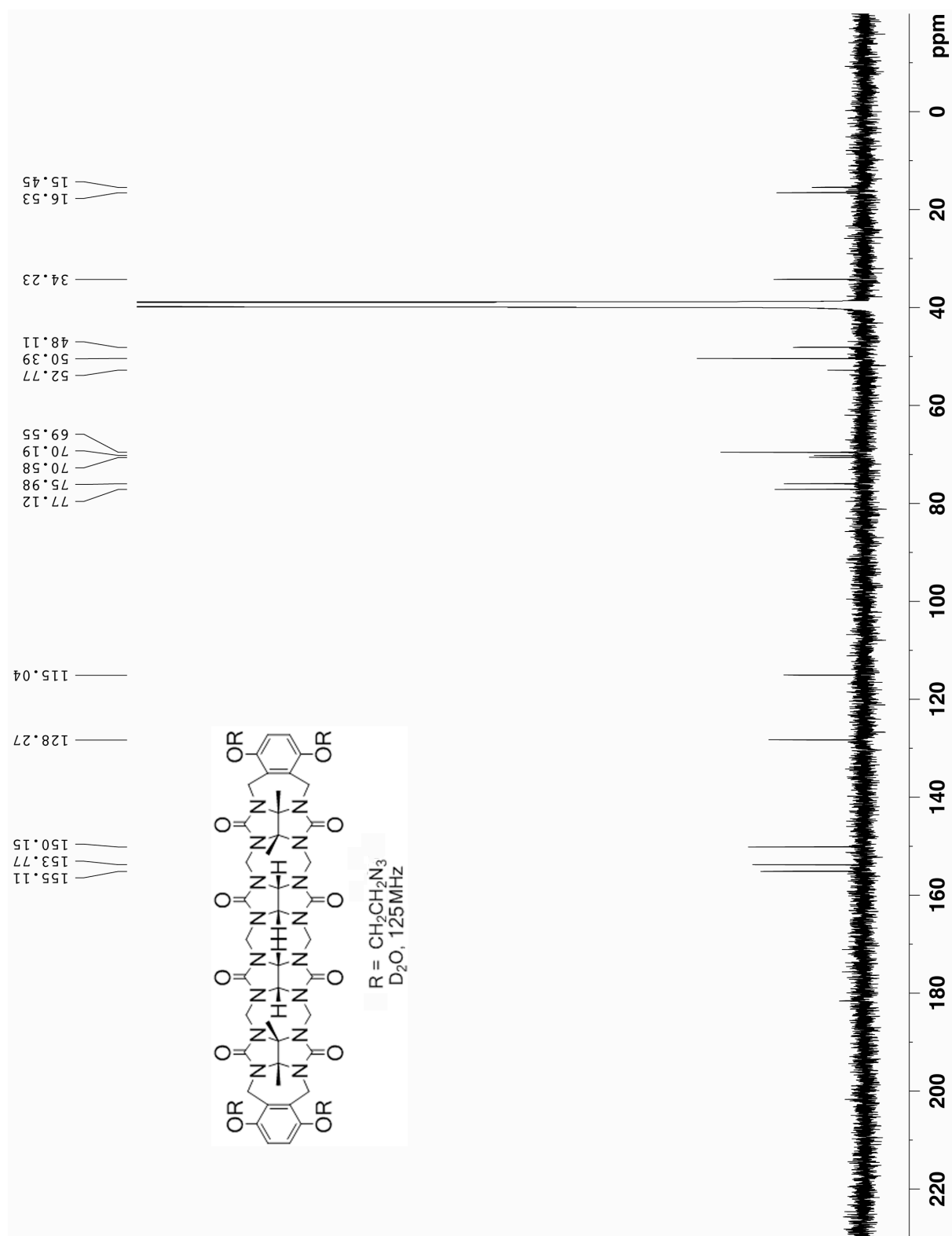


Figure S15. ^{13}C NMR spectra (125 MHz, D_2O , RT, 1,4-dioxane as internal reference) recorded for **2e**.

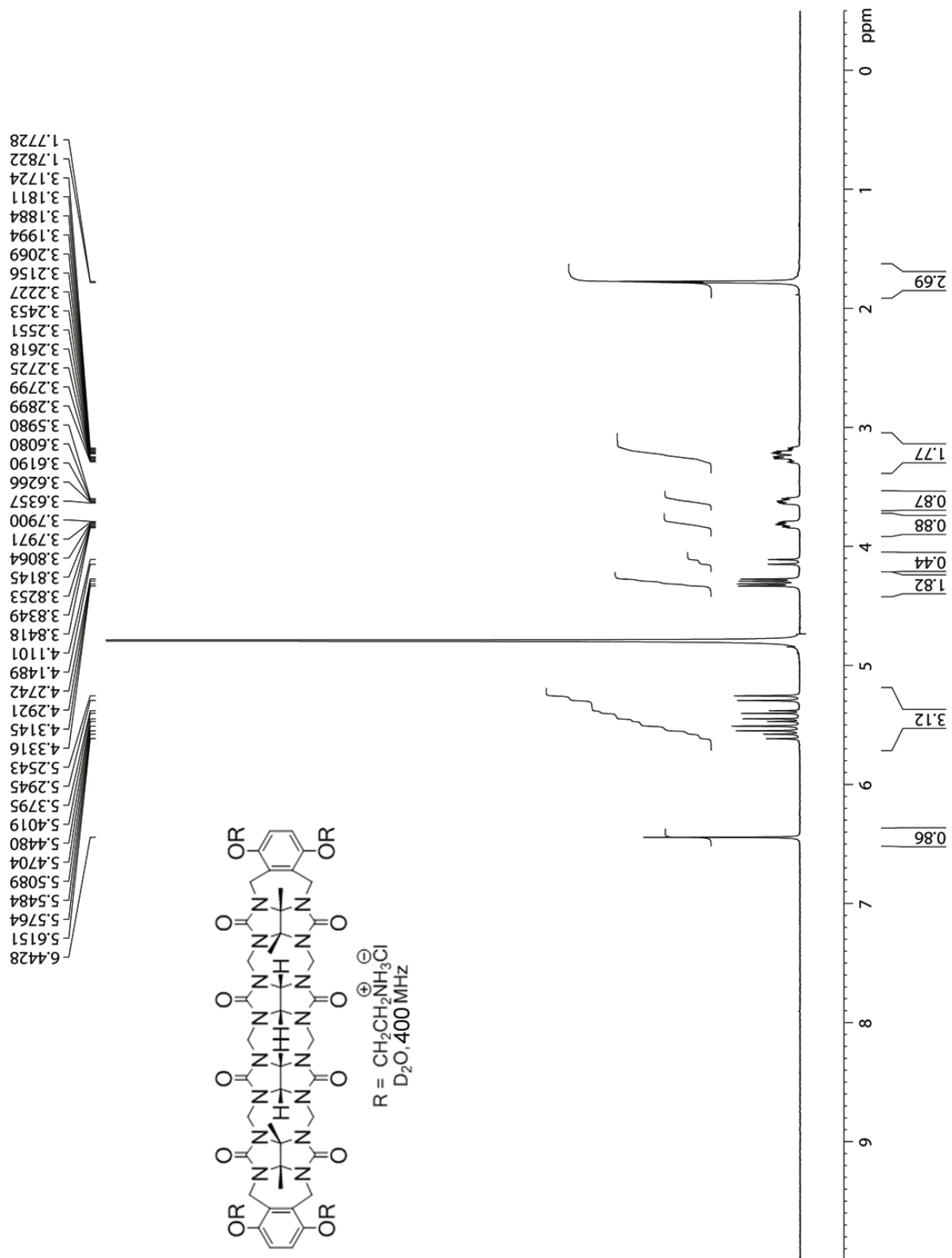


Figure S16. ^1H NMR spectra (400 MHz, D_2O , RT) recorded for **2f**.

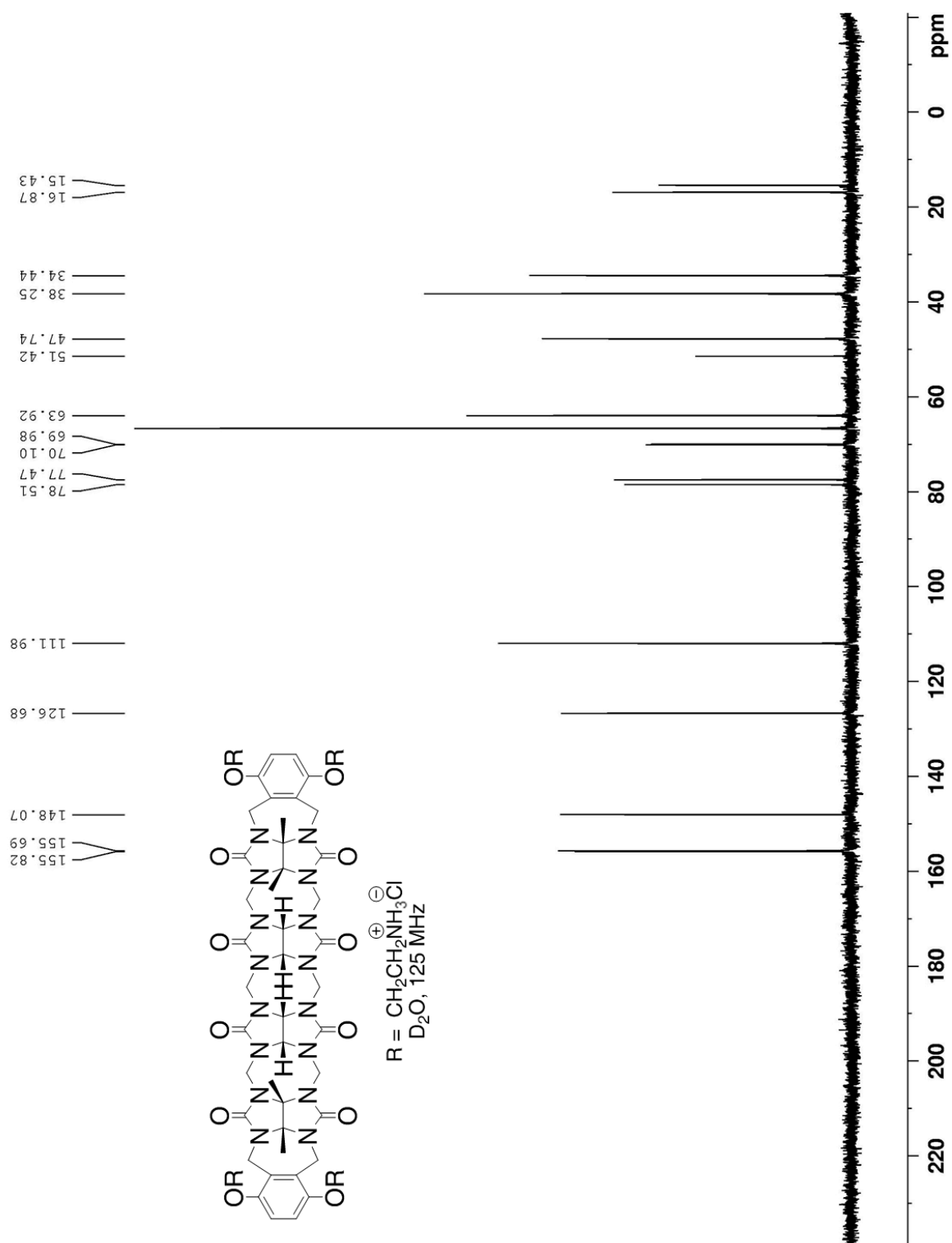


Figure S17. ^{13}C NMR spectra (125 MHz, D_2O , RT, 1,4-dioxane as internal reference) recorded for **2f**.

Procedure to measure the solubility of drugs with Host 2a, 2h and 2f. Excess amount of drug was added into a solution of host **2a/2f/2h** of known concentration in deuterated sodium phosphate buffer (20 mM, pD = 7.4). The suspended mixture was magnetically stirred at room temperature for 6 h. During this period, the pD value of the solution was monitored and adjusted back to 7.4 if it changed. The mixture was then centrifuged twice (4200 rpm, 10 min). The ^1H NMR spectrum of the supernatant was measured (400 MHz) with 1,3,5-benzenetricarboxylic acid (1.03 mM) as internal standard. The signal for the reference shows up at 8.35 ppm (s, 3H). Diagnostic signals for the dissolved drug were also integrated. From the ratio of integrations of reference peak relative to the drug peak, and the concentration of reference, the concentration of the drug can be calculated.

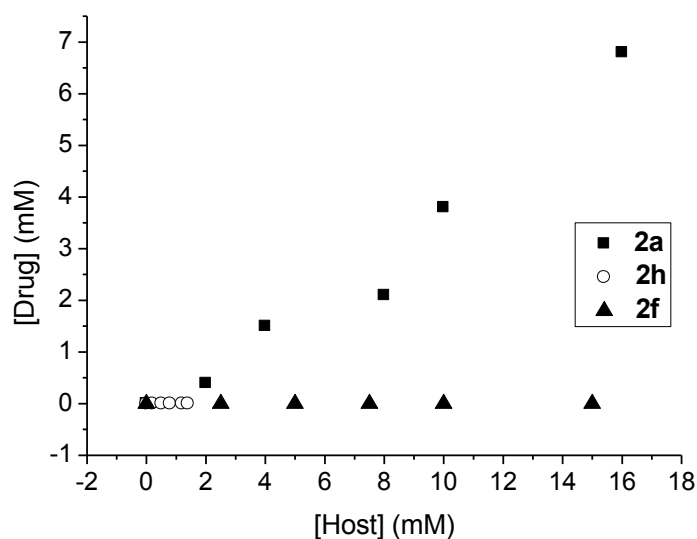


Figure S18. Phase diagram of mixtures of indomethacin and host **2a**, **2f** and **2h**, in 20 mM sodium phosphate buffer (pH = 7.4).

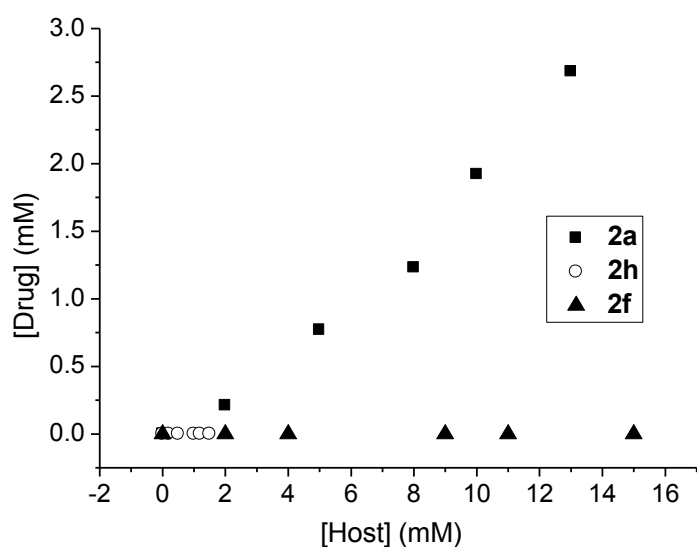


Figure S19. Phase diagram of mixtures of 17 α -ethynylestradiol and host **2a**, **2f** and **2h**, in 20 mM sodium phosphate buffer (pH = 7.4).

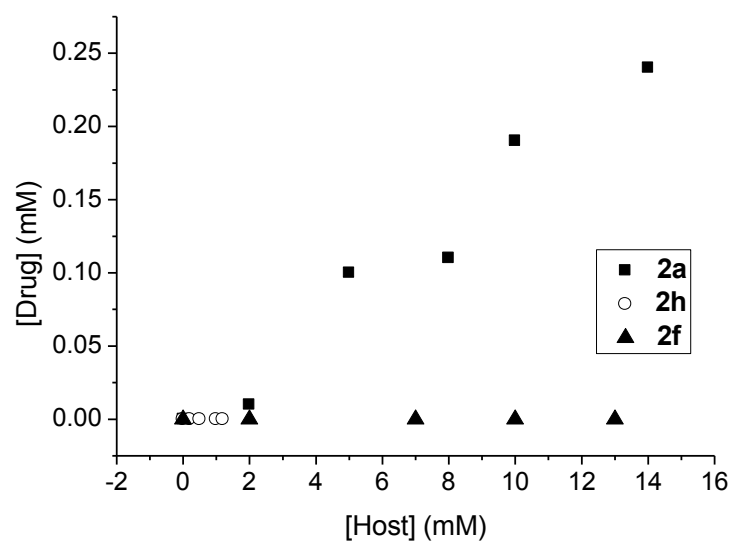


Figure S20. Phase diagram of mixtures of tamoxifen and host **2a**, **2f** and **2h**, in 20 mM sodium phosphate buffer (pH = 7.4).

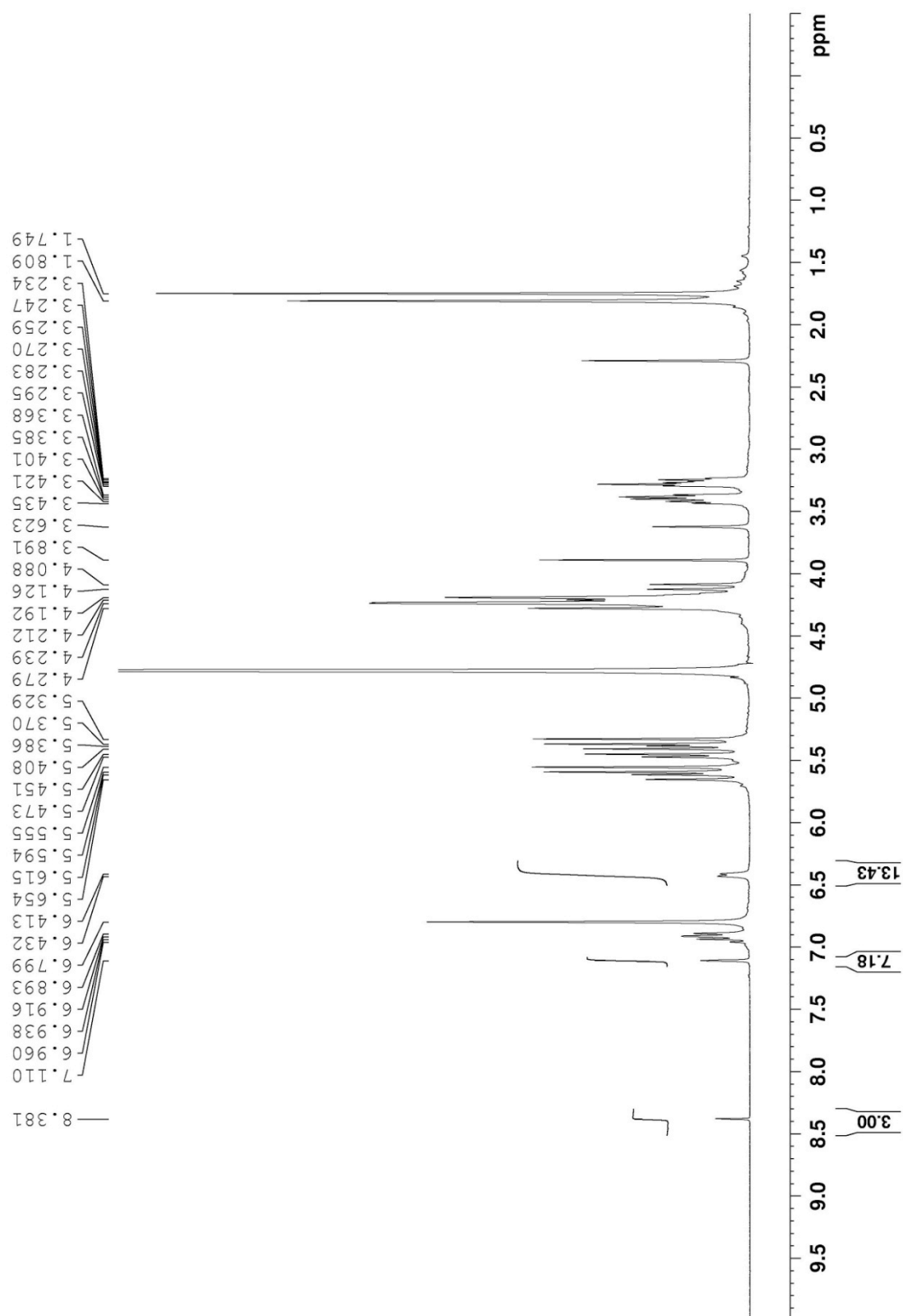


Figure S21. ^1H NMR recorded for pharmaceutical agent indomethacin with **2a** (16 mM) (400 MHz, 20 mM NaD_2PO_4 , pD = 7.4, RT, 1,3,5-benzenetricarboxylic acid as reference).

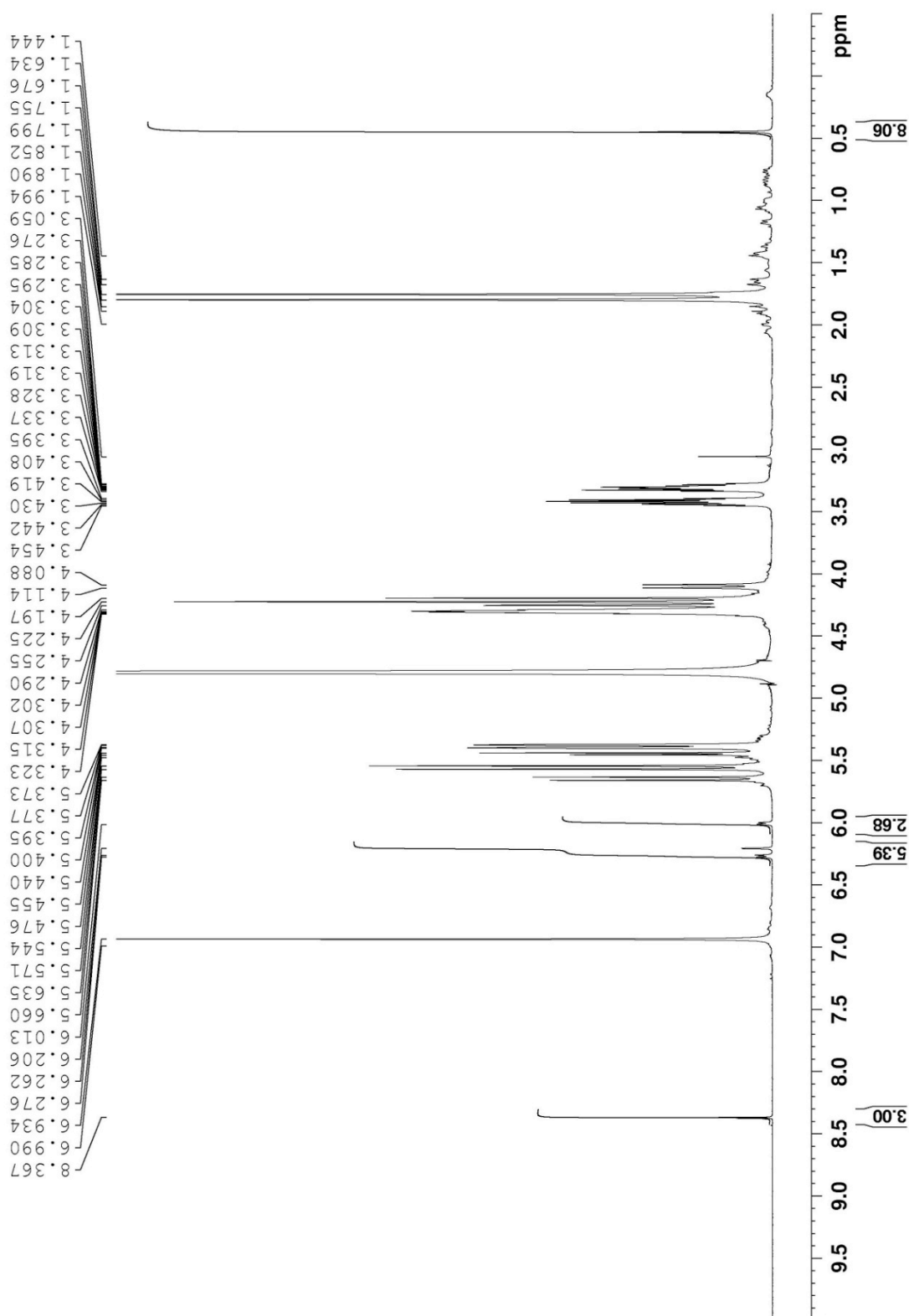


Figure S22. ^1H NMR recorded for pharmaceutical agent 17α -ethynylestradiol with **2a** (13 mM) (400 MHz, 20 mM NaD_2PO_4 , pD = 7.4, RT, 1,3,5-benzenetricarboxylic acid as reference).

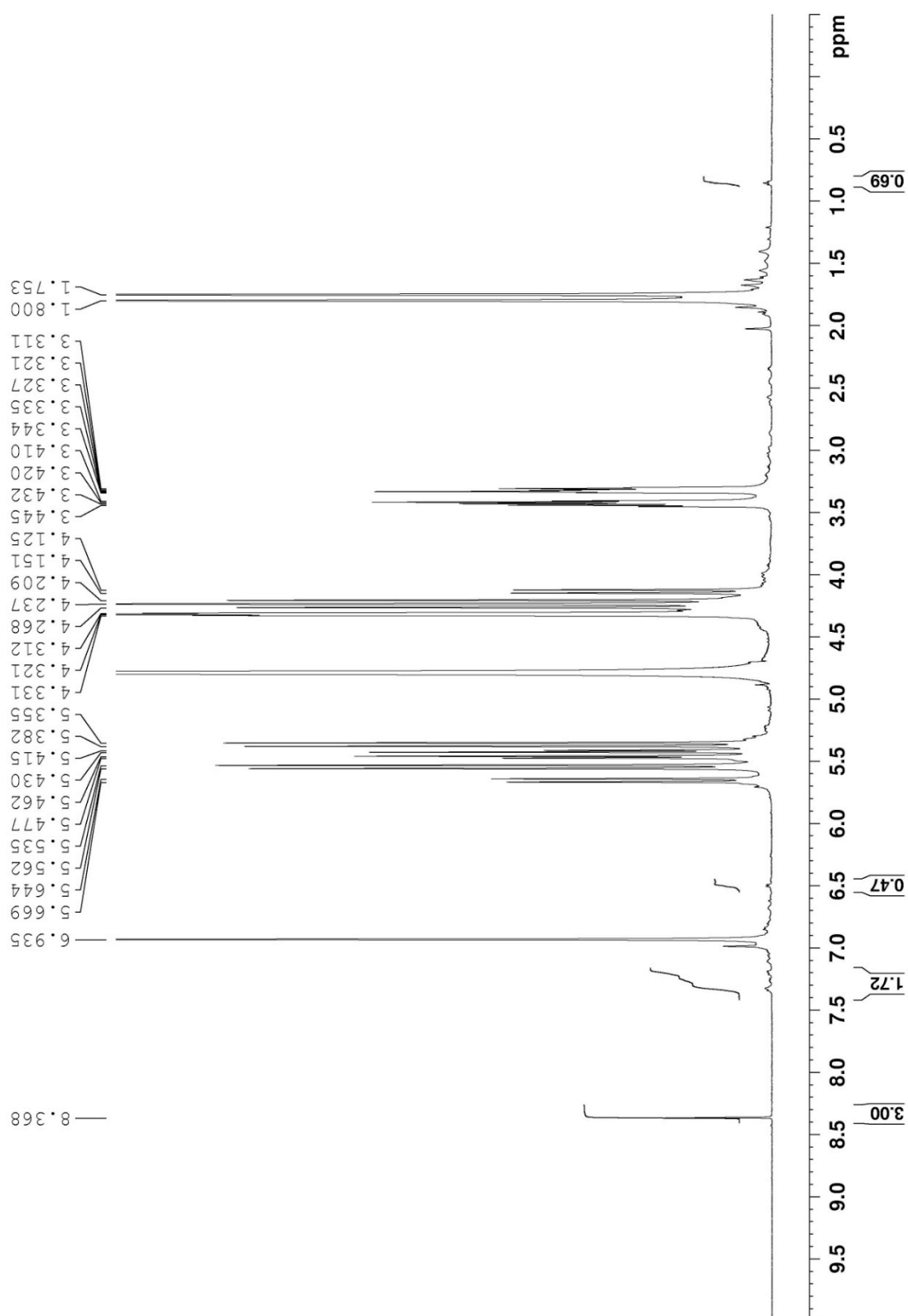


Figure S23 ¹H NMR recorded for pharmaceutical agent tamoxifen with **2a** (14 mM) (400 MHz, 20 mM NaD₂PO₄, pD = 7.4, RT, 1,3,5-benzenetricarboxylic acid as reference).

Determination of K_a Between Host 2a – 2h and Various Compounds. In this work, ^1H NMR and UV/Vis spectroscopic methods were used in order to determine the K_a values for various host•guest complexes. ^1H NMR spectroscopic method can measure K_a values up to 10^4 M^{-1} but for measurements of higher binding constants we need to use UV/Vis titration. The K_a value of hosts **2a – 2c** with dye **4** was obtained from direct UV/Vis titrations of fixed concentration of the dye by fitting the change of absorbance *versus* the concentration of host to a 1:1 binding model. Then dye **4** was used as an indicator in the displacement assays to measure the binding constants of host **2a – 2c** towards guest **5a**, **5b** and guest **6** by fitting the change of absorbance *versus* the concentration of guest to a competitive binding model. Similarly, the binding constant between host **2h** and dye **8** was determined by direct UV/Vis titration and K_a values between host **2h** and guest **6** was determined by indicator displacement assays with dye **8** as the indicator. Binding constants of **2a**, **2h** and **2f** toward guest **5c**, **2b** toward **5b**, and **2h** toward **5a** and **5b** are determined by direct ^1H NMR titration and the chemical shift change versus the change of concentration was fitted to a 1:1 binding model to give K_a values. The binding constant between **2f** and **5c** was also determined by ^1H NMR methods. The host•guest complex has a slow exchange on ^1H NMR, and the concentrations of free host, free guest, binding host, binding guest can be determined by the ratio of the integrals of their own NMR signals. The concentration was then used to calculate the binding constant of **2f** towards guest **5c**

Binding Models Used to Determine Values of Ka with Micromath Scientist

1:1 Binding Model (NMR).

```
// Micromath Scientist Model File
// 1:1 Host:Guest binding model for NMR
//This model assumes the guest concentration is fixed and host concentration is varied
IndVars: ConcHostTot
DepVars: Deltaobs
Params: Ka, ConcGuestTot, Deltasat, Deltazero
Ka = ConcHostGuest/(ConcHostFree*ConcGuestFree)
ConcHostTot=ConcHostFree + ConcHostGuest
ConcGuestTot=ConcGuestFree + ConcHostGuest
Deltaobs = Deltazero + (Deltasat - Deltazero) * (ConcHostGuest/ConcGuestTot)
//Constraints
0 < ConcHostFree < ConcHostTot
0 < Ka
0 < ConcGuestFree < ConcGuestTot
0 < ConcHostGuest < ConcHostTot
```

1:1 Binding Model (UV/Vis).

```
// Micromath Scientist Model File
// 1:1 Host:Guest binding model
//This model assumes the guest concentration is fixed and host concentration is varied
IndVars: ConcHostTot
DepVars: SpectroscopicSignal
Params: Ka, ConcGuestTot, SpectroscopicSignalMin, SpectroscopicSignalMax
Ka = ConcHostGuest/(ConcHostFree*ConcGuestFree)
ConcHostTot=ConcHostFree + ConcHostGuest
ConcGuestTot=ConcGuestFree + ConcHostGuest
SpectroscopicSignal = SpectroscopicSignalMin + (SpectroscopicSignalMax -
SpectroscopicSignalMin) * (ConcHostGuest/ConcGuestTot)
//Constraints
0 < ConcHostFree < ConcHostTot
0 < Ka
0 < ConcGuestFree < ConcGuestTot
0 < ConcHostGuest < ConcHostTot
```

Competitive Binding (Indicator Displacement) Model.

```
// MicroMath Scientist Model File
IndVars: ConcAntot
DepVars: Absorb
Params: ConcHtot, ConcGtot, Khg, Kha, AbsorbMax, AbsorbMin
Khg = ConcHG / (ConcH * ConcG)
Kha = ConcHAn / (ConcH * ConcAn)
```

$$\text{Absorb} = \text{AbsorbMin} + (\text{AbsorbMax} - \text{AbsorbMin}) * (\text{ConcHG} / \text{ConcGtot})$$

$$\text{ConcHtot} = \text{ConcH} + \text{ConcHG} + \text{ConcHAn}$$

$$\text{ConcGtot} = \text{ConcHG} + \text{ConcG}$$

$$\text{ConcAntot} = \text{ConcAn} + \text{ConcHAn}$$

$$0 < \text{ConcHG} < \text{ConcHtot}$$

$$0 < \text{ConcH} < \text{ConcHtot}$$

$$0 < \text{ConcG} < \text{ConcGtot}$$

$$0 < \text{ConcAn} < \text{ConcAntot}$$

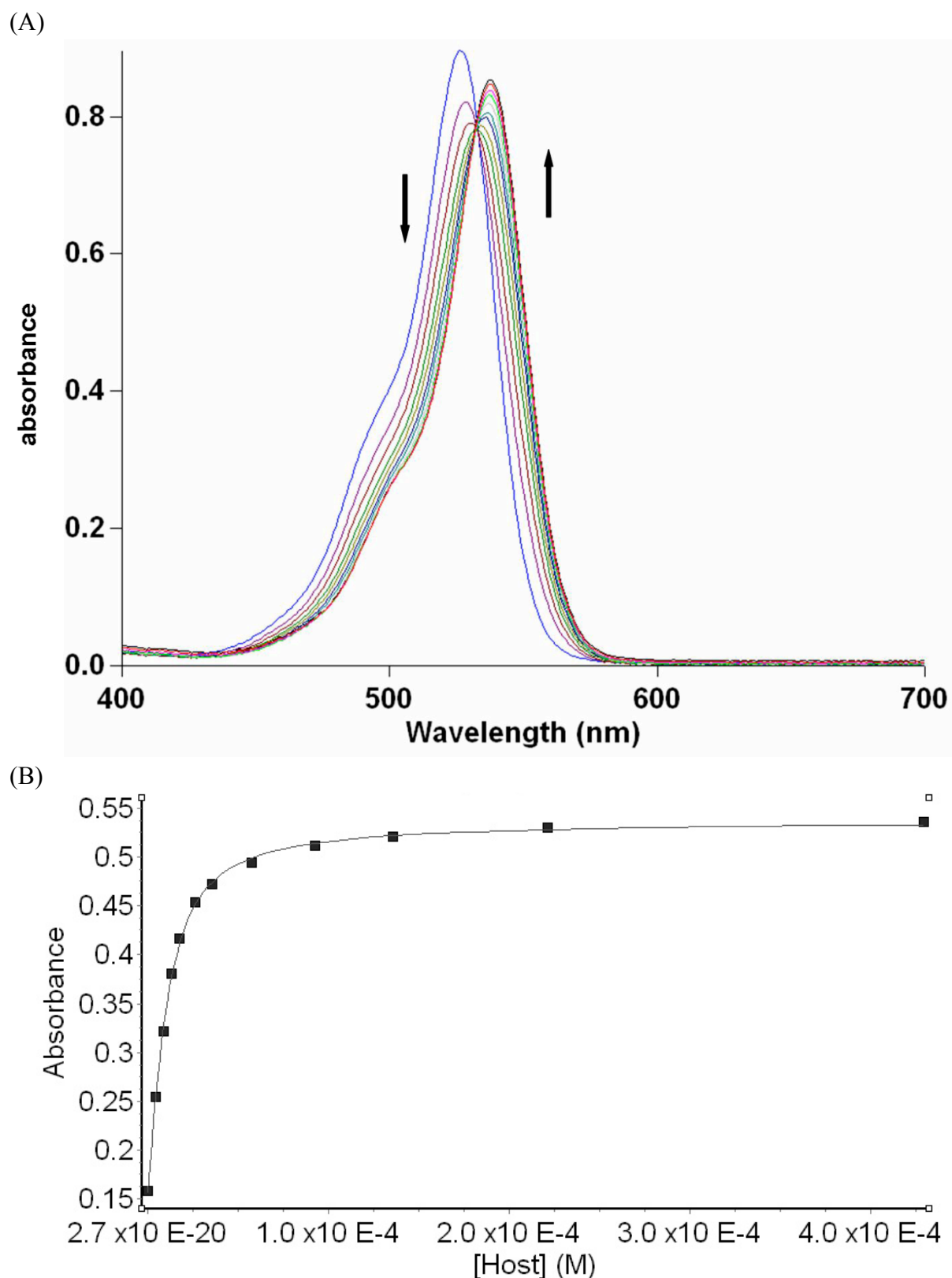


Figure S24. (A) UV/Vis spectra from the titration of dye **4** (10.0 μM) with **2a** (0 – 480 μM) in 20 mM NaH_2PO_4 buffer (pH 7.4); (B) plot of the ΔA_{550} as a function of **2a** concentration. The solid line represents the best non-linear fit of the data to a 1:1 binding model ($K_a = 1.83 (\pm 0.08) \times 10^5 \text{ M}^{-1}$).

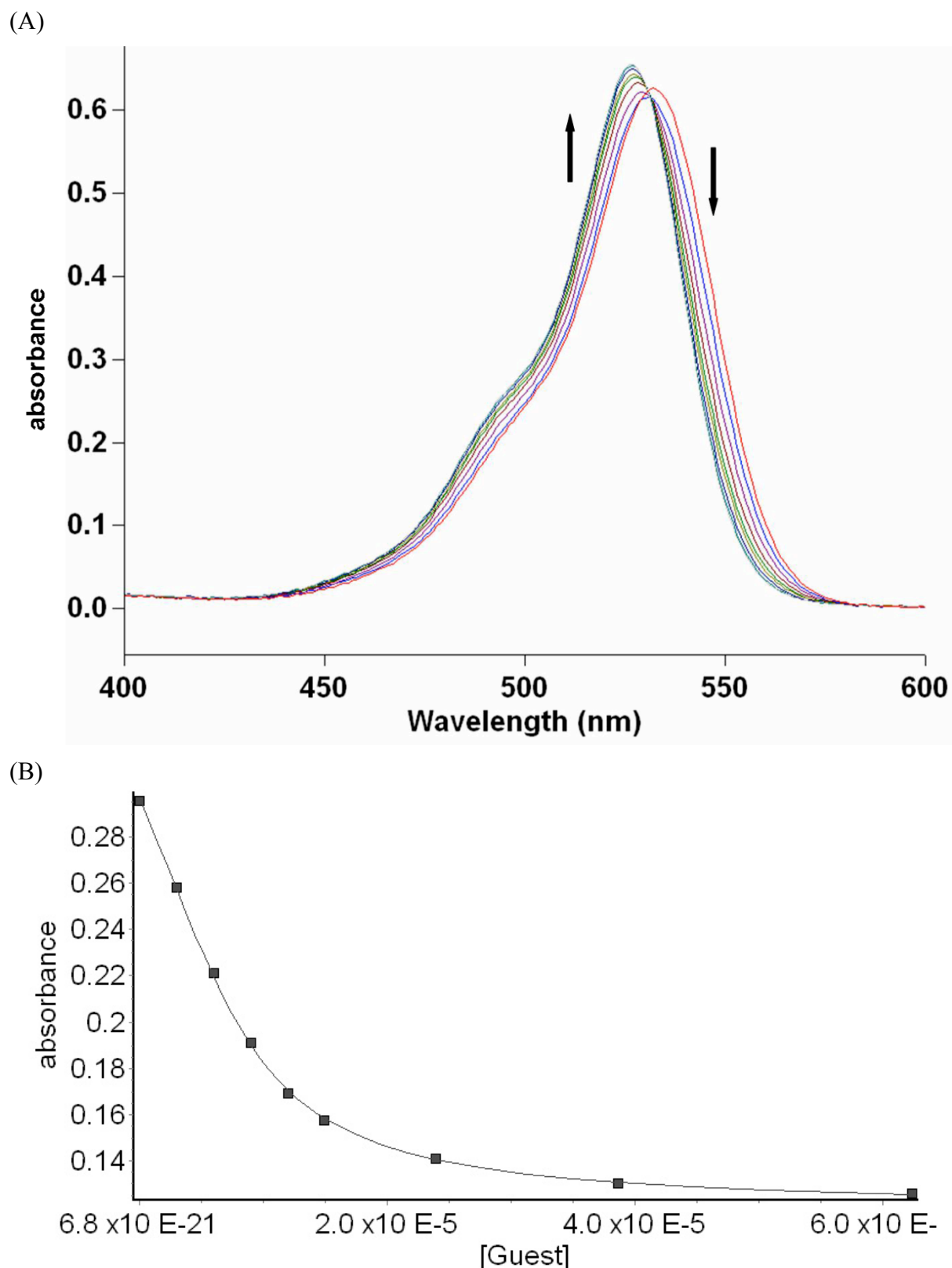


Figure S25. (A) Displacement titration of a solution of dye **4** (10.0 μM) and host **2a** (9.15 μM) solution with **5a** (0 – 65 μM) (20 mM NaH_2PO_4 buffer, pH 7.4). (B) Non-linear fitting plot of absorbance *versus* concentration for the displacement titration of **5a** using a model implemented in ScientistTM. K_a was evaluated as $1.68 (\pm 0.09) \times 10^6 \text{ M}^{-1}$.

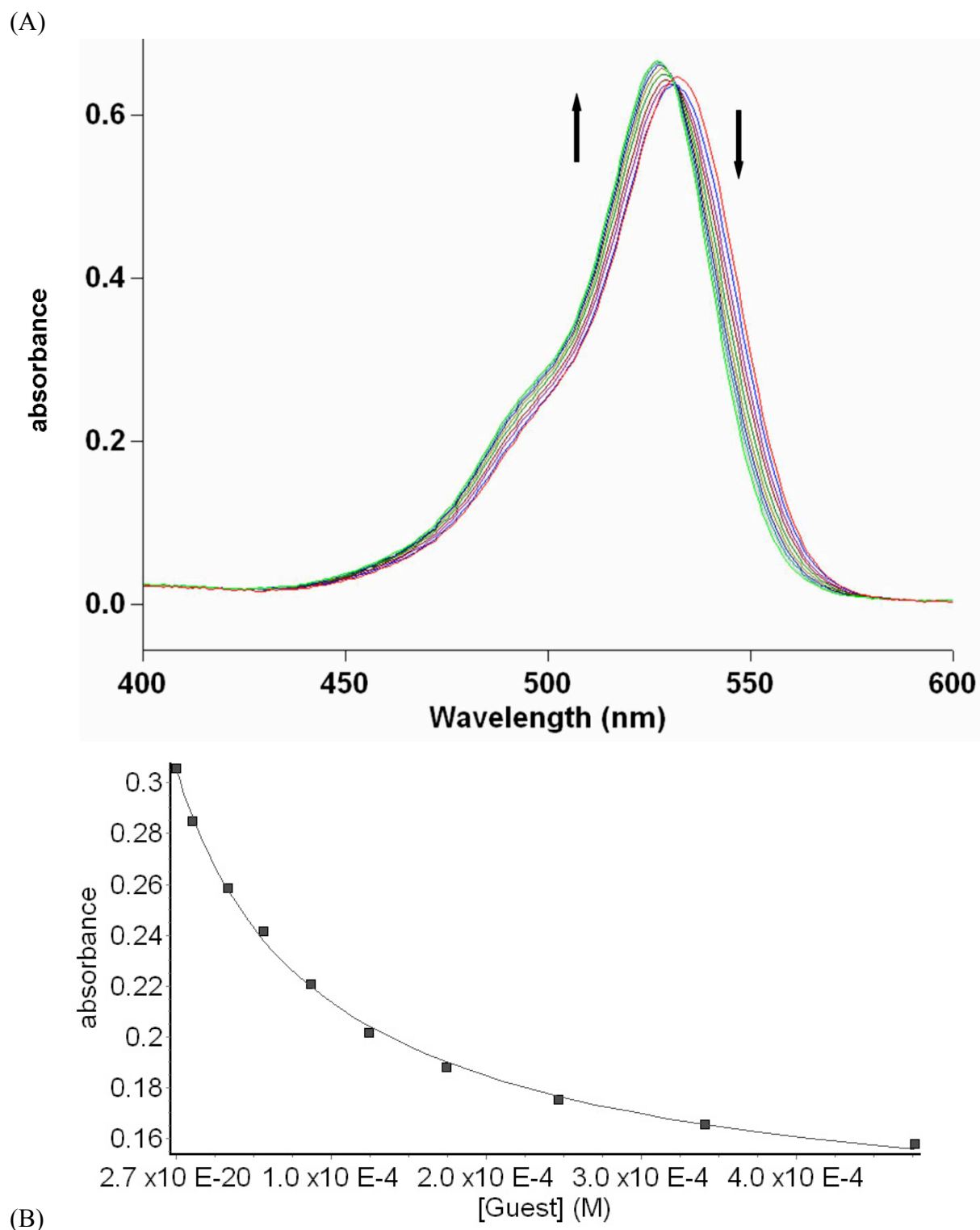
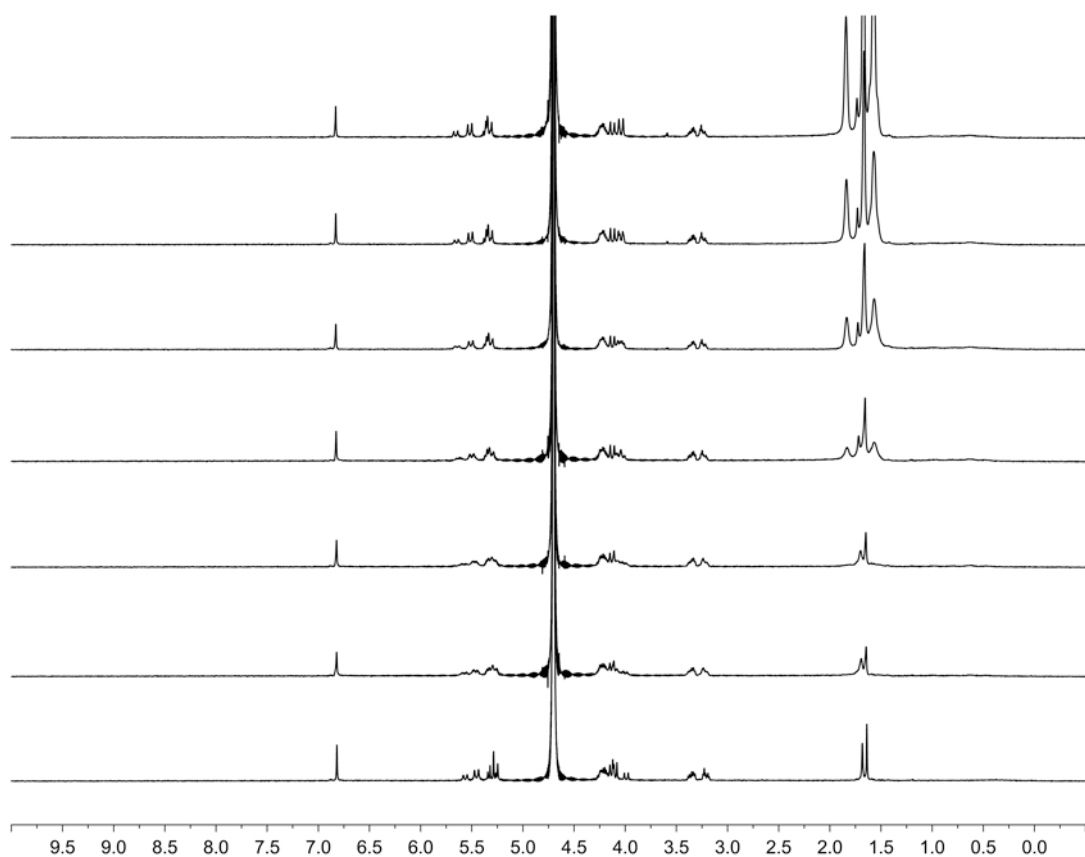


Figure S26. (A) Displacement titration of a solution of dye **4** (10.0 μM) and host **2a** (9.15 μM) solution with **5b** (0 – 480 μM) (20 mM NaH_2PO_4 buffer, pH 7.4). (B) Non-linear fitting plot of absorbance *versus* concentration for the displacement titration of **5b** using a model implemented in ScientistTM. K_a was evaluated as $4.47 (\pm 0.34) \times 10^4 \text{ M}^{-1}$.

(A)



(B)

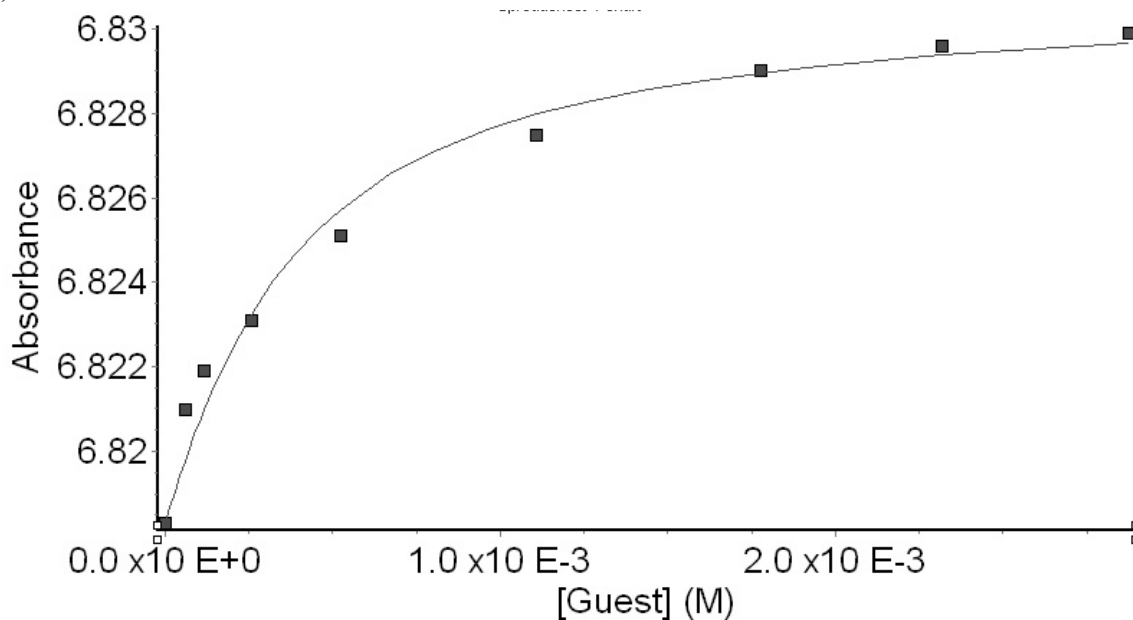


Figure S27. (A) ^1H NMR spectra (400 MHz, 20 mM sodium phosphate buffer, pD = 7.4) recorded for a solution of **2a** (181 μM) and **5c** of variable concentrations (0 – 3.1 mM). (B) Plot of the chemical shift of **2a** as a function of **5c** concentration. The solid line represents the best non-linear fitting of the data to a 1:1 binding model ($K_a = 3.50 (\pm 0.83) \times 10^3 \text{ M}^{-1}$).

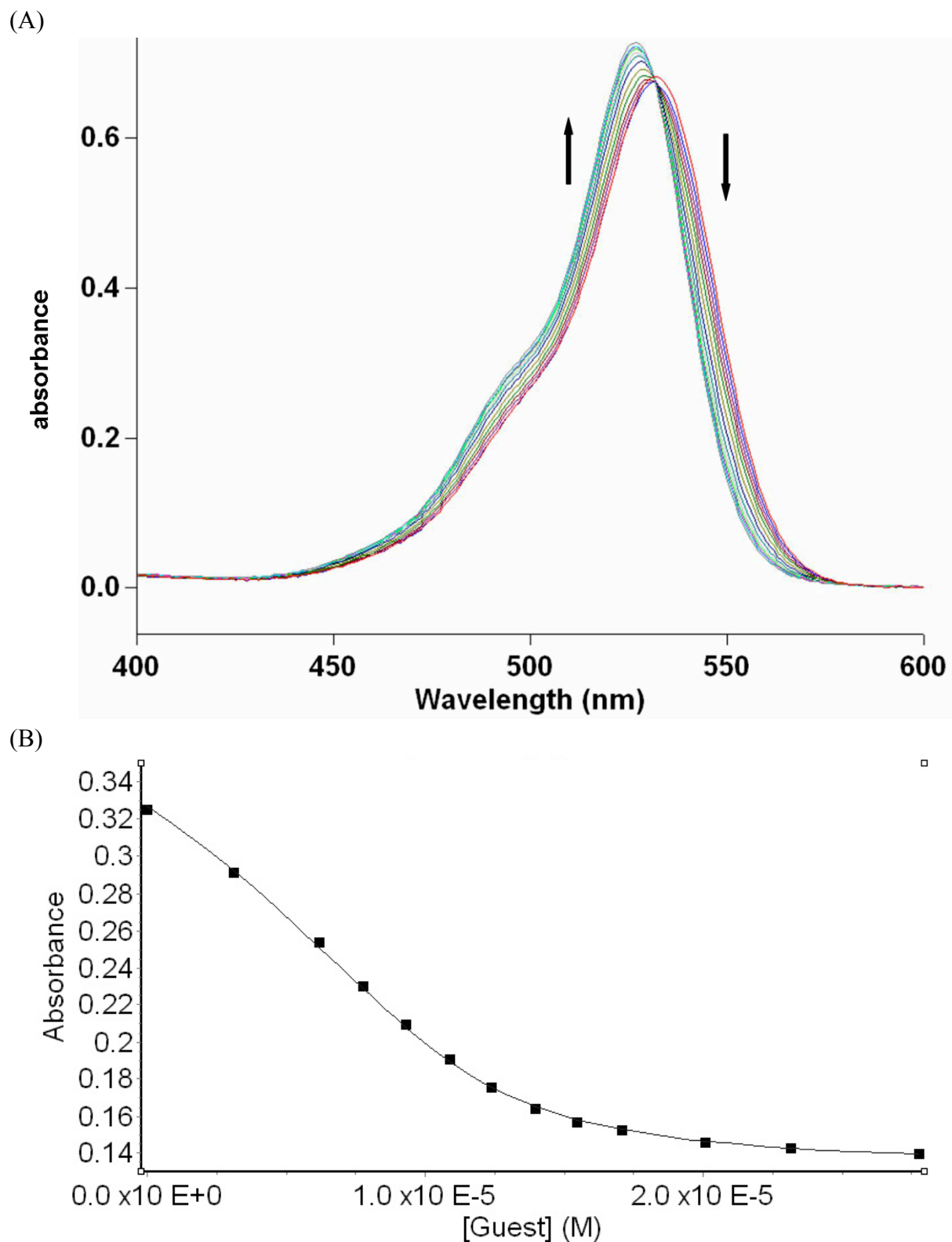


Figure S28. (A) Displacement titration of a solution of dye **4** (10.0 μM) and host **2a** (9.15 μM) solution with **6** (0 – 32 μM) (20 mM NaH_2PO_4 buffer, pH 7.4). (B) Non-linear fitting plot of absorbance *versus* concentration for the displacement titration of **6** using a model implemented in ScientistTM. K_a was evaluated as $4.59 (\pm 0.44) \times 10^6 \text{ M}^{-1}$.

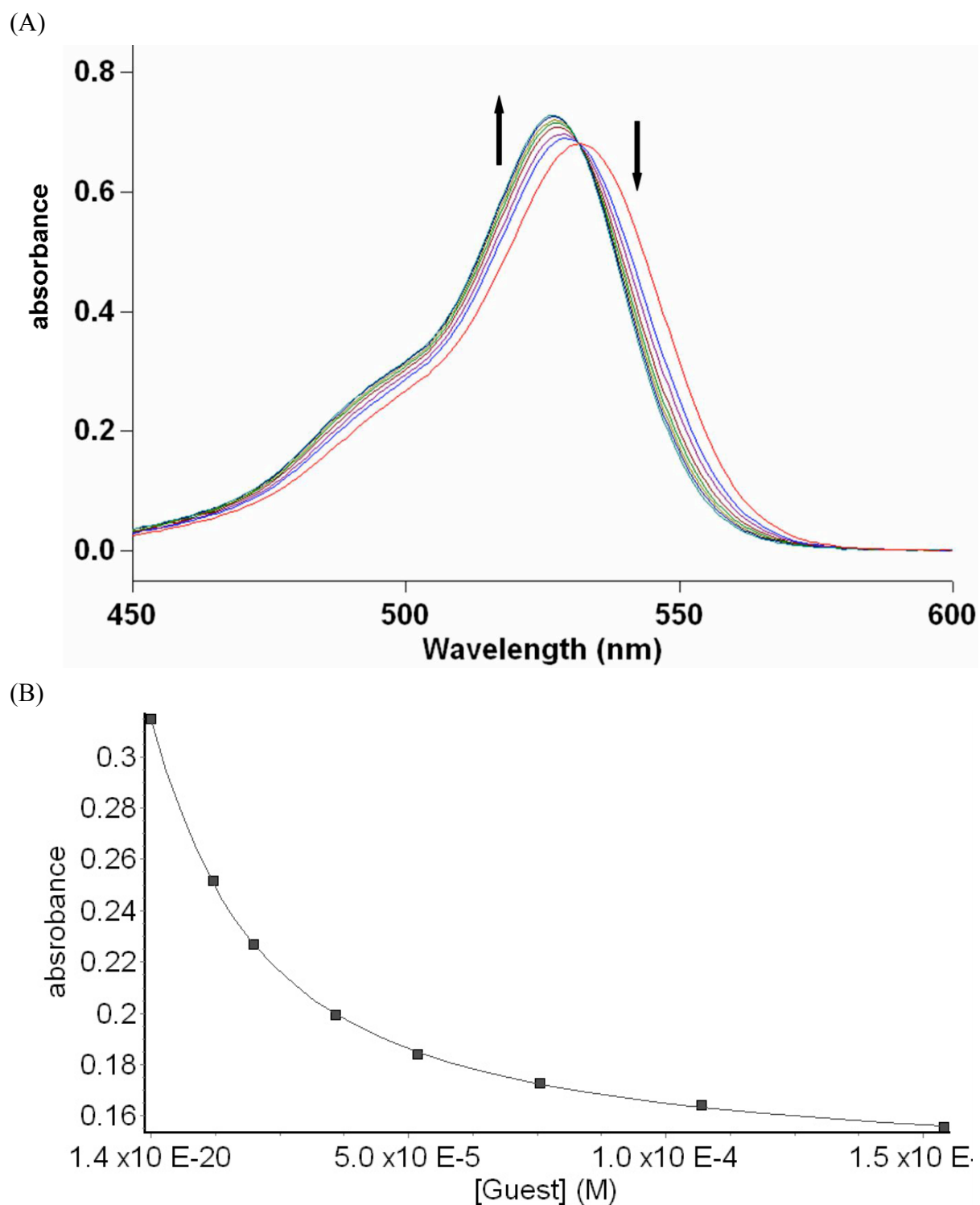


Figure S29. (A) Displacement titration of a solution of dye **4** (10.0 μM) and host **2a** (9.15 μM) solution with **7** (0 – 32 μM) (20 mM NaH_2PO_4 buffer, pH 7.4). (B) Non-linear fitting plot of absorbance *versus* concentration for the displacement titration of **7** using a model implemented in ScientistTM. K_a was evaluated as $2.74 (\pm 0.06) \times 10^5 \text{ M}^{-1}$.

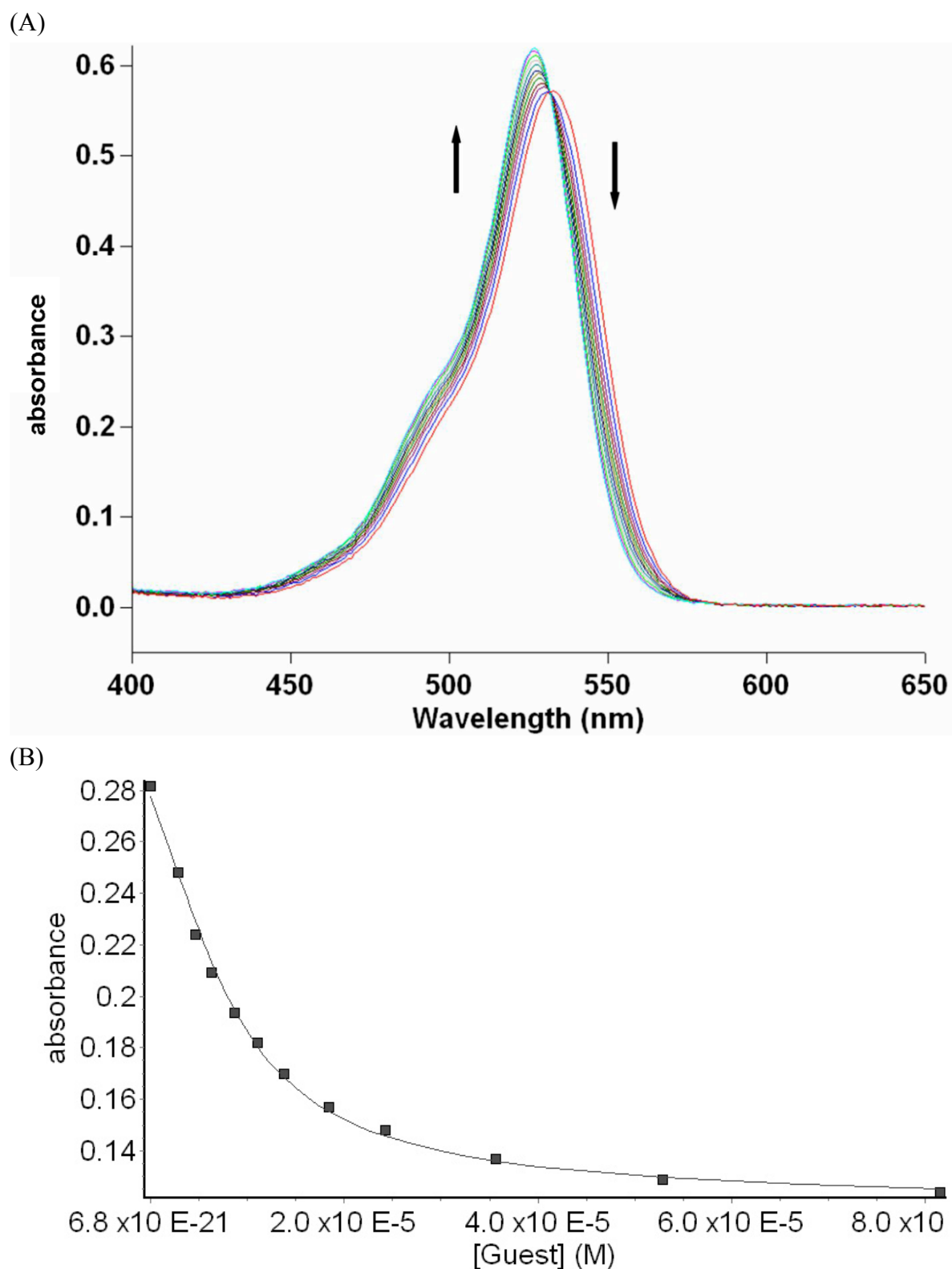


Figure S30. (A) Displacement titration of a solution of dye **4** (10.0 μM) and host **2b** (9.18 μM) solution with **5a** (0 – 32 μM) (20 mM NaH_2PO_4 buffer, pH 7.4). (B) Non-linear fitting plot of absorbance *versus* concentration for the displacement titration of **5a** using a model implemented in ScientistTM. K_a was evaluated as $1.78 (\pm 0.21) \times 10^6 \text{ M}^{-1}$.

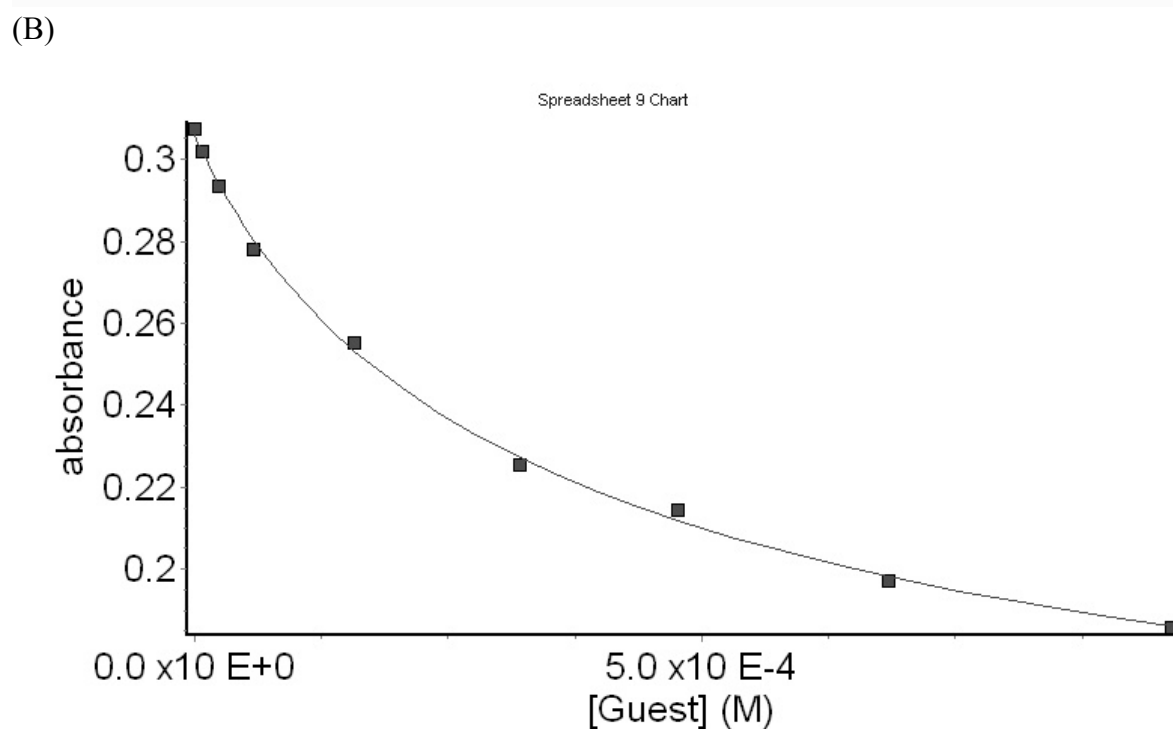
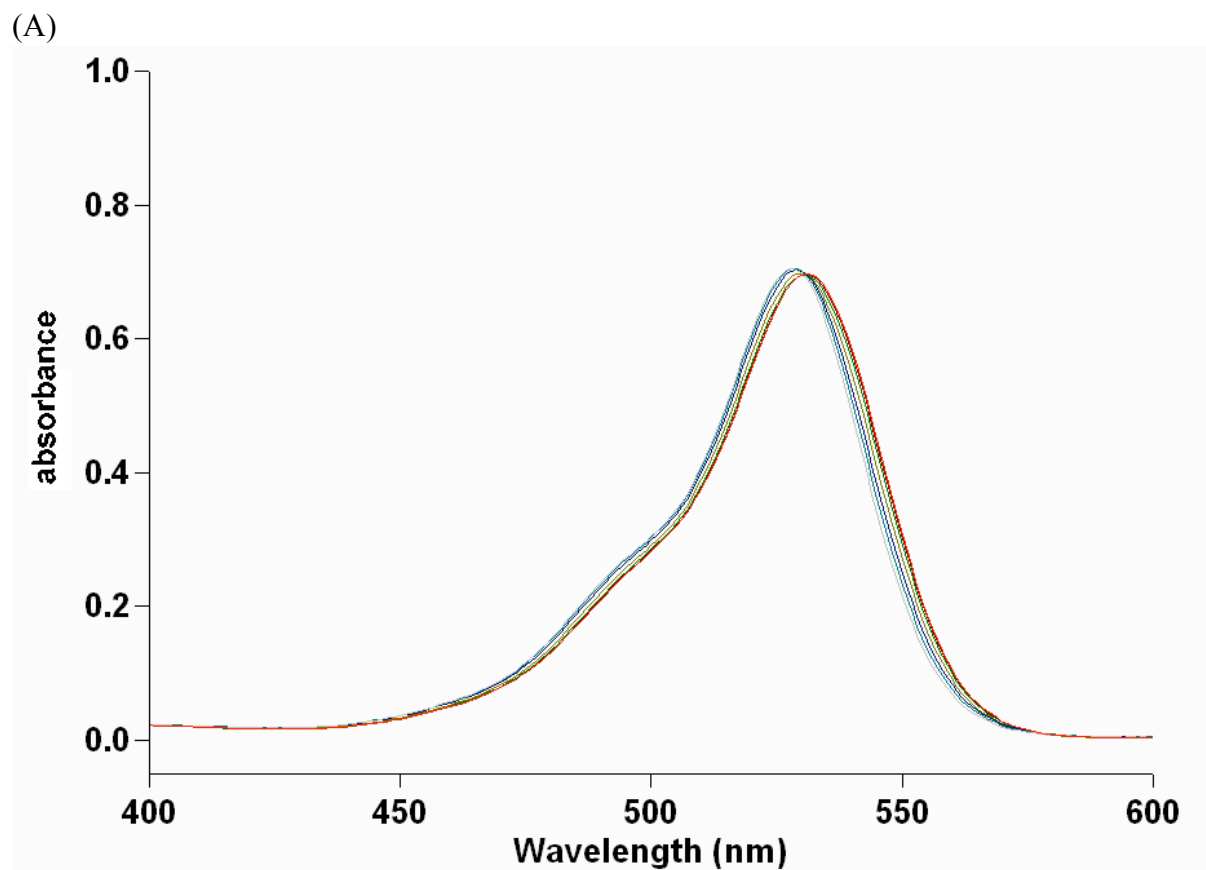
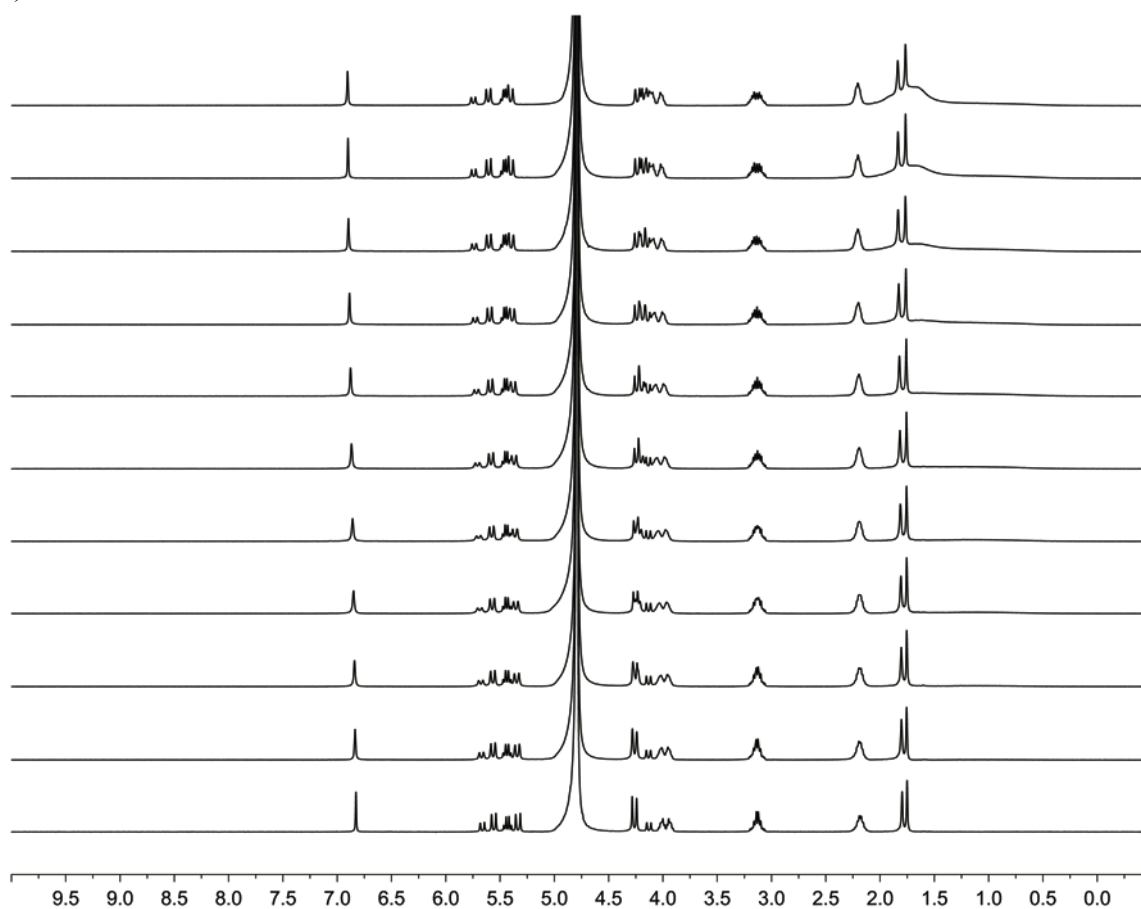


Figure S31. (A) Displacement titration of a solution of dye **4** (10.0 μM) and host **2b** (9.15 μM) solution with **5b** (0 – 32 μM) (20 mM NaH_2PO_4 buffer, pH 7.4). (B) Non-linear fitting plot of absorbance *versus* concentration for the displacement titration of **5b** using a model implemented in ScientistTM. K_a was evaluated as $1.67 (\pm 0.18) \times 10^3 \text{ M}^{-1}$

(A)



(B)

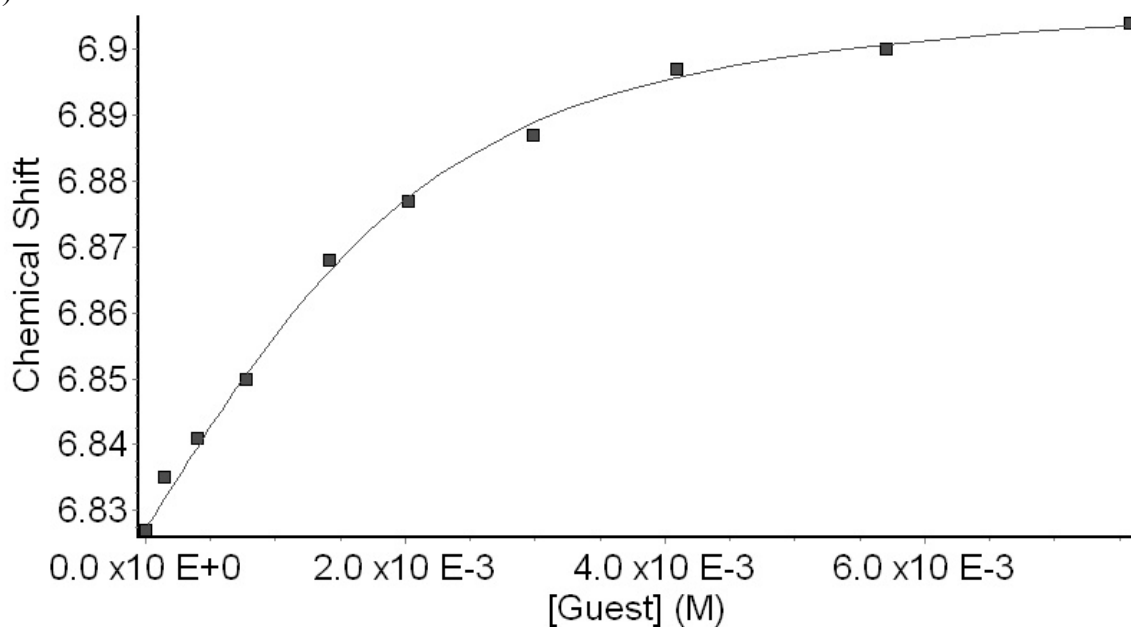


Figure S32. (A) ¹H NMR spectra (400 MHz, 20 mM sodium phosphate buffer, pD = 7.4) recorded for a solution of **2b** (2.0 mM) and **5c** of variable concentrations (0 – 8.0 mM). (B) Plot of the chemical shift of **2b** as a function of **5c** concentration. The solid line represents the best non-linear fitting of the data to a 1:1 binding model ($K_a = 1.87 (\pm 0.31) \times 10^3 \text{ M}^{-1}$).

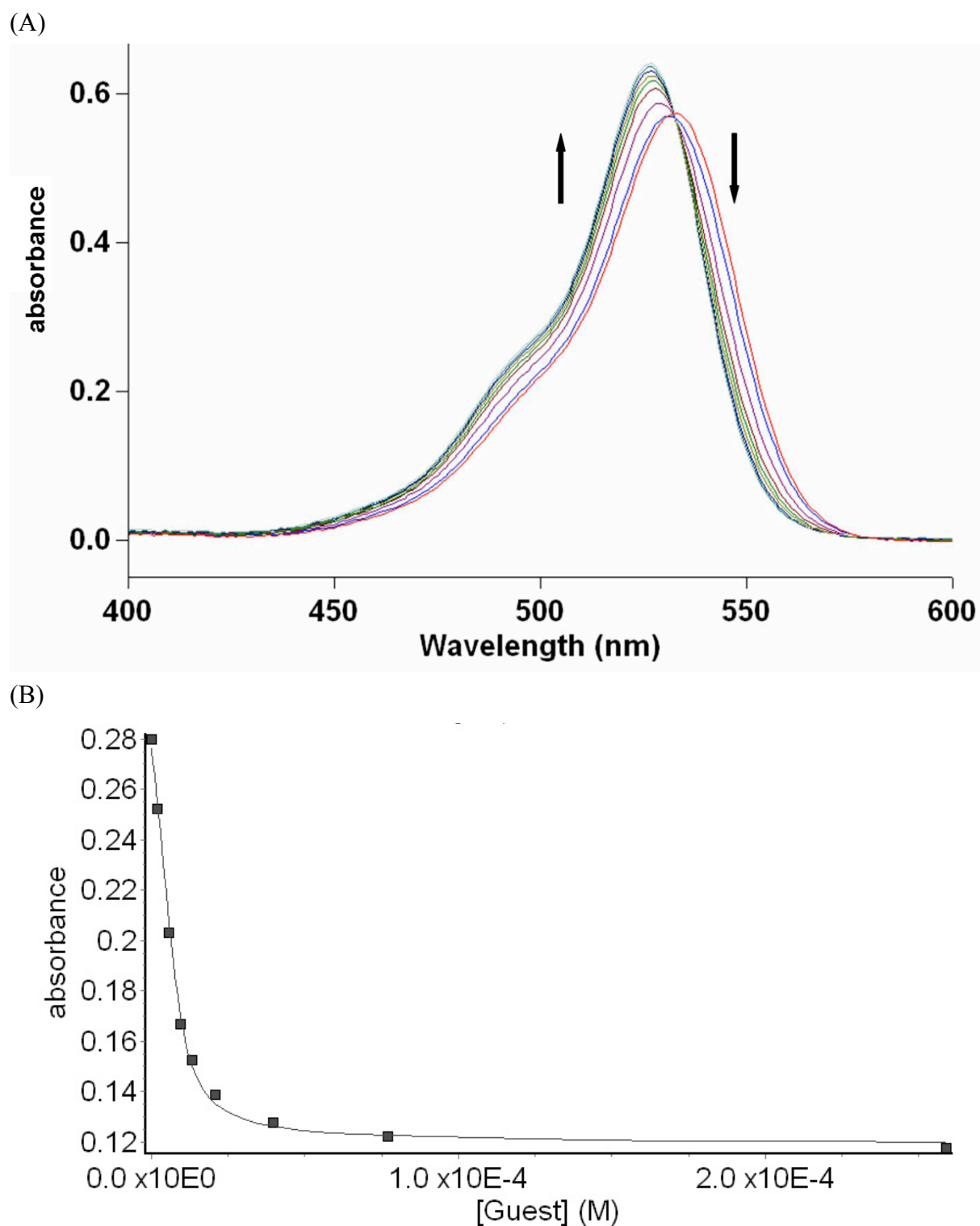


Figure S33. (A) Displacement titration of a solution of dye **4** (10.0 μM) and host **2b** (9.18 μM) solution with **6** (0 – 270 μM) (20 mM NaH₂PO₄ buffer, pH 7.4). (B) Non-linear fitting plot of absorbance *versus* concentration for the displacement titration of **6** using a model implemented in Scientist™. K_a was evaluated as $4.37 (\pm 0.46) \times 10^6 \text{ M}^{-1}$.

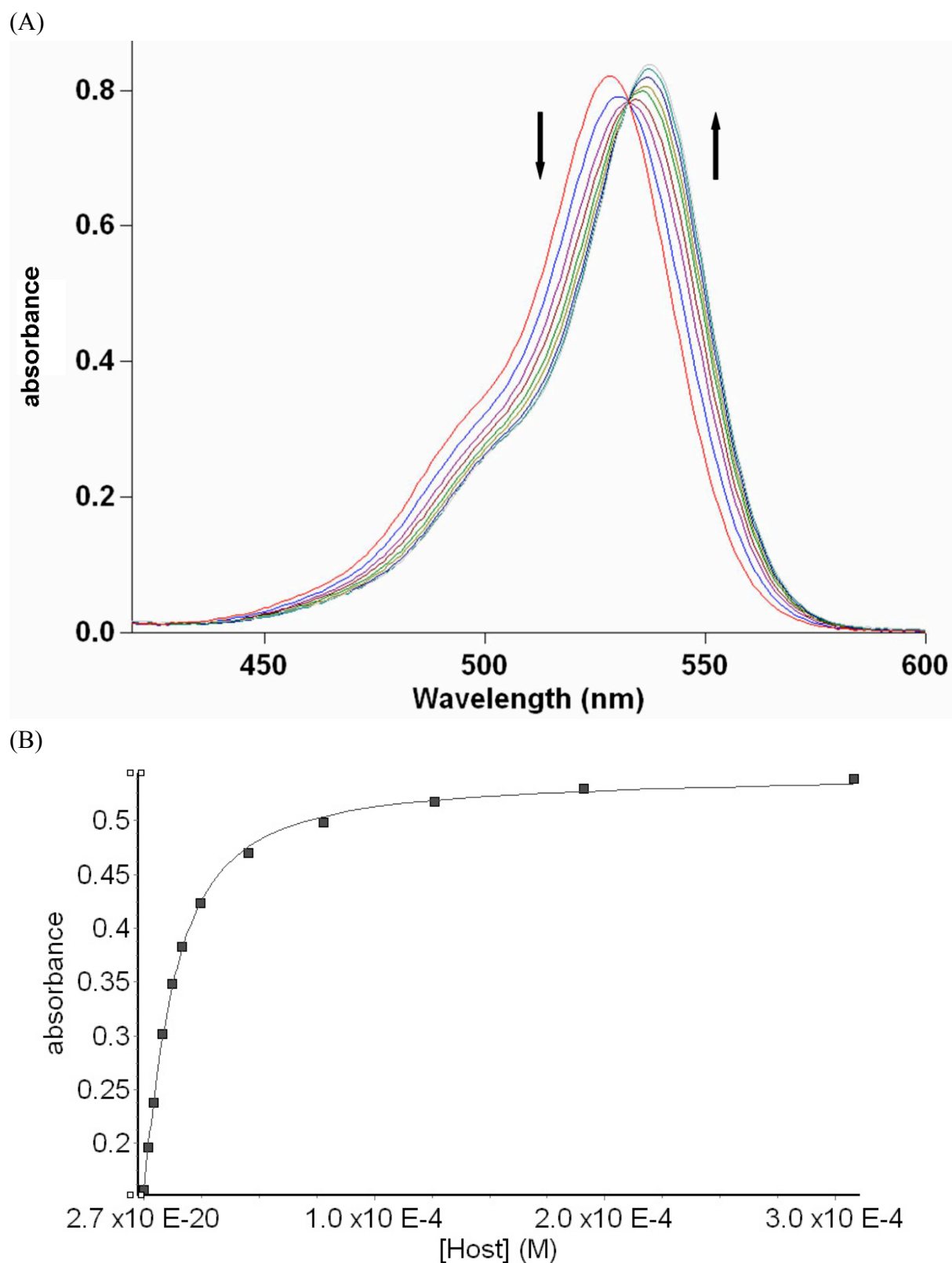


Figure S34. (A) UV/Vis spectra from the titration of dye **4** (10.0 μM) with **2c** (0 – 400 μM) in 20 mM NaH_2PO_4 buffer (pH 7.4); (B) plot of the ΔA_{550} as a function of **2c** concentration. The solid line represents the best non-linear fit of the data to a 1:1 binding model ($K_a = 1.29 (\pm 0.05) \times 10^5 \text{ M}^{-1}$).

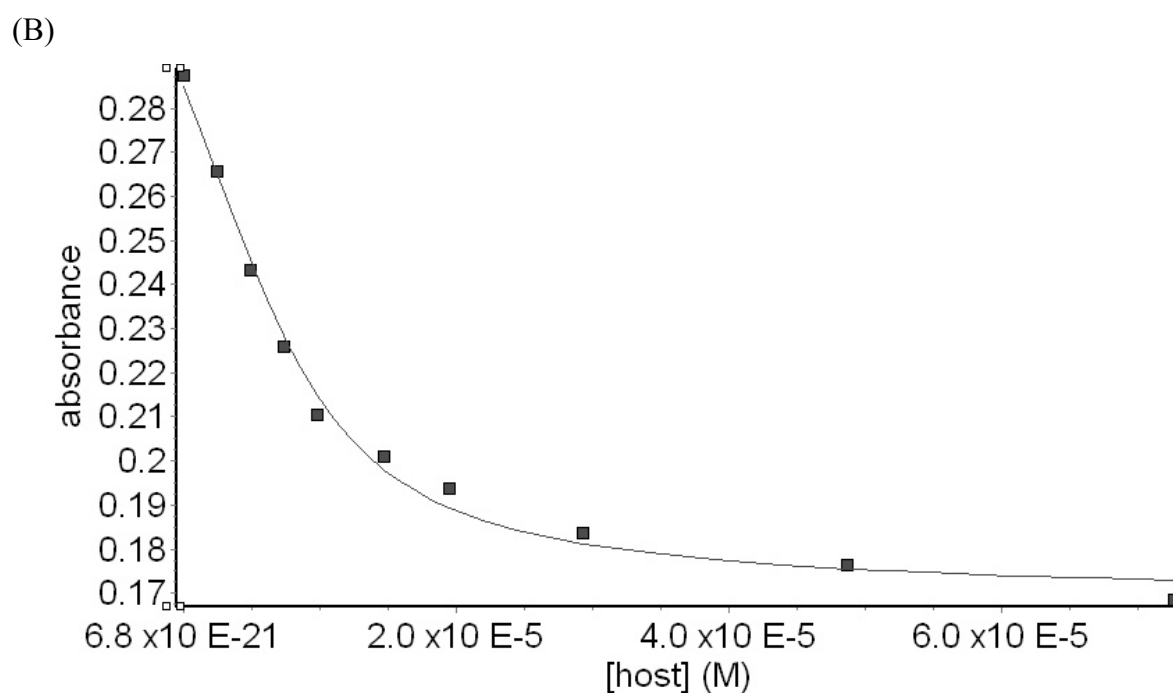
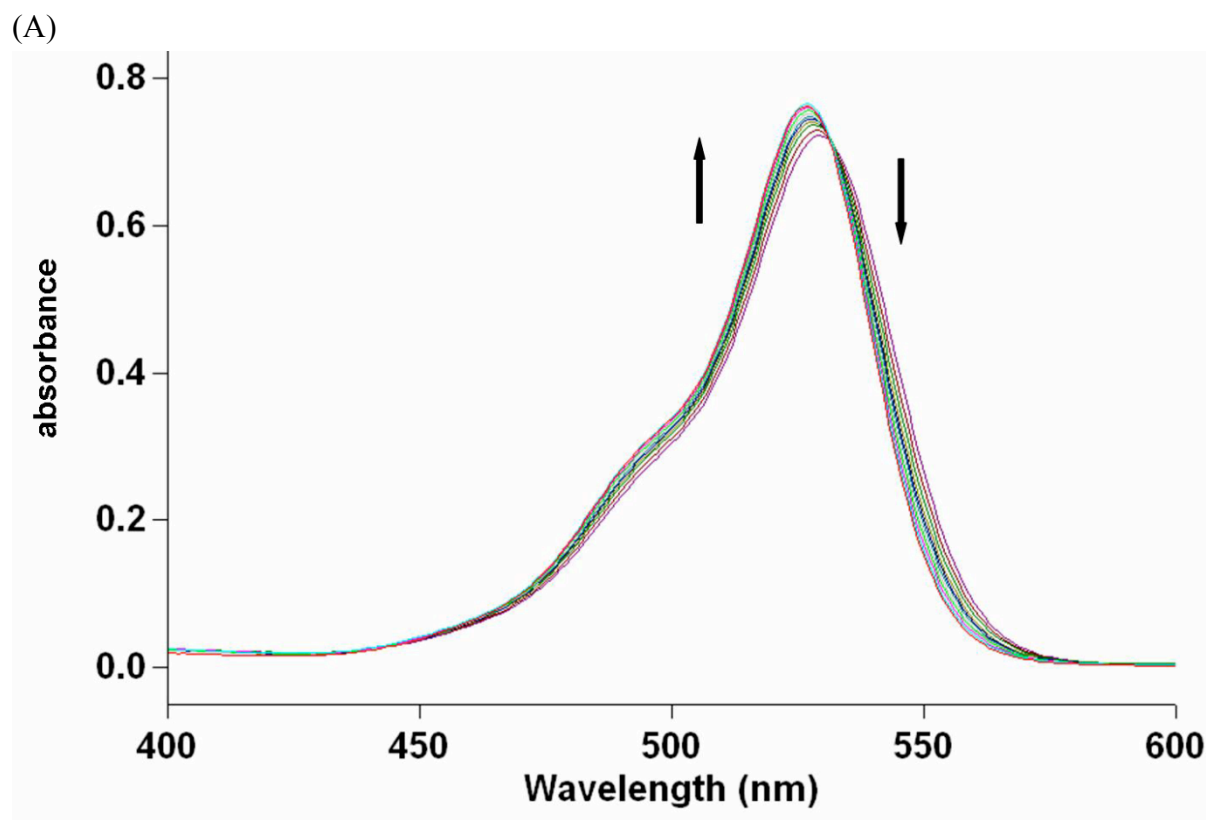


Figure S35. (A) Displacement titration of a solution of dye **4** (10.0 μM) and host **2c** (9.19 μM) solution with **6** (0 – 74 μM) (20 mM NaH_2PO_4 buffer, pH 7.4). (B) Non-linear fitting plot of absorbance *versus* concentration for the displacement titration of **6** using a model implemented in ScientistTM. K_a was evaluated as $1.12 (\pm 0.24) \times 10^6 \text{ M}^{-1}$.

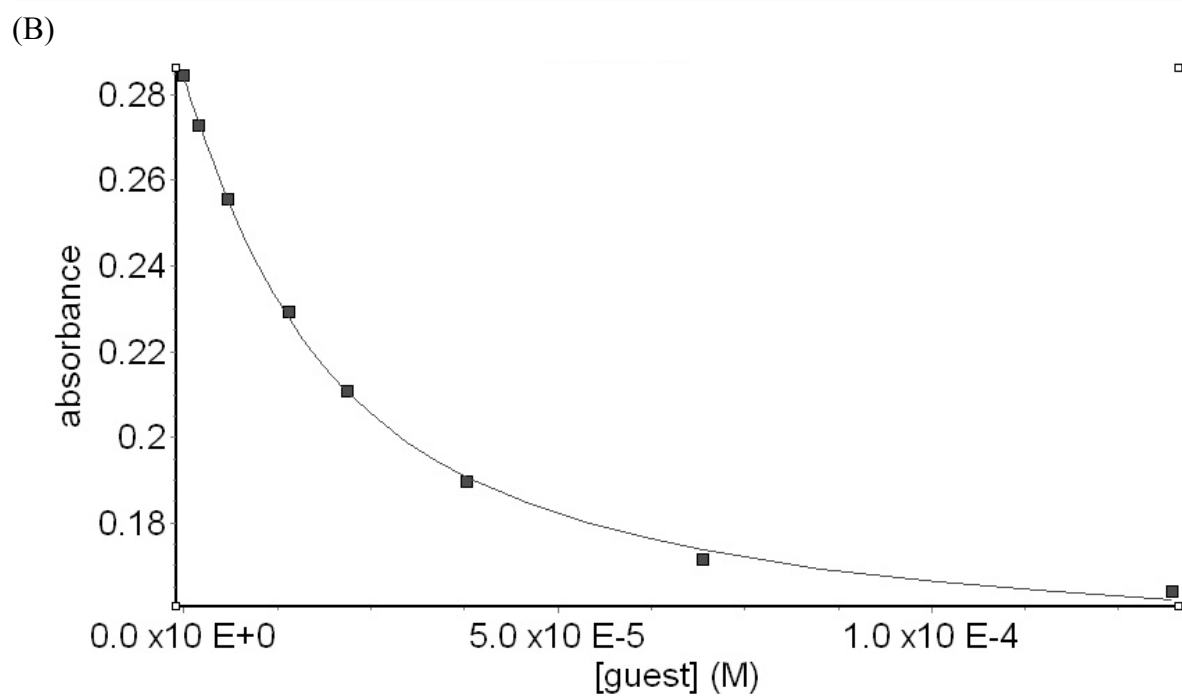
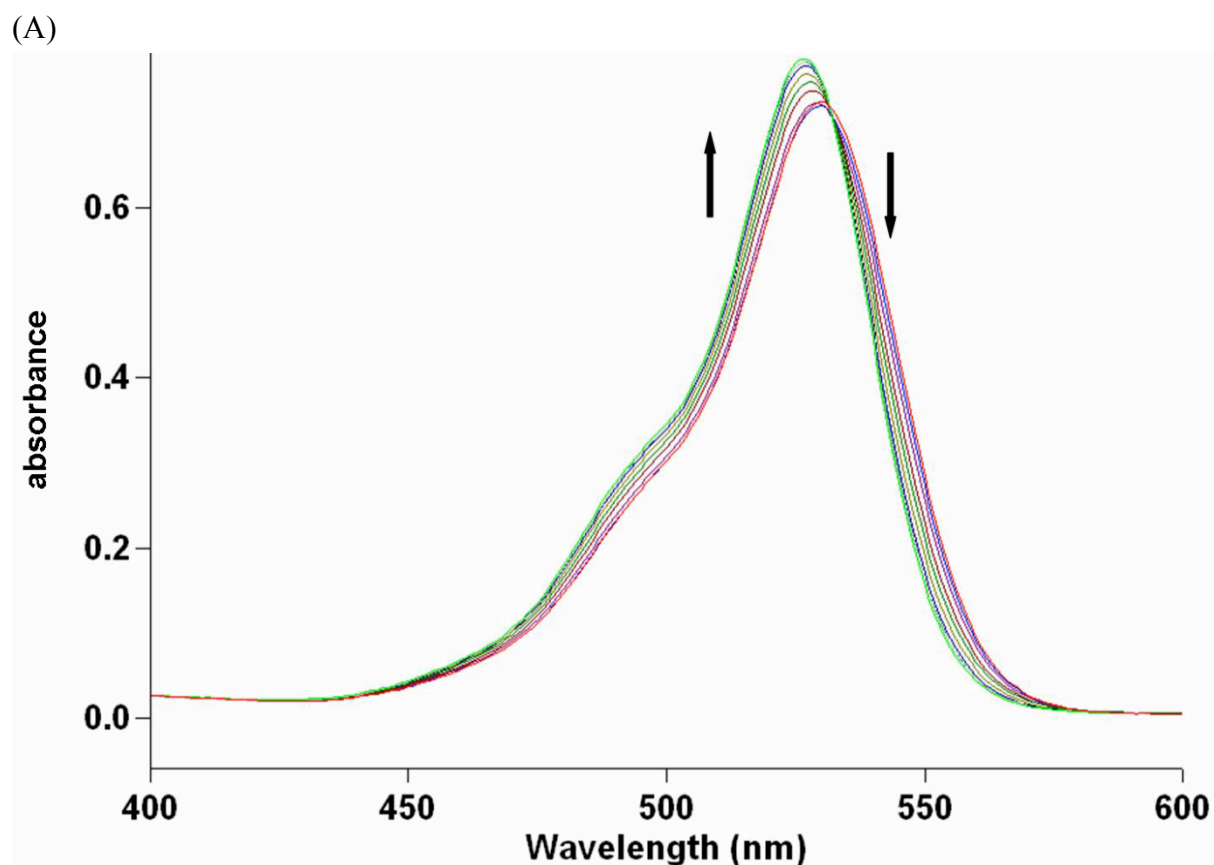


Figure S36. (A) Displacement titration of a solution of dye **4** (10.0 μM) and host **2c** (9.19 μM) solution with **5a** (0 – 130 μM) (20 mM NaH_2PO_4 buffer, pH 7.4). (B) Non-linear fitting plot of absorbance *versus* concentration for the displacement titration of **5a** using a model implemented in ScientistTM. K_a was evaluated as $1.94 (\pm 0.18) \times 10^5 \text{ M}^{-1}$.

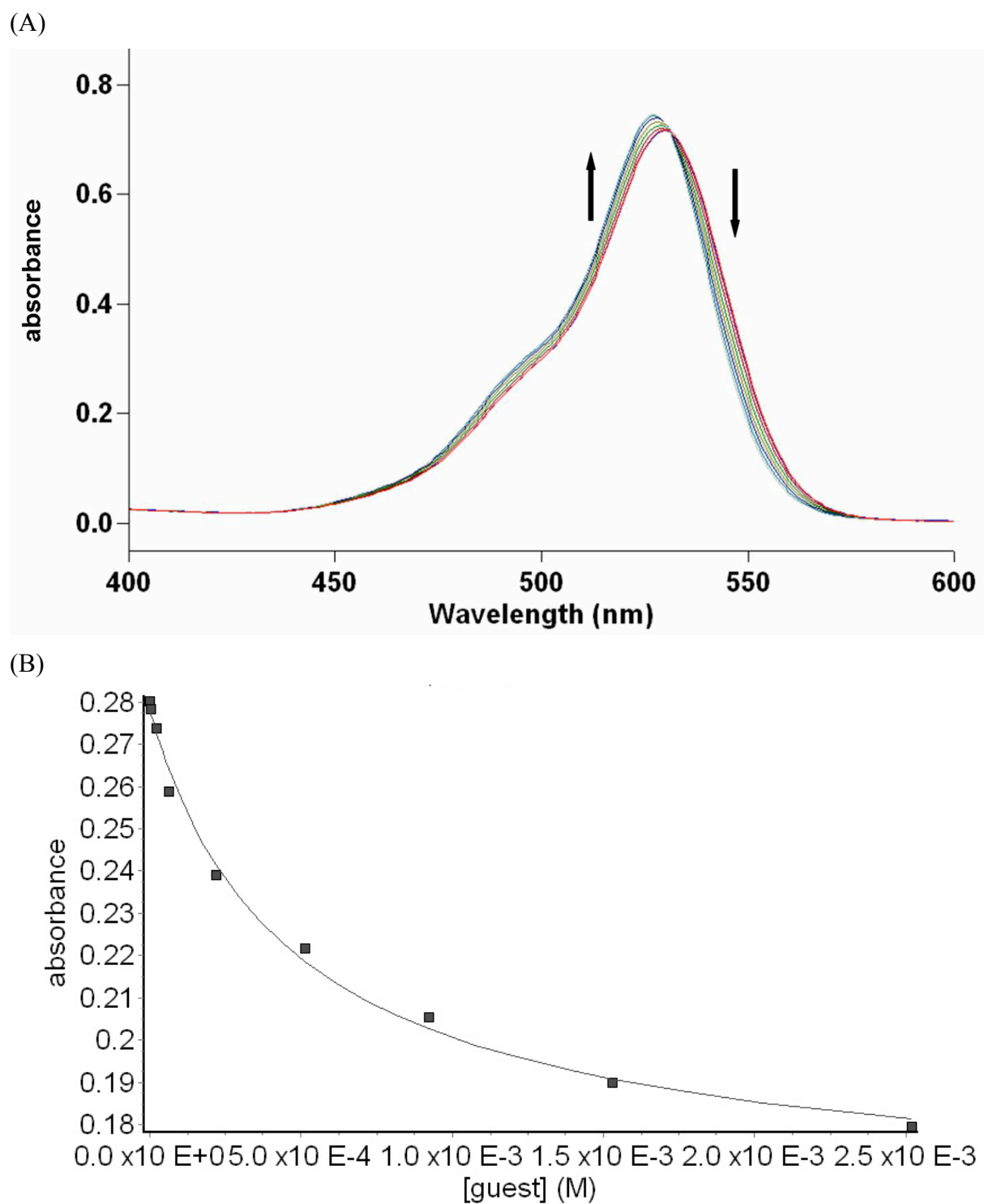
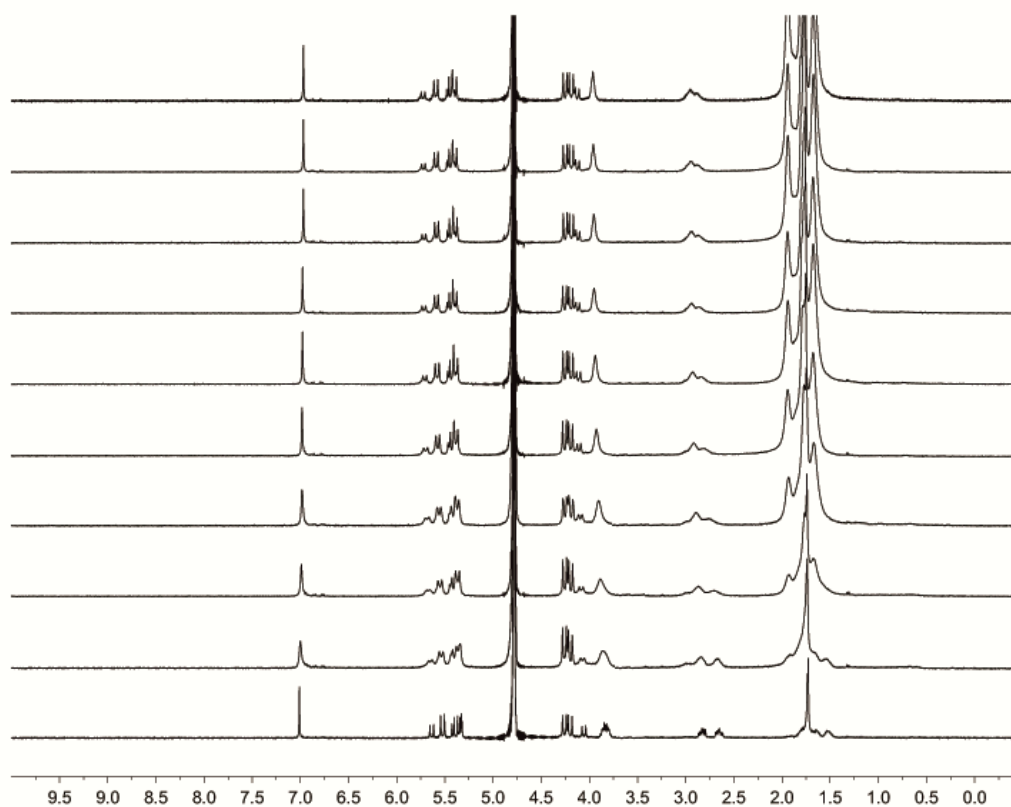


Figure S37. (A) Displacement titration of a solution of dye **4** (10.0 μM) and host **2c** (9.19 μM) solution with **5b** (0 – 2.6 mM) (20 mM NaH_2PO_4 buffer, pH 7.4). (B) Non-linear fitting plot of absorbance *versus* concentration for the displacement titration of **5b** using a model implemented in ScientistTM. K_a was evaluated as $5.54 (\pm 0.83) \times 10^4 \text{ M}^{-1}$.

(A)



(B)

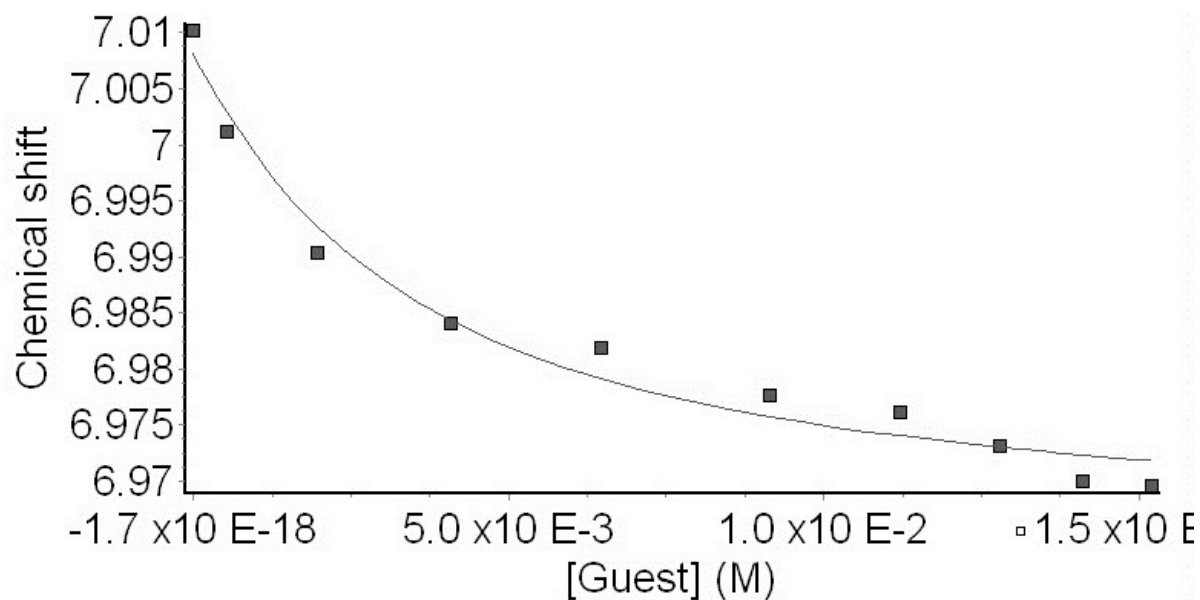


Figure S38. (A) ¹H NMR spectra (400 MHz, 20 mM sodium phosphate buffer, pD = 7.4) recorded for a solution of **2c** (1.055 mM) and **5c** of variable concentrations (0 – 16 mM). (B) Plot of the chemical shift of **2c** as a function of **5c** concentration. The solid line represents the best non-linear fitting of the data to a 1:1 binding model ($K_a = 345 \pm 118 \text{ M}^{-1}$)

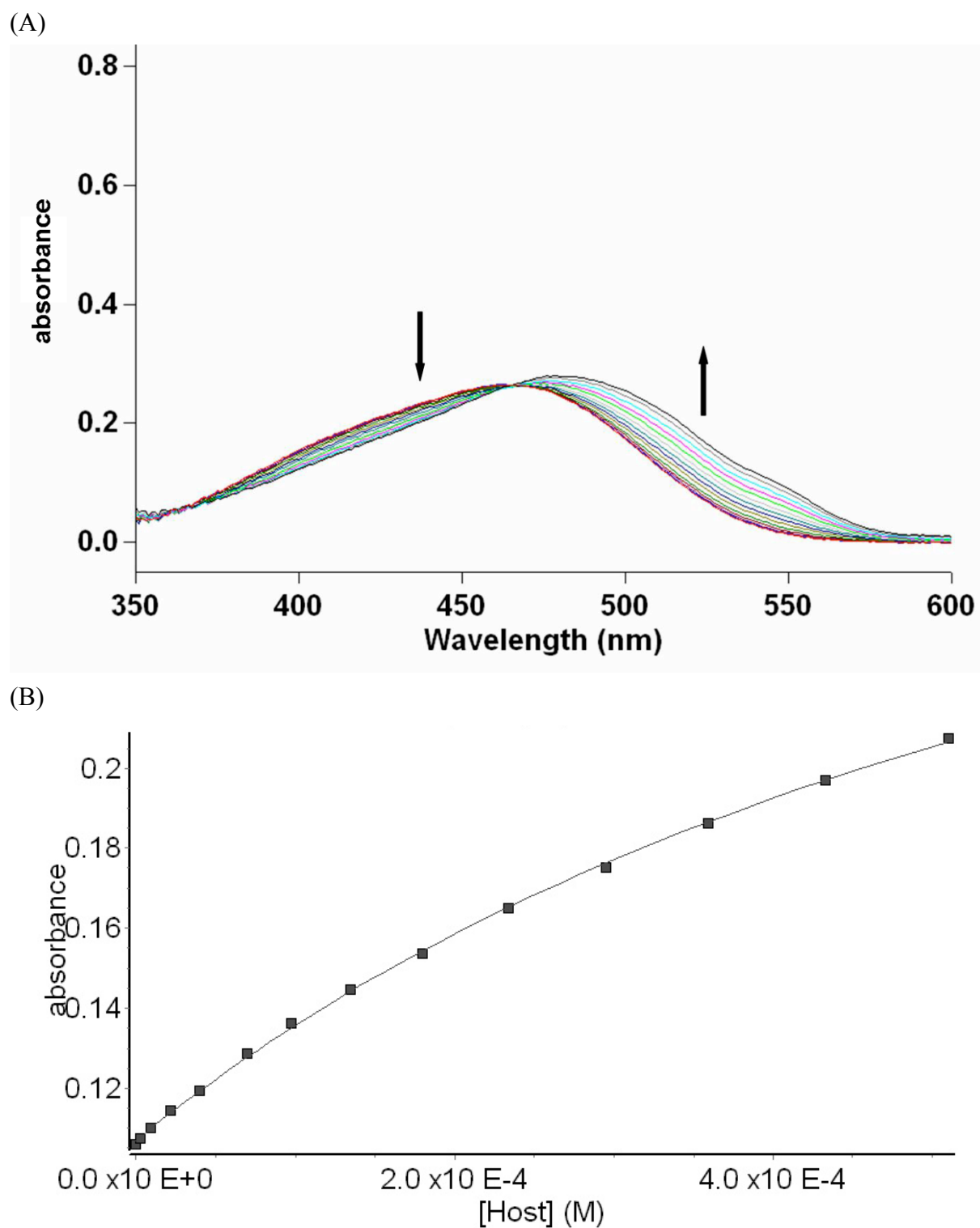


Figure S39. (A) UV/Vis spectra from the titration of dye **8** (11.0 μM) with **2h** (0 – 500 μM) in 20 mM NaH_2PO_4 buffer (pH 7.4); (B) plot of the ΔA_{550} as a function of **2h** concentration. The solid line represents the best non-linear fit of the data to a 1:1 binding model ($K_a = 1.32 (\pm 0.01) \times 10^3 \text{ M}^{-1}$).

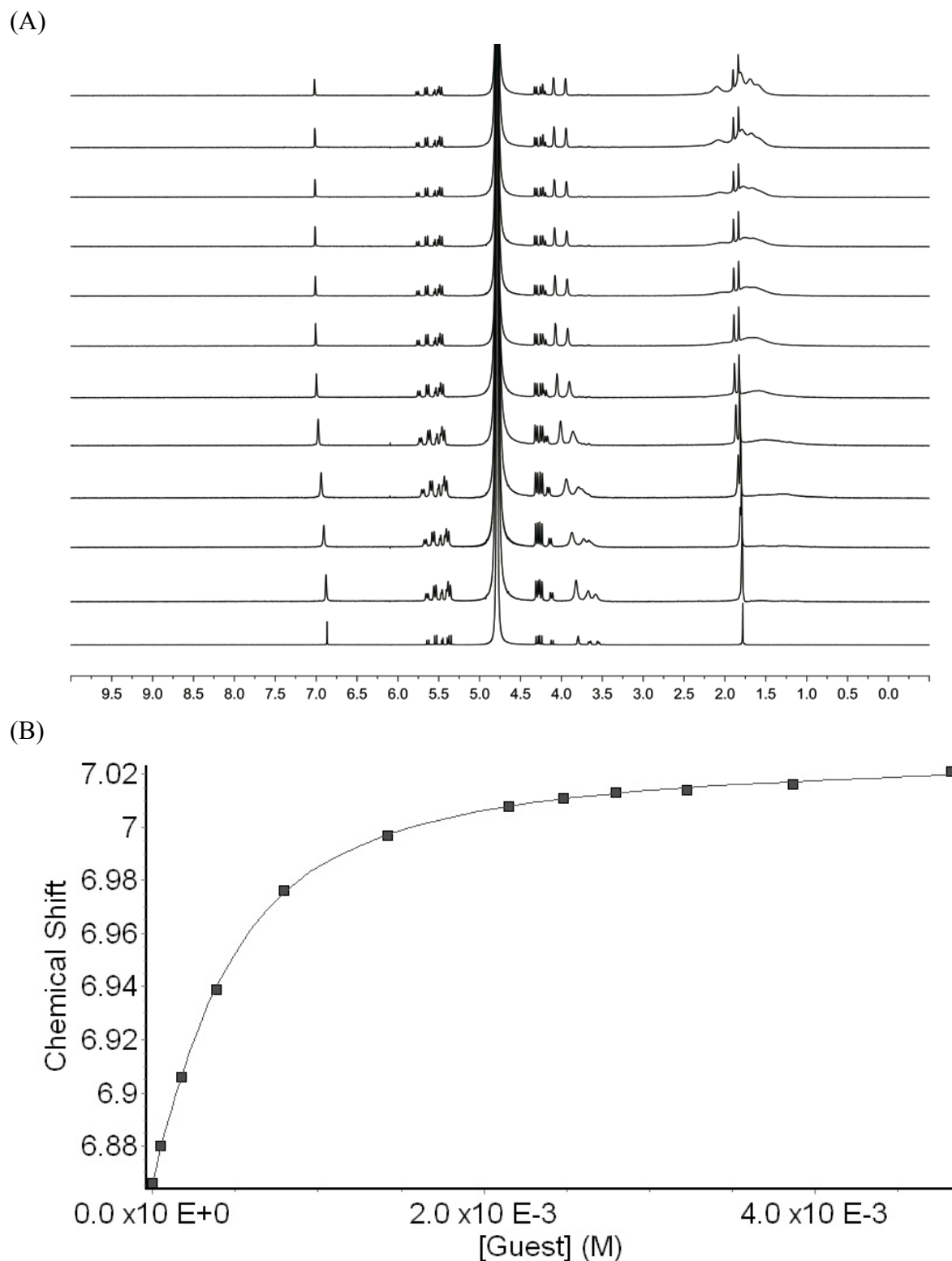
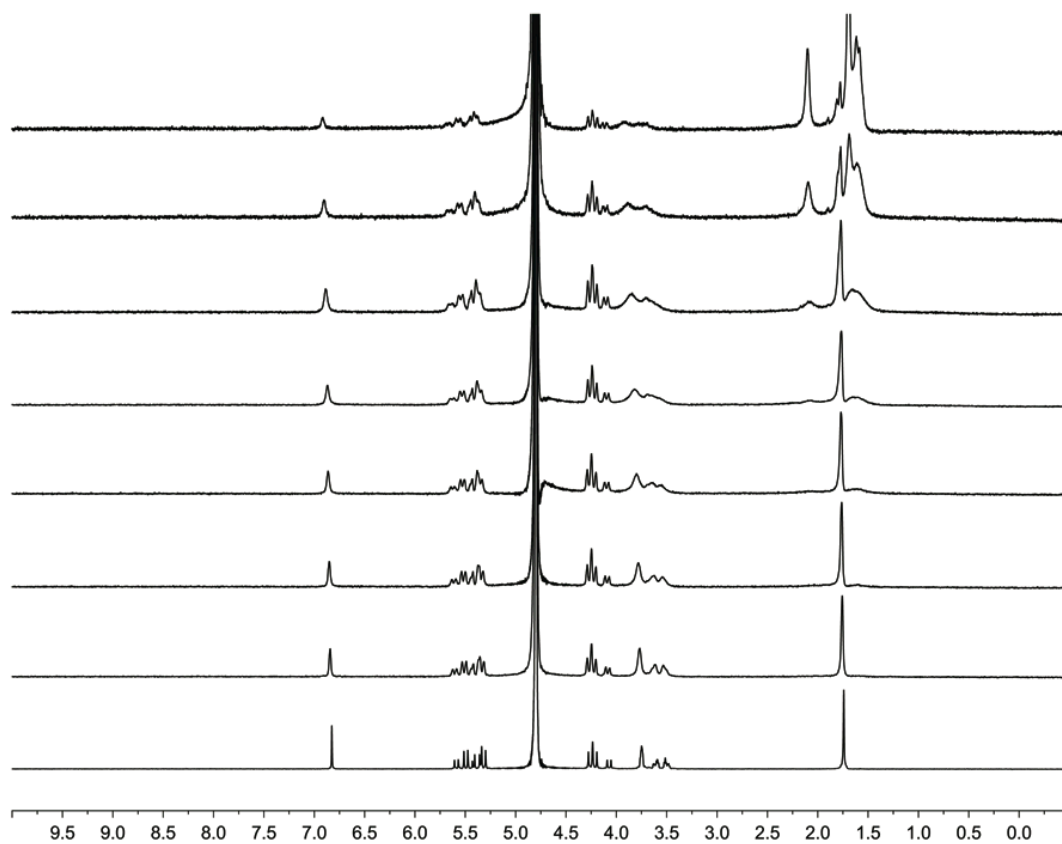


Figure S40. (A) ^1H NMR spectra (400 MHz, 20 mM sodium phosphate buffer, pD = 7.4) recorded for a solution of **2h** (0.350 mM) and **5a** of variable concentrations (0 – 5.0 mM). (B) Plot of the chemical shift of **2h** as a function of **5a** concentration. The solid line represents the best non-linear fitting of the data to a 1:1 binding model ($K_a = 3.64 (\pm 0.10) \times 10^3 \text{ M}^{-1}$).

(A)



(B)

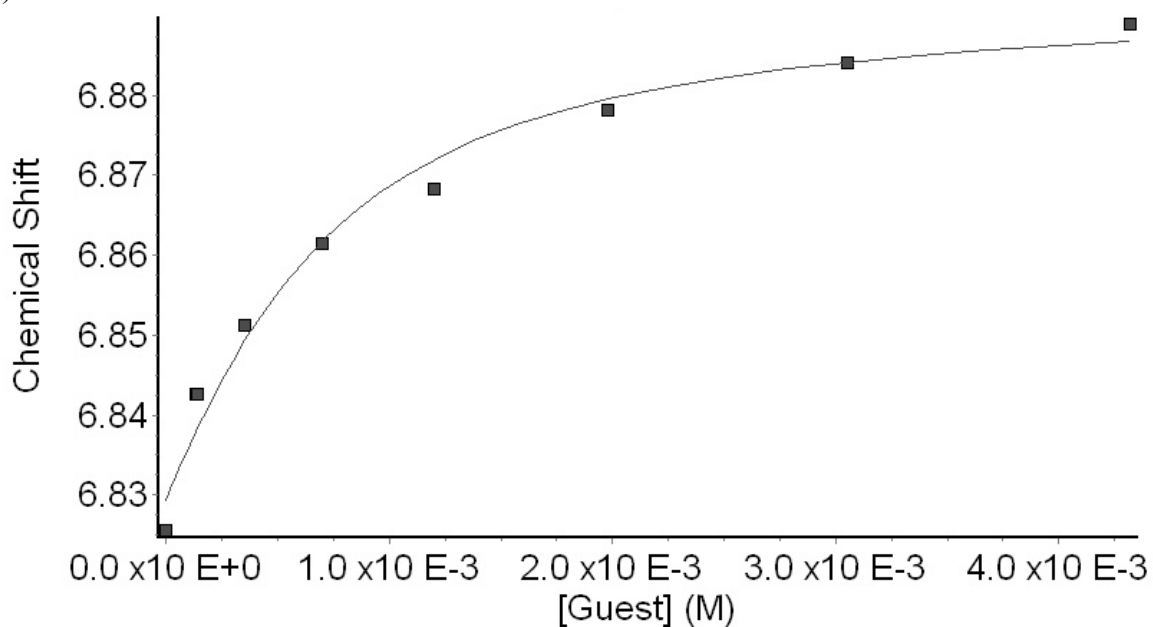
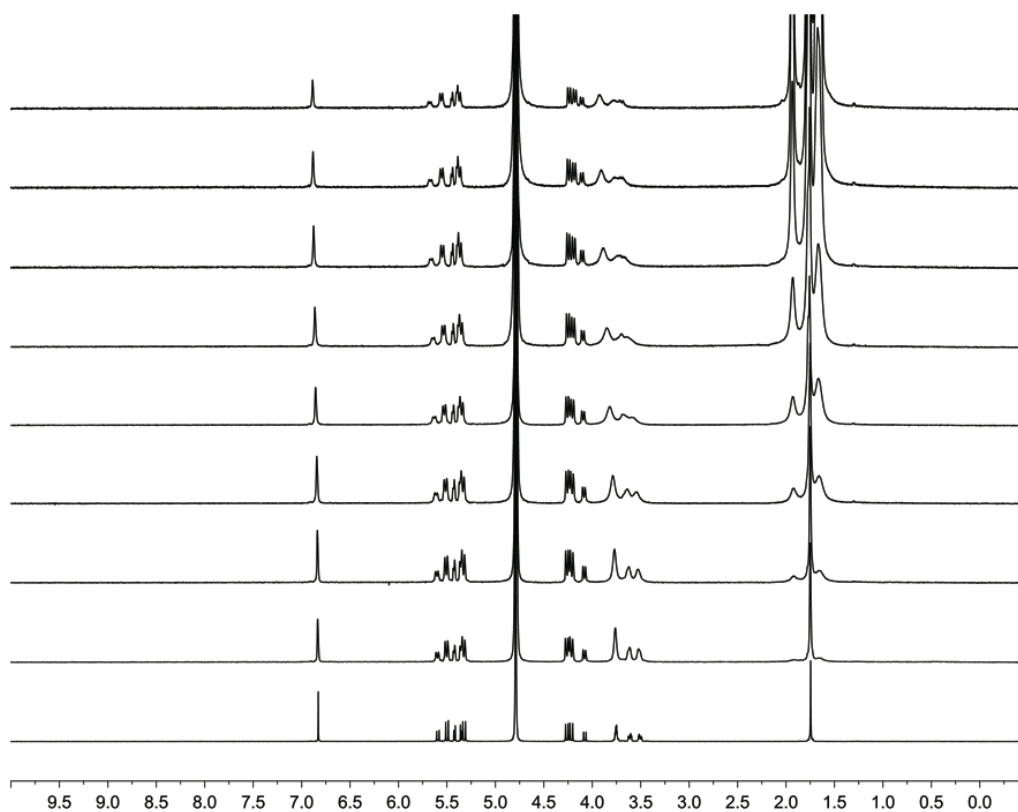


Figure S41. (A) ¹H NMR spectra (400 MHz, 20 mM sodium phosphate buffer, pD = 7.4) recorded for a solution of **2h** (0.350 mM) and **5b** of variable concentrations (0 – 5.0 mM). (B) Plot of the chemical shift of **2h** as a function of **5b** concentration. The solid line represents the best non-linear fitting of the data to a 1:1 binding model ($K_a = 2.36 \pm 0.41 \times 10^3 \text{ M}^{-1}$).

(A)



(B)

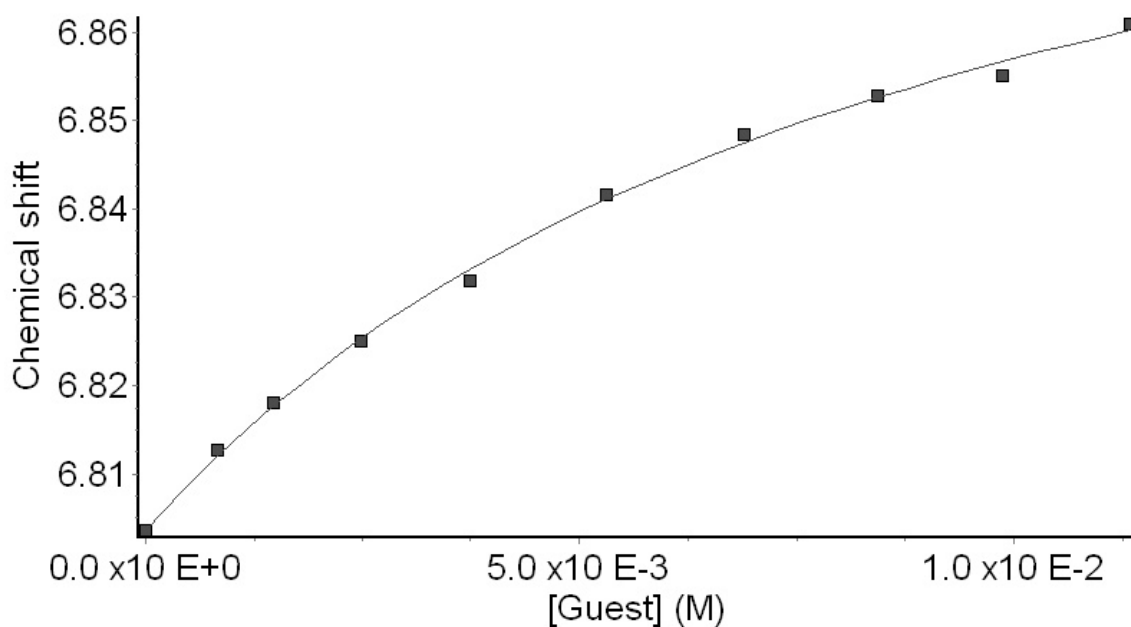


Figure S42. (A) ^1H NMR spectra (400 MHz, 20 mM sodium phosphate buffer, pD = 7.4) recorded for a solution of **2h** (0.350 mM) and **5c** of variable concentrations (0 – 11 mM). (B) Plot of the chemical shift of **2h** as a function of **5c** concentration. The solid line represents the best non-linear fitting of the data to a 1:1 binding model ($K_a = 108 \pm 8.3 \text{ M}^{-1}$).

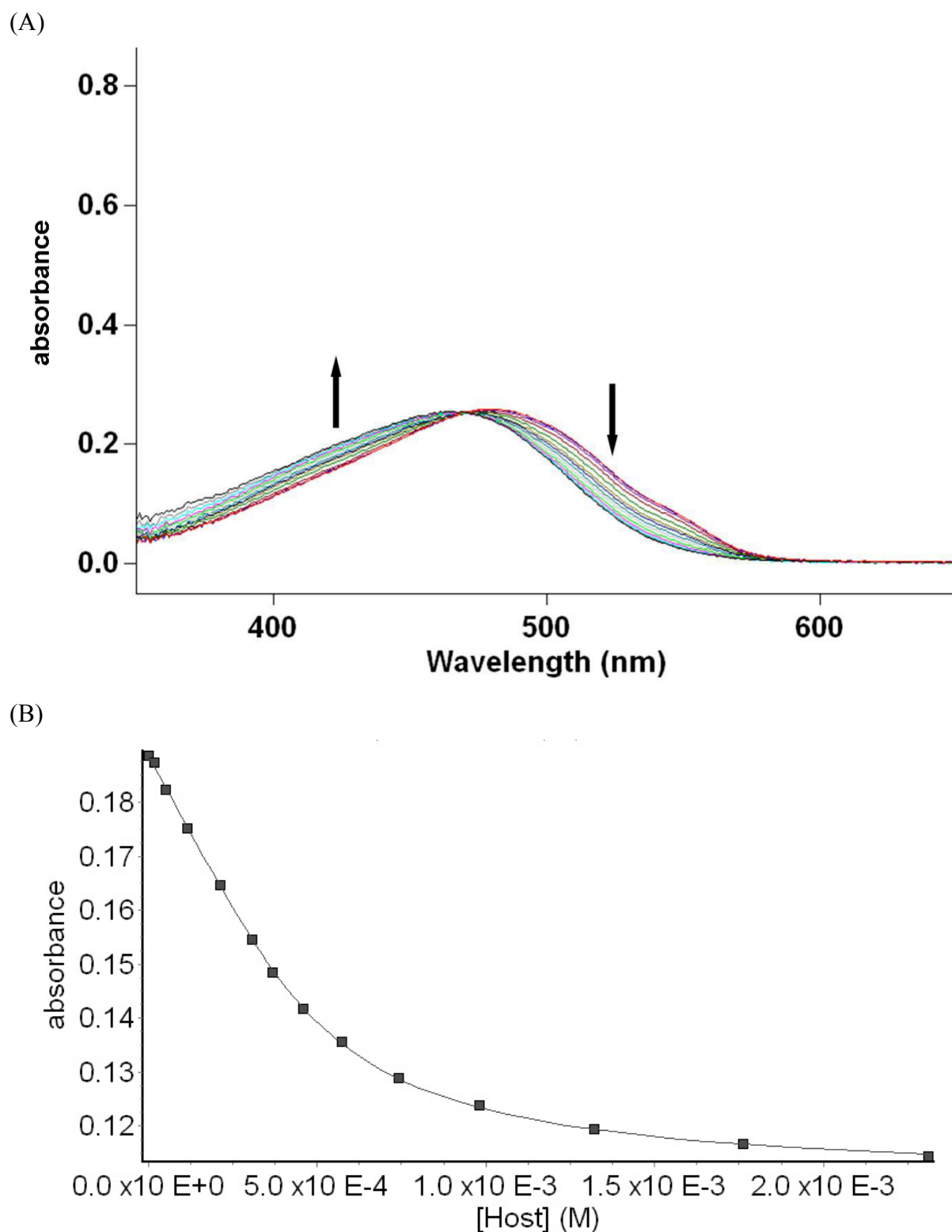


Figure S43. (A) Displacement titration of a solution of dye **8** (11.0 μM) and host **2h** (385 μM) solution with **6** (0 – 2.6 mM) (20 mM NaH_2PO_4 buffer, pH 7.4). (B) Non-linear fitting plot of absorbance *versus* concentration for the displacement titration of **6** using a model implemented in ScientistTM. K_a was evaluated as $1.13 \pm 0.10 \times 10^4 \text{ M}^{-1}$.

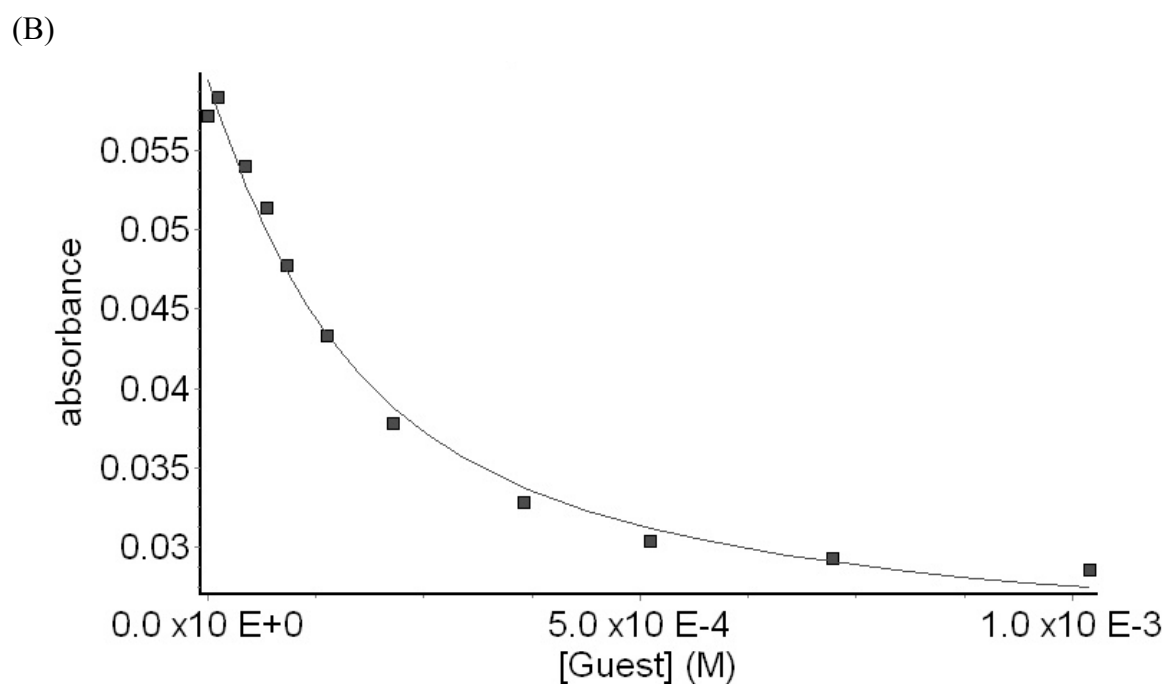
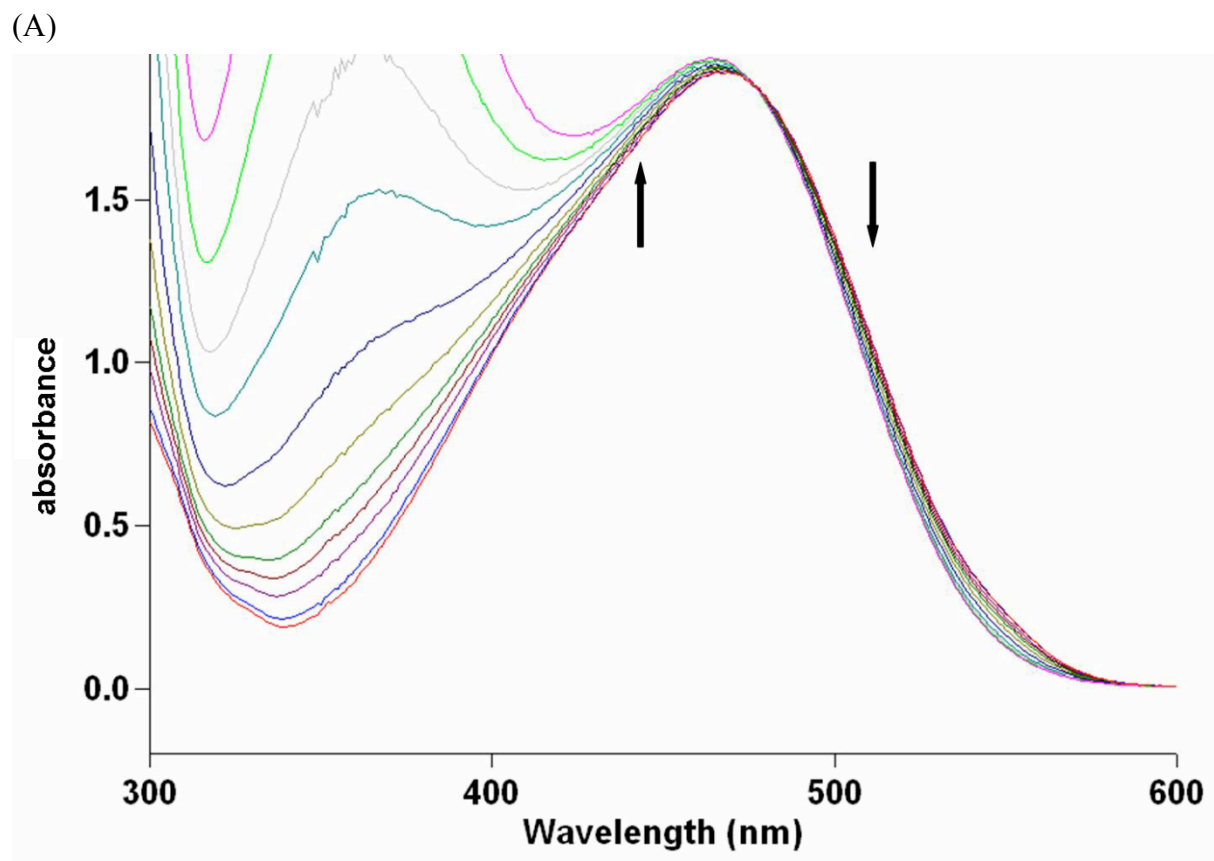
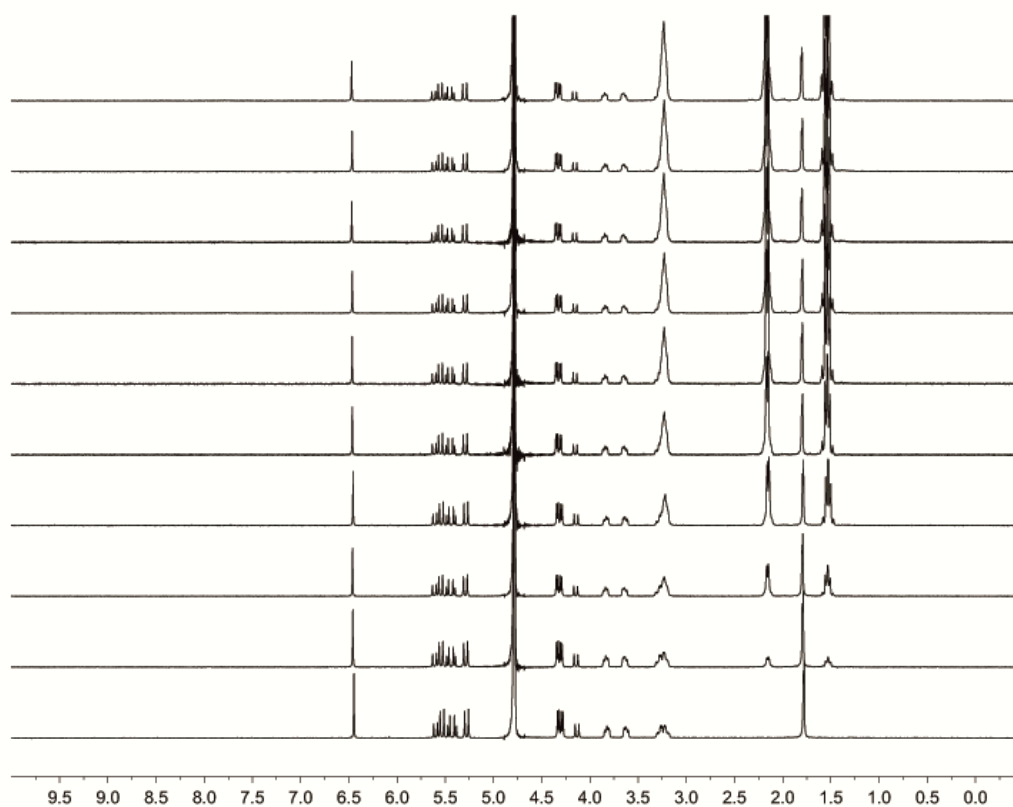


Figure S44. (A) Displacement titration of a solution of dye **8** (76.5 μM) and host **2h** (83.2 μM) solution with **7** (0 – 1.2 mM) (20 mM NaH_2PO_4 buffer, pH 7.4). (B) Non-linear fitting plot of absorbance *versus* concentration for the displacement titration of **7** using a model implemented in ScientistTM. K_a was evaluated as $9.59 \pm 1.2 \times 10^3 \text{ M}^{-1}$.

(A)



(B)

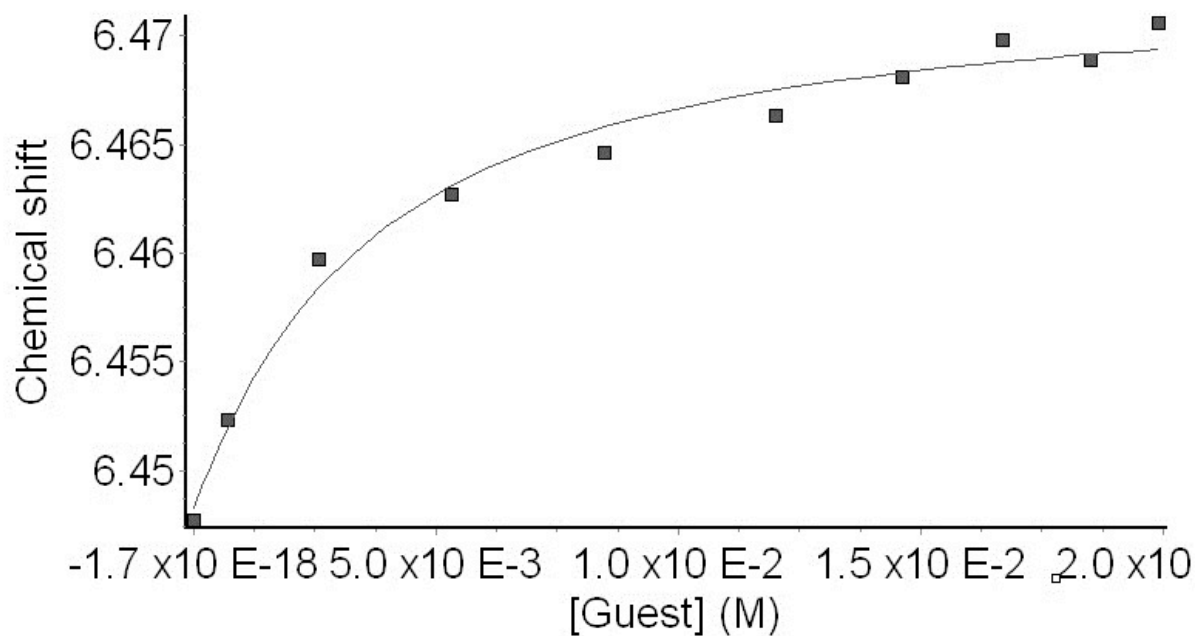
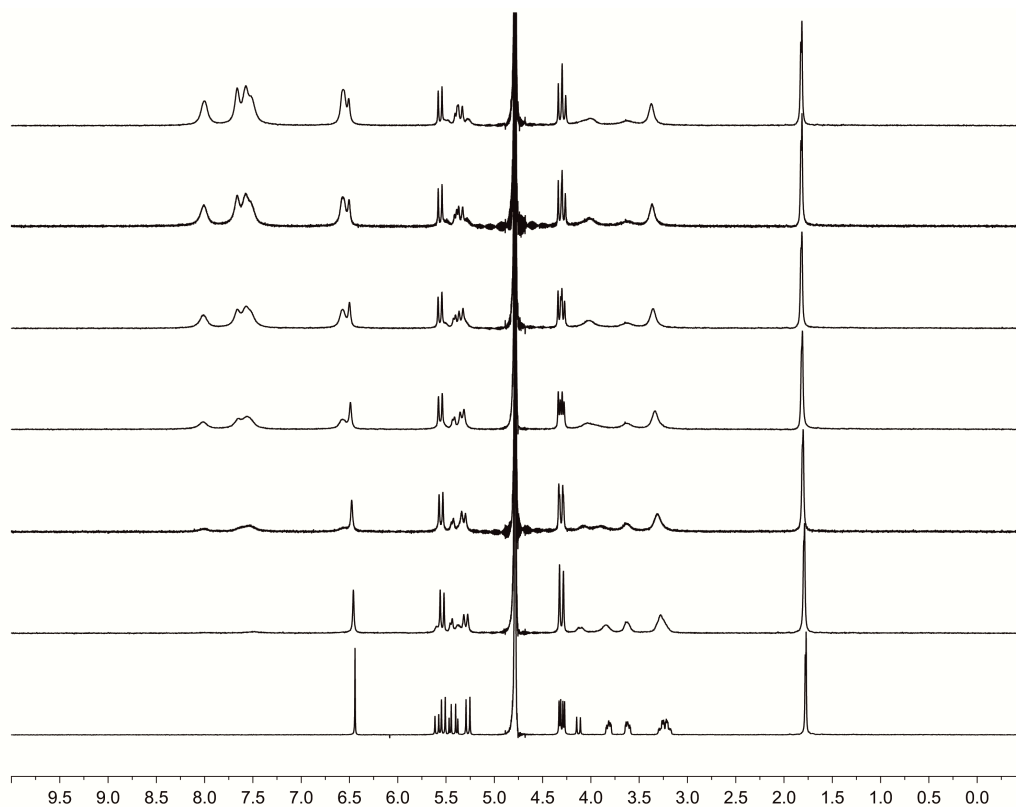


Figure S45. (A) ¹H NMR spectra (400 MHz, 20 mM sodium phosphate buffer, pD = 7.4) recorded for a solution of **2f** (1.055 mM) and **6** of variable concentrations (0 – 22 mM). (B) Plot of the chemical shift of **2f** as a function of **6** concentration. The solid line represents the best non-linear fitting of the data to a 1:1 binding model ($K_a = 327 (\pm 82) \text{ M}^{-1}$)

(A)



(B)

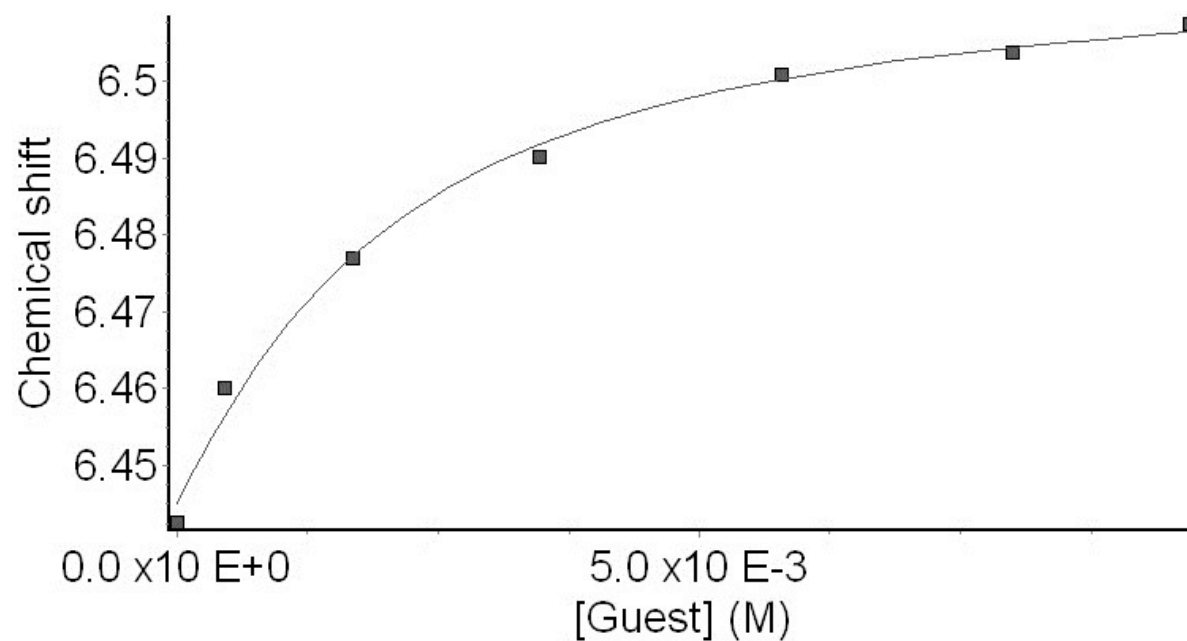


Figure S46. (A) ¹H NMR spectra (400 MHz, 20 mM sodium phosphate buffer, pD = 7.4) recorded for a solution of **2f** (1.055 mM) and **7** of variable concentrations (0 – 11 mM). (B) Plot of the chemical shift of **2f** as a function of **7** concentration. The solid line represents the best non-linear fitting of the data to a 1:1 binding model ($K_a = 678 \pm 171 \text{ M}^{-1}$).

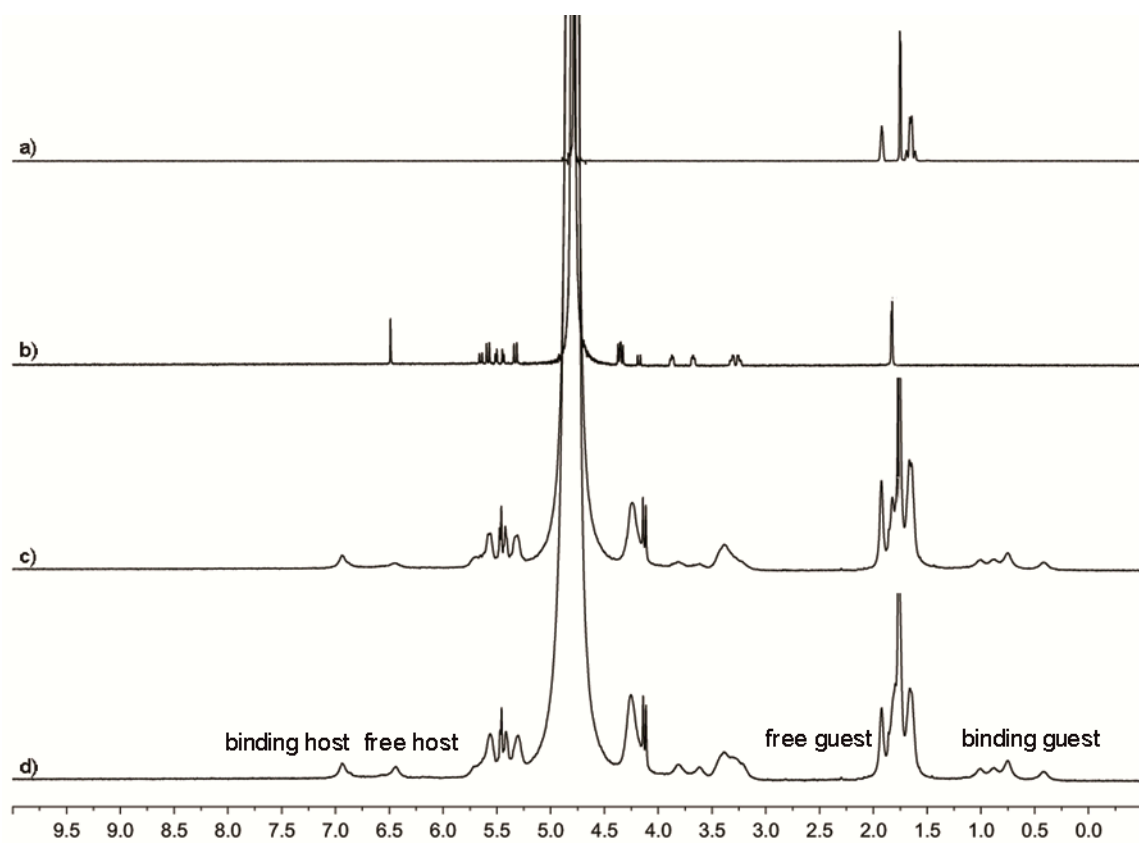


Figure S47. ¹H NMR spectra recorded (D₂O, 400 MHz, RT) for: a) **5c** (0.5 mM), b) **2f** (0.5 mM), c) a mixture of **2f** (0.5 mM) and **5c** (4.0 mM), and d) a mixture of **2f** (0.5 mM) and **5c** (2.5 mM).

Determination of pK_a shift of guest 7 when forming complexes with 2a, 2f and 2h
UV/Vis spectroscopy was used in this work to determine the pK_a values. The direct pH titration of fixed concentrations of UV/Vis dye 7 and different hosts allowed us to determine their values of pK_a by fitting to a pK_a model.

pK_a Models Used to Determine Values of K_a with Micromath Scientist

```
// Micromath Scientist Model File
IndVars: pH
DepVars: Iobs
Params: Imax, Imin, pKa
Iobs=Imax/(1+10^(pH-pKa))+Imin/(1+10^(pKa-pH))

0<pKa<14
0<pH
0<Imax
0<Imin
***
```

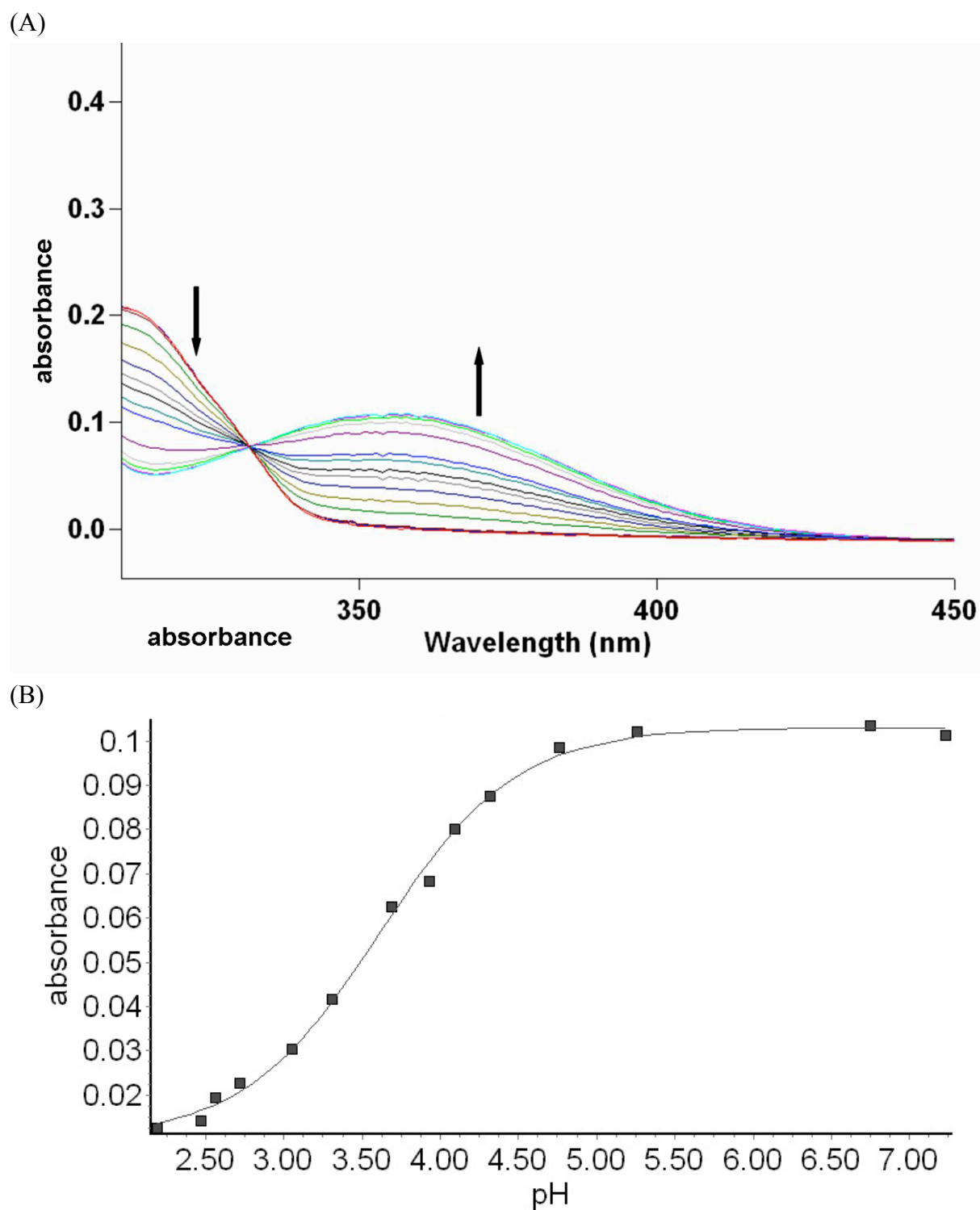


Figure S48. (A) pH titration of a solution of dye 7 (36.5 μM) solution (B) Non-linear fitting plot of absorbance *versus* pH for the pH titration of 7 with using a model implemented in ScientistTM. pK_a was evaluated as 3.6.

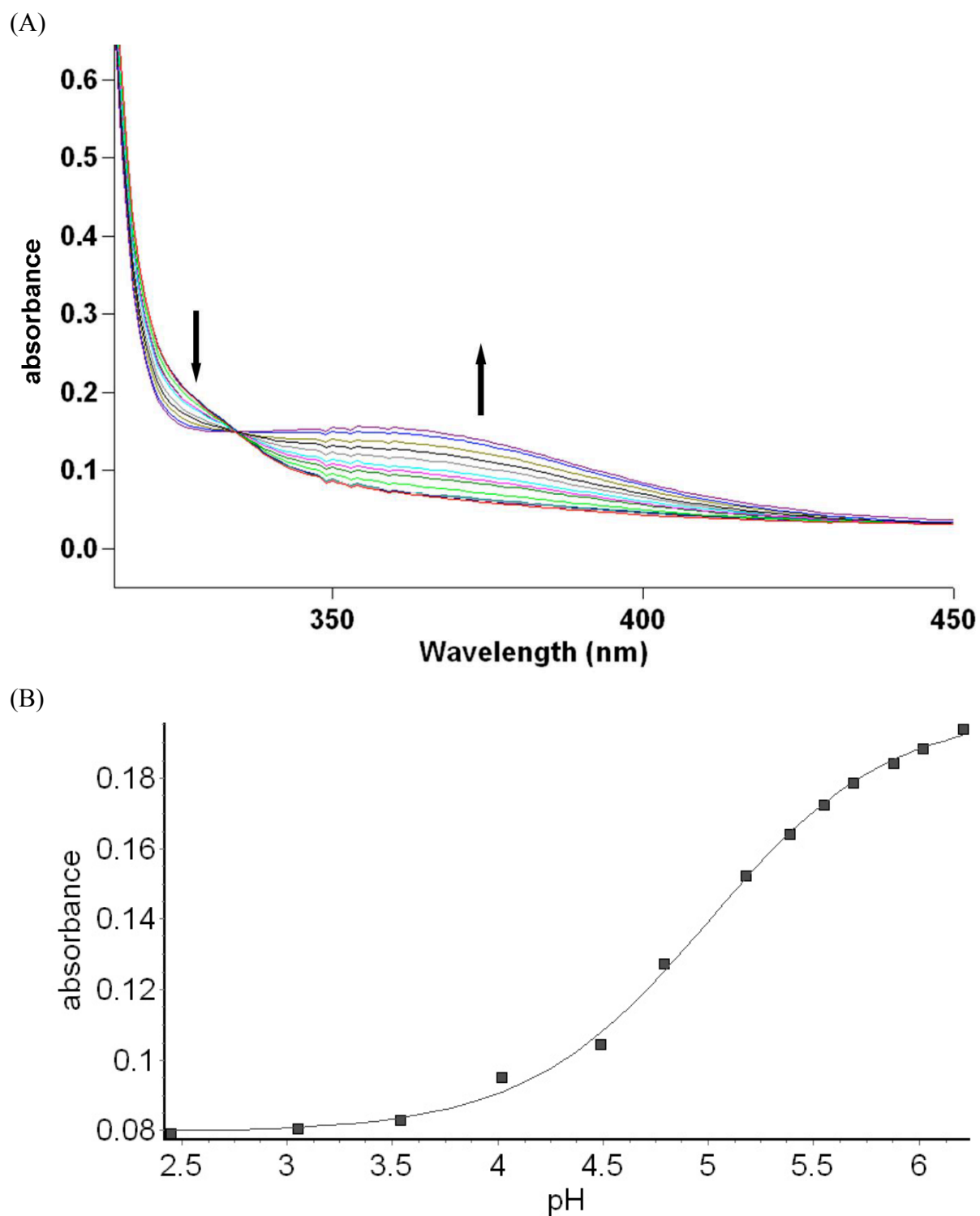


Figure S49. (A) pH titration of a solution of dye **7** ($36.5 \mu\text{M}$) solution with **2a** (1.5 mM) (B) Non-linear fitting plot of absorbance *versus* pH for the pH titration of **7** with using a model implemented in ScientistTM. pK_a was evaluated as 4.9.

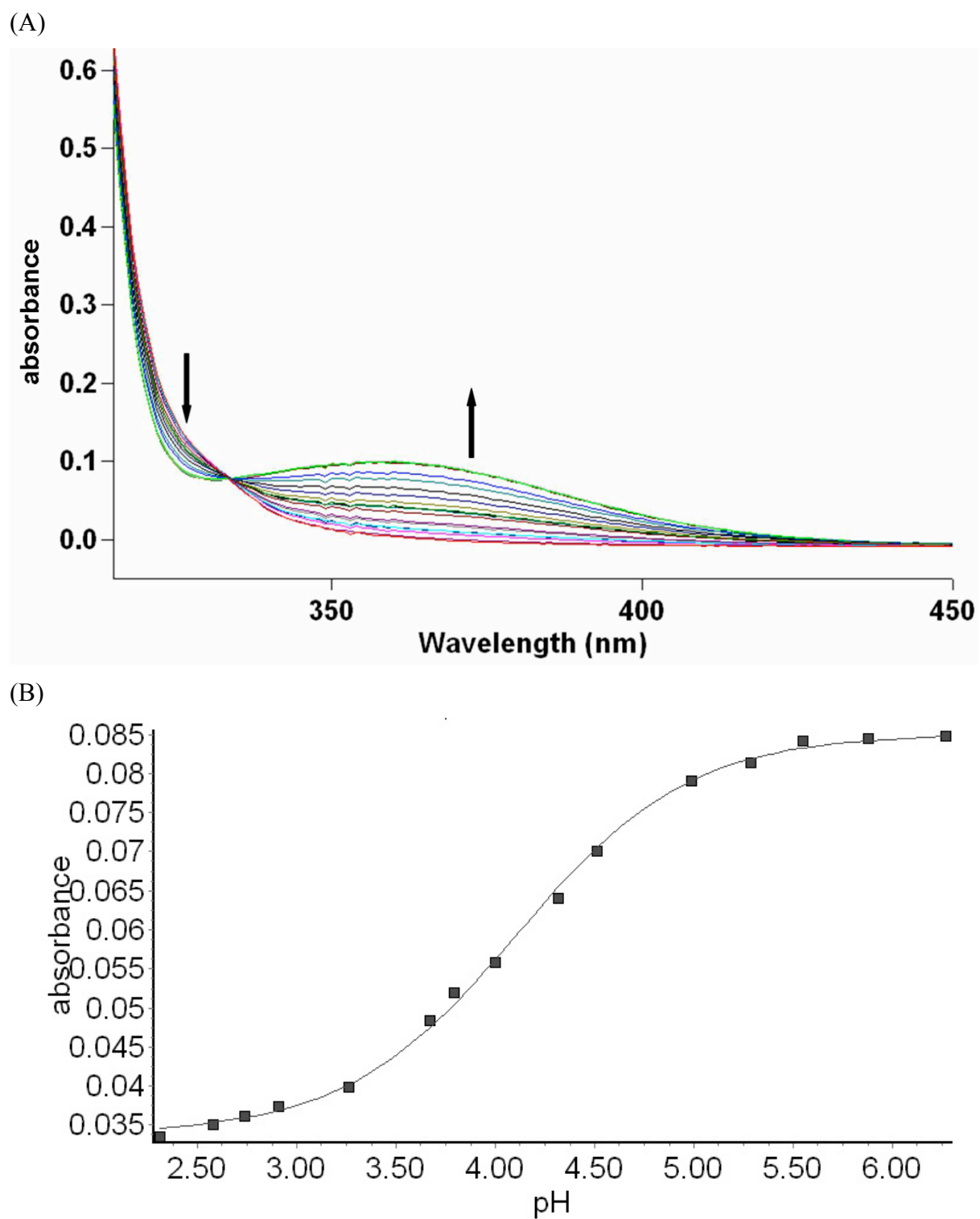
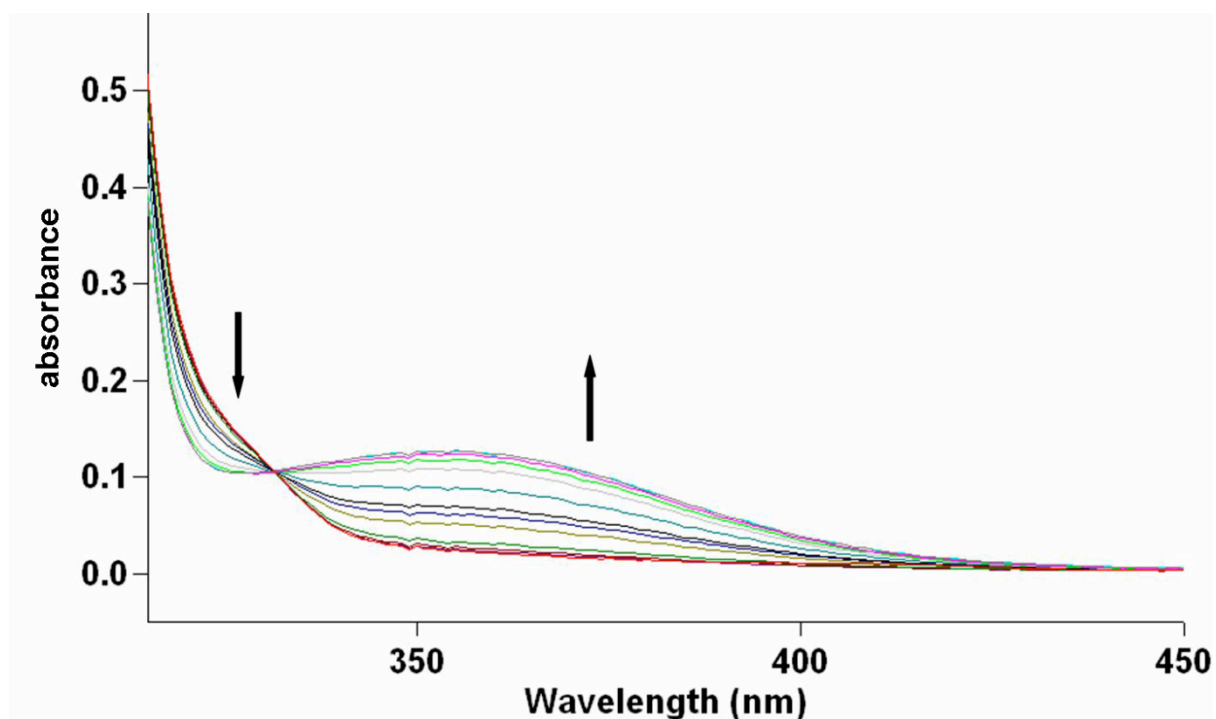


Figure S50. (A) pH titration of a solution of dye **7** ($36.5 \mu\text{M}$) solution with **2h** (1.5 mM) (B) Non-linear fitting plot of absorbance *versus* pH for the pH titration of **7** with using a model implemented in ScientistTM. pK_a was evaluated as 4.1.

(A)



(B)

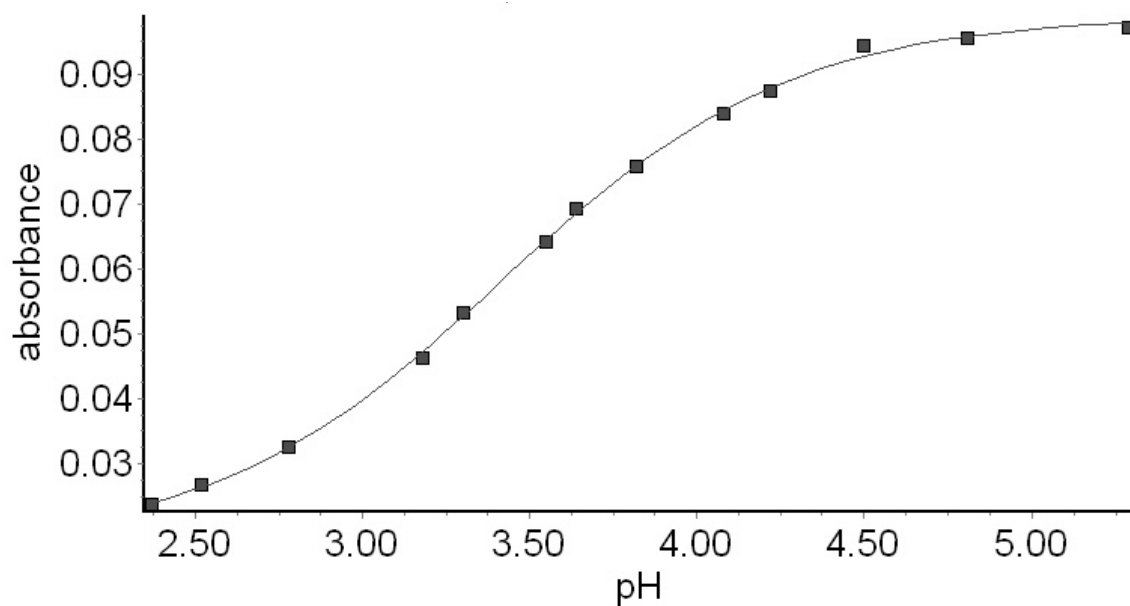


Figure S51. (A) pH titration of a solution of dye **7** ($36.5 \mu\text{M}$) solution with **2f** (1.5 mM) (B) Non-linear fitting plot of absorbance *versus* pH for the pH titration of **7** using a model implemented in ScientistTM. pK_a was evaluated as 3.4.

Details of the X-ray crystallographic structure of 2h. A colorless prism-like specimen of $C_{100}H_{155}N_{32}O_{49.50}$, approximate dimensions 0.21 mm \times 0.30 mm \times 0.42 mm, was used for the X-ray crystallographic analysis. The X-ray intensity data were measured on a Bruker APEX-II CCD system equipped with a graphite monochromator and a MoK α sealed tube ($\lambda = 0.71073$ Å). Data collection temperature was 150 K.

The total exposure time was 16.72 hours. The frames were integrated with the Bruker SAINT software package using a narrow-frame algorithm. The integration of the data using a monoclinic unit cell yielded a total of 116519 reflections to a maximum θ angle of 25.00° (0.84 Å resolution), of which 21005 were independent (average redundancy 5.547, completeness = 99.9%, $R_{\text{int}} = 3.15\%$, $R_{\text{sig}} = 2.19\%$) and 16835 (80.15%) were greater than $2\sigma(F^2)$. The final cell constants of $a = 29.339(3)$ Å, $b = 13.8631(13)$ Å, $c = 29.715(3)$ Å, $\beta = 99.2288(16)^\circ$, $V = 11930.2(2)$ Å³, are based upon the refinement of the XYZ-centroids of 9901 reflections above $20 \sigma(I)$ with $4.649^\circ < 2\theta < 56.33^\circ$. Data were corrected for absorption effects using the multi-scan method (SADABS). The calculated minimum and maximum transmission coefficients (based on crystal size) are 0.9526 and 0.9759.

The structure was solved and refined using the Bruker SHELXTL Software Package, using the space group P 1 21/n 1, with $Z = 4$ for the formula unit, $C_{100}H_{155}N_{32}O_{49.50}$. The final anisotropic full-matrix least-squares refinement on F^2 with 1867 variables converged at $R_1 = 5.88\%$, for the observed data and $wR_2 = 12.11\%$ for all data. The goodness-of-fit was 1.008. The largest peak in the final difference electron density synthesis was $0.798 \text{ e}^-/\text{Å}^3$ and the largest hole was $-0.470 \text{ e}^-/\text{Å}^3$ with an RMS deviation of $0.057 \text{ e}^-/\text{Å}^3$. On the basis of the final model, the calculated density was 1.446 g/cm^3 and $F(000)$, 5500 e^- .

APEX2 Version 2010.11-3 (Bruker AXS Inc.)

SAINT Version 7.68A (Bruker AXS Inc., 2009)

SADABS Version 2008/1 (G. M. Sheldrick, Bruker AXS Inc.)

XPREP Version 2008/2 (G. M. Sheldrick, Bruker AXS Inc.)

XS Version 2008/1 (G. M. Sheldrick, *Acta Cryst.* (2008). **A64**, 112-122)

XL Version 2008/4 (G. M. Sheldrick, *Acta Cryst.* (2008). **A64**, 112-122)

Platon (A. L. Spek, *Acta Cryst.* (1990). **A46**, C-34)

Table 1. Sample and crystal data for UM2316a.

Identification code	2316a	
Chemical formula	$C_{100}H_{155}N_{32}O_{49.50}$	
Formula weight	2597.56	
Temperature	150(2) K	
Wavelength	0.71073 Å	
Crystal size	0.21 \times 0.30 \times 0.42 mm	
Crystal habit	colorless prism	
Crystal system	monoclinic	
Space group	P 1 21/n 1	
Unit cell dimensions	$a = 29.339(3)$ Å	$\alpha = 90^\circ$

	$b = 13.8631(13) \text{ \AA}$	$\beta = 99.2288(16)^\circ$
	$c = 29.715(3) \text{ \AA}$	$\gamma = 90^\circ$
Volume	11930.(2) \AA^3	
Z	4	
Density (calculated)	1.446 Mg/cm^3	
Absorption coefficient	0.117 mm^{-1}	
F(000)	5500	

Table 2. Data collection and structure refinement for UM2316a.

Diffractometer	Bruker APEX-II CCD	
Radiation source	sealed tube, MoK α	
Theta range for data collection	2.07 to 25.00 $^\circ$	
Index ranges	$-34 \leq h \leq 34$, $-16 \leq k \leq 16$, $-35 \leq l \leq 35$	
Reflections collected	116519	
Independent reflections	21005 [R(int) = 0.0315]	
Coverage of independent reflections	99.9%	
Absorption correction	multi-scan	
Max. and min. transmission	0.9759 and 0.9526	
Structure solution technique	direct methods	
Structure solution program	SHELXS-97 (Sheldrick, 2008)	
Refinement method	Full-matrix least-squares on F^2	
Refinement program	SHELXL-97 (Sheldrick, 2008)	
Function minimized	$\Sigma w(F_o^2 - F_c^2)^2$	
Data / restraints / parameters	21005 / 440 / 1867	
Goodness-of-fit on F^2	1.008	
$\Delta/\sigma_{\text{max}}$	0.009	
Final R indices	16835 data; $I > 2\sigma(I)$	$R_1 = 0.0588$, $wR_2 = 0.1160$
	all data	$R_1 = 0.0737$, $wR_2 = 0.1211$
Weighting scheme	$w = 1/[\sigma^2(F_o^2) + (0.0100P)^2 + 26.5000P]$, $P = (F_o^2 + 2F_c^2)/3$	
Extinction coefficient	0.0002(0)	
Largest diff. peak and hole	0.798 and -0.470 e\AA^{-3}	

R.M.S. deviation from mean $0.057 \text{ e}\text{\AA}^{-3}$

$$R_{\text{int}} = \Sigma |F_o^2 - F_o^2(\text{mean})| / \Sigma [F_o^2]$$

$$R_1 = \Sigma ||F_o| - |F_c|| / \Sigma |F_o|$$

$$\text{GOOF} = S = \{ \Sigma [w(F_o^2 - F_c^2)^2] / (\text{n} - \text{p}) \}^{1/2}$$

$$wR_2 = \{ \Sigma [w(F_o^2 - F_c^2)^2] / \Sigma [w(F_o^2)^2] \}^{1/2}$$

Details of the X-ray crystallographic structure of 2f. A colorless plate-like specimen of $C_{50}H_{94.28}Cl_4N_{20}O_{25.14}$, approximate dimensions 0.18 mm \times 0.44 mm \times 0.48 mm, was used for the X-ray crystallographic analysis. The X-ray intensity data were measured on a Bruker APEX-II CCD system equipped with a graphite monochromator and a MoK α sealed tube ($\lambda = 0.71073$ Å). Data collection temperature was 150 K.

The total exposure time was 22.73 hours. The frames were integrated with the Bruker SAINT software package using a narrow-frame algorithm. The integration of the data using a monoclinic unit cell yielded a total of 118279 reflections to a maximum θ angle of 30.00° (0.71 Å resolution), of which 39291 were independent (average redundancy 3.010, completeness = 99.5%, $R_{\text{int}} = 4.30\%$, $R_{\text{sig}} = 4.63\%$) and 34631 (88.14%) were greater than $2\sigma(F^2)$. The final cell constants of $a = 13.7177(10)$ Å, $b = 27.048(2)$ Å, $c = 18.9817(14)$ Å, $\beta = 92.5526(12)^\circ$, $V = 7035.9(9)$ Å³, are based upon the refinement of the XYZ-centroids of 9755 reflections above $20 \sigma(I)$ with $4.685^\circ < 2\theta < 61.03^\circ$. Data were corrected for absorption effects using the multi-scan method (SADABS). The calculated minimum and maximum transmission coefficients (based on crystal size) are 0.8858 and 0.9549.

The structure was solved and refined using the Bruker SHELXTL Software Package, using the space group P 1 21 1, with $Z = 4$ for the formula unit, $C_{50}H_{94.28}Cl_4N_{20}O_{25.14}$. The final anisotropic full-matrix least-squares refinement on F^2 with 1686 variables converged at $R_1 = 5.29\%$, for the observed data and $wR_2 = 12.34\%$ for all data. The goodness-of-fit was 1.011. The largest peak in the final difference electron density synthesis was $0.689 \text{ e}^-/\text{Å}^3$ and the largest hole was $-0.916 \text{ e}^-/\text{Å}^3$ with an RMS deviation of $0.071 \text{ e}^-/\text{Å}^3$. On the basis of the final model, the calculated density was 1.435 g/cm^3 and $F(000)$, 3214 e^- .

APEX2 Version 2010.11-3 (Bruker AXS Inc.)

SAINT Version 7.68A (Bruker AXS Inc., 2009)

SADABS Version 2008/1 (G. M. Sheldrick, Bruker AXS Inc.)

XPREF Version 2008/2 (G. M. Sheldrick, Bruker AXS Inc.)

XS Version 2008/1 (G. M. Sheldrick, *Acta Cryst.* (2008). **A64**, 112-122)

XL Version 2012/4 (G. M. Sheldrick, (2012) University of Gottingen, Germany)

Platon (A. L. Spek, *Acta Cryst.* (1990). **A46**, C-34)

Table 1. Sample and crystal data for UM2349.

Identification code	2349
Chemical formula	$C_{50}H_{94.28}Cl_4N_{20}O_{25.14}$
Formula weight	1519.77
Temperature	150(2) K
Wavelength	0.71073 Å
Crystal size	0.18 \times 0.44 \times 0.48 mm
Crystal habit	colorless plate
Crystal system	monoclinic

Space group	P 1 21 1	
Unit cell dimensions	a = 13.7177(10) Å	$\alpha = 90^\circ$
	b = 27.048(2) Å	$\beta = 92.5526(12)^\circ$
	c = 18.9817(14) Å	$\gamma = 90^\circ$
Volume	7035.9(9) Å ³	
Z	4	
Density (calculated)	1.435 Mg/cm ³	
Absorption coefficient	0.259 mm ⁻¹	
F(000)	3214	

Table 2. Data collection and structure refinement for UM2349.

Diffractometer	Bruker APEX-II CCD	
Radiation source	sealed tube, MoK α	
Theta range for data collection	2.28 to 30.00°	
Index ranges	-19 ≤ h ≤ 19, -36 ≤ k ≤ 38, -26 ≤ l ≤ 26	
Reflections collected	118279	
Independent reflections	39291 [R(int) = 0.0430]	
Coverage of independent reflections	99.5%	
Absorption correction	multi-scan	
Max. and min. transmission	0.9549 and 0.8858	
Structure solution technique	direct methods	
Structure solution program	SHELXS-97 (Sheldrick, 2008)	
Refinement method	Full-matrix least-squares on F ²	
Refinement program	SHELXL-97 (Sheldrick, 2008)	
Function minimized	$\Sigma w(F_o^2 - F_c^2)^2$	
Data / restraints / parameters	39291 / 31 / 1686	
Goodness-of-fit on F²	1.011	
Δ/σ_{\max}	0.001	
Final R indices	34631 data; I > 2 σ (I)	R ₁ = 0.0529, wR ₂ = 0.1210
	all data	R ₁ = 0.0583, wR ₂ = 0.1234
Weighting scheme	w = 1/[$\sigma^2(F_o^2) + (0.0100P)^2 + 9.0000P$], P = (F _o ² + 2F _c ²)/3	

Absolute structure parameter	0.5(0)
Largest diff. peak and hole	0.689 and -0.916 eÅ ⁻³
R.M.S. deviation from mean	0.071 eÅ ⁻³

$$R_{\text{int}} = \Sigma |F_o^2 - F_o^2(\text{mean})| / \Sigma [F_o^2]$$

$$R_1 = \Sigma ||F_o| - |F_c|| / \Sigma |F_o|$$

$$\text{GOOF} = S = \{ \Sigma [w(F_o^2 - F_c^2)^2] / (n - p) \}^{1/2}$$

$$wR_2 = \{ \Sigma [w(F_o^2 - F_c^2)^2] / \Sigma [w(F_o^2)^2] \}^{1/2}$$